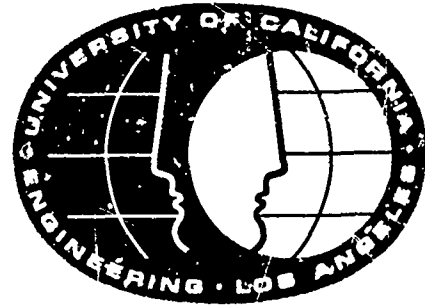


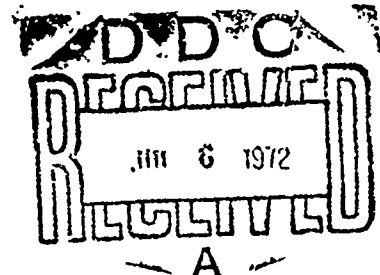
AROD-10048.3 MC.

AD 744531



Technical Report No. 1

DA-ARO-D-31-214-71-G124



Prepared for the U.S. Army Research Office -- Durham

UCLA-ENG-7234

April 1972

EMBRITTLEMENT BY LIQUID METALS

H. Kamdar

Reproduced by
NATIONAL TECHNICAL
INFORMATION SERVICE
U.S. Department of Commerce
Springfield VA 22151

Approved for public release; distribution unlimited. The findings in this report are not to be construed as an official Department of the Army position, unless so designated by other authorized documents.

Materials Department
School of Engineering and Applied Science
University of California
Los Angeles

171
SK

Unclassified

Security Classification

DOCUMENT CONTROL DATA - R & D

(Security classification of title, body of abstract and indexing annotation must be entered when the overall report is classified)

1. ORIGINATING ACTIVITY (Corporate author)		2a. REPORT SECURITY CLASSIFICATION	
University of California, Los Angeles		Unclassified	
		2b. GROUP	
		NA	
3. REPORT TITLE			
Embrittlement by Liquid Metals			
4. DESCRIPTIVE NOTES (Type of report and inclusive dates)			
Technical Report			
5. AUTHOR(S) (First name, middle initial, last name)			
M. H. Kamdar			
6. REPORT DATE		7a. TOTAL NO. OF PAGES	7b. NO. OF REFS
April 1972		164	
8a. CONTRACT OR GRANT NO.		9a. ORIGINATOR'S REPORT NUMBER(S)	
DA-ARO-D-31-124-71-G124		NA	
b. PROJECT NO.		9b. OTHER REPORT NO(S) (Any other numbers that may be assigned this report)	
20061102B32D		10048.4-MC	
c.			
d.			
10. DISTRIBUTION STATEMENT			
Approved for public release; distribution unlimited.			
11. SUPPLEMENTARY NOTES		12. SPONSORING MILITARY ACTIVITY	
None		U. S. Army Research Office-Durham Box CM, Duke Station Durham, North Carolina 27705	
13. ABSTRACT			
<p>This paper reviews the results of a number of investigations of liquid metal embrittlement and discusses the prerequisites and possible mechanisms for its occurrence. It also reviews the effects of variables on the severity of embrittlement that normally influence the fracture behavior of a solid. Additionally this paper describes effects on the occurrence and severity of embrittlement caused by the liquid phase. Other topics discussed are the possible correlation between the severity of embrittlement and the electro-negativities of the solid and liquid metals, the use of the concept of "inert carrier" liquid metals and possible means for enhancing or inhibiting embrittlement.</p>			
14. KEY WORDS			
Solid Metals Liquid Metals Embrittlement Liquid Metal Embrittlement Fracture Behavior			

DD FORM 1473

NOV 66

REPLACES DD FORM 1473, 1 JAN 64, WHICH IS OBSOLETE FOR ARMY USE.

Unclassified

EMBRITTLEMENT BY LIQUID METALS

Dr. M.H. Kamdar

Research Engineer, Materials Department
School of Engineering and Applied Science
University of California
Los Angeles, California
90024

Technical Report #1, April 1, 1972

DA-ARO-D-31-214-71-G124

Prepared for the U.S. Army Research Office — Durham

"Requests for additional copies by Agencies
of the Department of Defense, their contractors
and other government agencies should be directed
to:

Defense Documentation Center
Cameron Station
Alexandria, Virginia 22314

Department of Defense contractors must be established for
DDC services or have their "need-to-know" certified by the
cognizant military agency of their project or contract.

ACKNOWLEDGMENTS

It is a great pleasure to acknowledge helpful discussions with colleagues in the Materials Department at UCLA. Special thanks are extended to Professor Alan Tetelman, Chairman, Materials Department, UCLA, for his encouragement and for providing the facilities of the Materials Department to the author during the preparation of this paper. Thanks are also extended to Mrs. Mildred Hudson who patiently typed various drafts of this paper, and to Professor Robert Epp, of the Oriental Languages Department, UCLA who edited the entire manuscript and suggested improvements. Most importantly, thanks are extended to Drs. H.M. Davis, J.K. Magor, and G. Mayer of the Army Research Office, Durham for their encouragement, and for providing financial support to the author during the preparation of this paper. This work was supported by the Army Research Office, Durham under Grant No. DA-ARO(D)-31-214-71-G124.

ABSTRACT

Normally ductile metals become brittle when exposed to specific chemical environments; one example is the dramatic effects observed when ductile solid metals are exposed to certain surface active liquid metal environments. Polycrystalline as well as single crystal specimens loaded in air to some critical stress below the fracture stress, fracture almost instantly when contacted or "wetted" by an appropriate liquid metal. In liquid metal environment, the fracture mode changes from ductile to brittle either intergranular or transgranular. In some instances, propagation of cracks in liquid metal environments occurs at speeds of order 100 cm. per sec. or greater. Such effects are generally recognized as the phenomenon of "Liquid-Metal Embrittlement."

Liquid metal embrittlement is presently considered to result from a chemisorption-induced reduction in cohesion of atomic bonds at regions of high stress concentrations in a solid, such as at the tips of cracks or at the sites of crack nucleation. It is not considered to occur by either diffusion dependent penetration of liquid or corrosion type of processes. Moreover, adsorption-induced embrittlement is considered a special case of brittle fracture.

This paper reviews the results of a number of investigations of liquid metal embrittlement and discusses the prerequisites and possible mechanisms for its occurrence. It also reviews the effects of variables on the severity of embrittlement that normally influence the fracture behavior of a solid. These variables include grain size, alloying, strain rate, temperature, metallurgical structure, cold work, etc. Additionally this paper describes effects on the occurrence and severity of embrittlement caused by the liquid phase. These include time and temperature dependent diffusion or penetration

of the liquid into the solid, presence of liquid at the crack tip, composition of the liquid phase, etc. The effects of these variables on liquid metal embrittlement are discussed in terms of the effects of adsorption of the liquid metal atoms on the cohesive and shear strength of the solid at, or in the vicinity of the crack tip. Other topics discussed are the possible correlation between the severity of embrittlement and the electronegativities of the solid and liquid metals, the use of the concept of "inert carrier" liquid metals and possible means for enhancing or inhibiting embrittlement.

CONTENTS

	<u>Page</u>
FIGURES	ix
TABLES	xv
1. INTRODUCTION	1
2. OCCURANCE OF LIQUID METAL EMBRITTLEMENT.	7
2.1 Embrittlement by Liquid Metals.	7
2.2 Embrittlement by Vapor Phase.	9
3. MECHANISMS OF LIQUID METAL EMBRITTLEMENT	13
3.1 Reduction in Surface Energy Model	13
3.2 Adsorption-Induced Reduction in Cohesion Model.	13
3.1 Crack Propagation in the Zinc-Mercury and Zinc-Gallium System	21
3.3.1 Determination of Cleavage Fracture Energies.	21
3.3.2 Effects of Plastic Deformation and Environment on ϕ_p	23
3.4 Stress-Assisted Dissolution Model	27
4. BRITTLE FRACTURE IN LIQUID METAL ENVIRONMENTS.	31
4.1 A Criterion for Ductile-Brittle Fracture and Embrittlement	31
4.2 Prerequisites for Embrittlement	40
4.3 The Stress Concentrator Requirement	41
4.4 Criteria for Crack Initiation	46
4.5 Crack Initiation in Pure Zinc	51
4.6 Crack Initiation in Zinc Alloys	55
5. EFFECTS OF METALLURGICAL AND PHYSICAL FACTORS	71
5.1 Effects of Grain Size	73
5.2 Effects of Temperature.	78
5.3 Effects of Alloying	88
5.3.1 Embrittlement of Dilute Zinc Alloys	89
5.3.2 Embrittlement of Solid-Solution and Age- Hardenable Alloys	93
5.4 Effects of Prestrain and Cold Work.	105
6. EFFECTS OF LIQUID METAL ENVIRONMENTS	117
6.1 Effects of Minor Additions to the Embrittling Liquid Metal.	118
6.2 The Concept of "Inert Carriers"	121
6.3 Severity of Embrittlement and Electronegativity	124
6.4 Effects of Exposure to the Liquid Metal Environ- ment Prior to Stressing	134
6.5 Effects of Liquid Metal Environment on Static Fatigue	139
6.6 Effects of Variation in the Composition of the Environment	141

CONTENTS (Cont'd)

	<u>Page</u>
6.7 Effects of Liquid Metal Solutions on Static Fatigue Behavior.	143
6.8 Effects of Liquid Metal Solutions on Brittle- Ductile Transitions	147
7. SUMMARY.	153
8. SUGGESTIONS FOR FUTURE WORK	155
REFERENCES	159

FIGURES

		Page
Figure 1	Stress-strain curves for (a) unamalgamated and (b) amalgamated zinc monocrystals at room temperature. $\chi_0 = 48^\circ$ (after Likhtman and Shchukin ¹).	3
Figure 2	Illustrating (schematic) displacement of atoms at the tip of a crack. The bond A-A ₀ constitutes the crack tip and B is liquid metal atom.	15
Figure 3	Schematic potential energy, U(a) and U(a) _B , and resulting stress, $\sigma(a)$ and $\sigma(a)_B$, versus separation distance curves for bonds of type A-A ₀ (Fig. 2) in the absence and presence of chemisorbed atom B. For spontaneous chemisorption of B, $a_c = a_0$. For strain-activated chemisorption, $a_c > a_0$ (after Westwood and Kamdar ⁴).	16
Figure 4	Effects of temperature and liquid mercury environment on the cleavage crack propagation energy, ϕ_p , for the (0001) planes of zinc. The inset shows the formula and type of specimens used to determine ϕ_p (after Westwood and Kamdar ⁴).	22
Figure 5	A comparison of the fracture energy involved in the propagation of a plastically blunted cleavage crack in air, $\phi_{p,Zn}$, and in mercury, $\phi_{p,Zn-Hg}$, from a double propagation experiments. A line of slope 0.61 is drawn through the data (after Westwood and Kamdar ⁴).	25
Figure 6	Schematic illustration of an "equilibrium" crack in a solid, subjected to an increasing force F. The Bond A-A ₀ constitutes the crack tip. B is a surface active liquid metal atom.	32
Figure 7	Demonstrating cleavage of cadmium monocrystals at 25°C following coating with mercury - 60 at.pct indium solution (after Kamdar and Westwood ¹⁰⁸ and Kamdar ¹⁰).	36
Figure 8	Orientation dependence of shear strain at fracture for (a) amalgamated 1mm dia. zinc monocrystals (after Shchukin et al. ⁷¹) (b) uncoated or partially amalgamated 6mm square zinc monocrystals (Kamdar and Westwood ⁹).	43
Figure 9	The cleavage step pattern reveals that failure of this amalgamated zinc monocrystal was initiated at one of the dislocation walls which constitute the boundaries of the kink band K. Twins are visible at T (after Kamdar and Westwood ⁹).	44
Figure 10	Illustrating the formation of cleavage cracks at kink bands in amalgamated zinc monocrystals $\chi_0 = 25^\circ$. The kink band is denoted by arrows in (b) (after Kamdar and Westwood ⁹).	45

FIGURES (Cont'd)

Page

- Figure 11 Orientation dependence of the normal stress, σ_{NF} , and shear stress, τ_F , at fracture for Type 1 asymmetric zinc bicrystals in the partially amalgamated condition. For comparison, the theoretically constructed curves correspond to Eqs. (22) (solid lines - Likhtman-Shchukin or Kamdar-Westwood criteria) or Eqs. (24), (dashed lines) when $K_1=K_2=178 \text{ gm/mm}^2$ and $K=148 \text{ gm/mm}^2$ (after Kamdar and Westwood⁹). 52
- Figure 12 Same data as Fig. 11. The solid lines, B, correspond to Eqs. (18) (Bullough's⁶² analysis); the dashed lines, S, to Eqs. (23) (Stroh's⁶¹ analysis), and the other line, S-B, to Eq. (20) (Smith-Barnby's⁶⁵ analysis) when $K_3=K_5=178 \text{ gm/mm}^2$ and $K_4=359 \text{ gm/mm}^2$ (after Kamdar and Westwood⁹). 53
- Figure 13 Orientation dependence of (a) the strain at fracture, and (b) the product of the normal stress, σ_{NF} , shear stress, τ_F , and slip plane length, L_F , at fracture for asymmetric zinc bicrystals grown by the seeding technique, and tested in the partially amalgamated condition (after Kamdar and Westwood⁹). 56
- Figure 14 Effect of solute content on the room temperature fracture stress, σ_F , of polycrystalline zinc in liquid mercury. The grain diameter of the zinc was $\sim 1 \text{ mm}$, and its engineering flow stress $\sim 1.9 \text{ kg/mm}^2$. The strain rate was 4×10^{-5} per sec. (b). Variation of critical resolved shear stress, τ_C , with solute content for zinc monocrystals. Range of values for asymmetric bicrystals of Zn-0.05 at. % Cu and Zn-0.2 at. % Cu are given by bars (after Kamdar and Westwood⁵⁴). 57
- Figure 15 Orientation dependence of (a) the shear strain at failure, ϵ_F , and (b) the energy to initiate cleavage failure on the basal plane, ϕ_I , for asymmetric bicrystal of Zn-0.2 at. % Cu in the partially amalgamated condition at 298°K (after Kamdar and Westwood⁴). 60
- Figure 16 Illustrating linear relationship between the product $[(\tau_F - \tau_C)\sigma_{NF}]^{1/2}$ and $(L_F)^{-1/2}$ for partially amalgamated asymmetric bicrystals of zinc and its alloys tested in tension at 298°K. The correlation shown is equivalent to the Petch fracture stress-grain size relationship (after Kamdar and Westwood^{54,9}). 61
- Figure 17 Illustrating the variation of the energy to initiate basal cracks in zinc monocrystals at 77°K with χ_0 and crystal diameter (after Kamdar^{69,72}). 65

FIGURES (Cont'd)

Page

- Figure 18 Illustrating linear relationship between the product $[(\tau_F - \tau_C)\sigma_{NF}]^{1/2}$ and $(L_F)^{-1/2}$ for zinc monocrystals of 1mm and 6mm dia. tested in tension at 77°K. The correlation shown is equivalent to Petch fracture-stress grain size relationship when L_F varied from 6.02 to 14mm (after Kamdar⁷²). 66
- Figure 19 Orientation dependence of i) the shear strain at fracture, ϵ_F , Fig. 19(a) and ii) the energy to initiate cleavage fracture on the basal plane, ϕ_I , for asymmetric bicrystals of zinc, Fig. 19(b) in liquid mercury at 298°K (after Kamdar⁶⁹). 67
- Figure 20 Summary of experimental results on fracture of polycrystals (after Gilman⁵⁹). 74
- Figure 21 Variation of the flow stress of amalgamated zinc polycrystalline specimens, $\sigma_{f,Zn}$, and fracture stress of amalgamated zinc specimens, $\sigma_{F,Zn-Hg}$, with grain size at 298°K (after Westwood⁸²). 76
- Figure 22 Dependence of strain at fracture on temperature for (a) unamalgamated, and (b) amalgamated zinc monocrystals of ~1mm diameter (after Rozhanskii et al.⁴¹). 79
- Figure 23 Fracture stress of annealed specimen of aluminum in mercury -3% zinc solution as a function of temperature and three grain sizes (after Ichinose⁸⁰). 81
- Figure 24 Correlation between brittle to ductile transition temperature for amalgamated 70-30 brass specimens and log of the grain diameter (after Nichols and Rostoker⁸⁴). 83
- Figure 25 Temperature and strain rates at which titanium -55A was tested in liquid cadmium. The attached numbers give the elongation at fracture for each test. The line separates the region of ductile behavior from the region of brittle behavior (after Robertson¹⁶). 84
- Figure 26 Variation of crack propagation rate with temperature for amalgamated polycrystalline brass or aluminum alloy specimens (after Rhines et al.⁸⁵). 87
- Figure 27 The effect of yield stress, σ_y , on the ratio of fracture stress, σ_F , to yield stress in copper base alloy tested in mercury at 298°K (after Rosenberg and Cadoff⁴⁸). 94
- Figure 28 Embrittlement of copper base alloys as a function of (a) stacking fault energy (after Stoloff et al.³⁹), and (b) electron/atom ratio (after Westwood et al.⁷). 95

FIGURES (Cont'd)

	<u>Page</u>
Figure 29 Illustrating the absence of the effect of environment on the yield stress and strain hardening rate on various iron-aluminum alloys tested in mercury-indium solutions (after Stoloff et al. ³⁹).	98
Figure 30 Illustrating the effects of aluminum additions to iron on its susceptibility to embrittlement in mercury and mercury-indium solution (after Stoloff et al. ³⁹).	99
Figure 31 Illustrating the effects of nickel additions to iron on the susceptibility (reduction in area, RA) of smooth tensile specimens tested in liquid mercury environments (after Hayden et al. ⁵³).	100
Figure 32 Fracture toughness parameter, G_C of doubly notched annealed specimens broken in mercury versus nickel content (after Hayden et al. ⁵³).	102
Figure 33 Correlation for aluminum alloys between (dark circles) fracture strength in air and in (Hg + 3% Zn) amalgam, and (open circle) yield strength in air and elongation at failure in (Hg + 3% Zn) amalgam (after Rostoker et al. ¹⁰⁰).	104
Figure 34 Variation with grain size of effects of prestrain in air on fracture stress of 70-30 brass in liquid mercury at 25°C (after Rosenberg and Cadoff ⁴⁸).	106
Figure 35 Effects of grain size and prestrain on fracture stress of amalgamated Al 5083 alloy specimens. Note that the data from prestrained specimens do not conform to a Petch relationship (after Roscoker ¹⁰⁰).	107
Figure 36 Influence of prestrain on fracture stress of amalgamated polycrystalline Al 2024 alloy specimens in aged condition (100°C for 30 min.) (after Nichols and Rostoker ¹⁰⁰).	108
Figure 37 Variation of time to failure with applied stress for zinc at room temperature. Curves (a) and (b) for un-amalgamated and amalgamated monocrystals ($\chi_0 = 50^\circ$, ~1mm dia.), respectively; curves (c) and (d) for un-amalgamated and amalgamated polycrystals, respectively (after Bryukhanova et al. ⁴²).	111
Figure 38 Strain rate dependence of the shear strain at fracture for (i) lower curve, 1mm dia. zinc monocrystals coated with Ga (after Shchukin et al. ¹⁰⁷). Note "plasticizing" effect at low strain rates. (ii) upper curves, 6mm square zinc monocrystals partially coated with Ga (black circles) or uncoated (open circles) (Kamdar and Westwood ⁹).	113

FIGURES (Cont'd)

	<u>Page</u>
Figure 39 Variation in ductility of polycrystalline cadmium specimens with indium content of mercury-indium surface coatings at 298°K (after Kamdar ¹⁰ and Kamdar and Westwood ¹⁰⁸).	123
Figure 40 Embrittlement of polycrystalline pure aluminum by various mercury solutions. Note apparent correlation between Pauling electronegativity of solute element and severity of embrittlement (Westwood et al. ⁷).	130
Figure 41 The variation of fracture stress of silver and cadmium with composition of the mercury indium environment (after Preece and Westwood ⁴³).	132
Figure 42 Fracture stress of polycrystalline aluminum or 70-30 brass as a function of time of exposure to liquid mercury prior to testing in this environment (after Ichinose ³).	136
Figure 43 Fracture strength of polycrystalline zinc as function of (i) time of exposure to mercury environment prior to testing in this environment (ii) ratio, C_o , of mass of Hg on the surface to mass of the specimen. Values of C_o are: a - 3×10^{-4} ; b - 7×10^{-4} ; c - 2×10^{-3} ; d - 3×10^{-3} ; e - 7×10^{-3} ; f - 1×10^{-2} (after Flegontova et al. ¹¹⁸).	137
Figure 44 Delayed failure of copper -2% beryllium alloy at room temperature wetted with mercury -2% sodium amalgam. The alloy was initially aged for one hour at 700°F (yield stress ~150000 psi) (after Rinovetore et al. ¹²⁰).	140
Figure 45 Effects of applied stress and (Hg-In) environments on the time to failure of statically loaded polycrystalline cadmium at room temperature. (Grain diam. = 1.0mm.) Note that for indium concentrations of more than ~7 a/o, severity of embrittlement increases with indium concentration (after Preece and Westwood ⁴³).	145
Figure 46 Influence of mercury, gallium or mercury-gallium environments on the strain at fracture of aluminum (grain diam \approx 1mm) as a function of temperature (after Preece and Westwood ¹²²).	148
Figure 47 Effects of gallium concentration of (Hg-Ga) environments on (a) fracture stress at -20°C and (b) transition temperatures, T_C for aluminum. Values of T_C were derived from the data of Fig. 46 (after Preece and Westwood ¹²²).	150

TABLES

	<u>Page</u>
Table 1 Examples of Transgranular and Intergranular Failure	2
Table 2 Occurrence of Embrittlement	7
Table 3 Values of ratios of σ/τ for some typical solid metals which are embrittled by liquid metals	33
Table 4 Summary of Test Data on Amalgamated Asymmetric Zinc Bicrystals	55
Table 5 Effects of Minor Solute Additions to Embrittling Liquid on Susceptibility of a Solid to Liquid Metal Embrittlement, (after Stoloff ¹¹ and Westwood et al. ⁷).	119
Table 6 Effects of Several Liquid Metal Environments on the Tensile Fracture Behavior of Polycrystalline Cadmium (after Kamdar and Westwood ¹⁰⁸ and Kamdar ¹⁰).	125
Table 7 Effects of Mercury and Mercury Solutions on the Tensile Fracture Load of Polycrystalline 2024-T3 Aluminum Alloy Specimens at Room Temperature, Data from Rostoker et al. ²	127
Table 8 Fracture Date for Polycrystalline Zinc Specimens Coated with Mercury or Gallium and Tested in Tension at 30°C (after Kamdar and Westwood ^{9,4}).	127
Table 9 Effects of Bismuth and Bismuth Solutions on the Tensile Fracture Stress of Polycrystalline Copper at 345°C. Data from Kraai et al. ⁴⁹ .	128

I. INTRODUCTION

When an oxide-free solid metal is coated with a thin film of a liquid metal only a few microns in thickness and then immediately deformed in tension, its yield and flow behavior are not significantly affected. Its fracture behavior, however, can be markedly different from that observed in air. In many instances a reduction in fracture stress or strain results, Figure 1, the magnitude of which is dependent on various chemical and mechanical parameters of the solid metal-liquid metal system. Under certain experimental conditions, embrittlement can be quite dramatic; specimens stressed above some critical value appear to fail "instantly" on wetting or contacting with an appropriate liquid metal. The polycrystalline metals usually fail by an intergranular mode in liquid metal environments. However, it is also possible to cleave monocrystals of otherwise ductile metals such as cadmium in certain liquid metal environments (See Table 1 and Figure 7). Also, brittle crack propagation rates of order 50-500 cm per sec. have been reported for ductile aluminum alloys in liquid mercury environments. Such effects occur only in specific solid metal-liquid metal couples and belong to the class of environment-sensitive fracture phenomena known as liquid-metal embrittlement.

Embrittlement by liquid metals can also occur in the absence or the presence of stress, by corrosion or by diffusion controlled intergranular penetration processes. Such time and temperature dependent processes, however, are not considered responsible for the occurrence of liquid metal embrittlement. For example, in most cases of liquid metal embrittlement, little or no penetration of liquid metal into the solid metal has been

Table 1

Examples of Transgranular Failure

<u>Solid</u>	<u>Liquids</u>
Cd	Ga, Cs, In
Zn	Ga, Hg, In
Al	Ga
Al-Cu	Hg
Fe-Si	Li, Hg, Hg-In, Ga
Cu-4% Ag (aged)	Hg

Examples of Intergranular Failure

Cu-4% Ag (quenched)	Hg
Cu and alpha Brass	Hg, Bi, Li
Ni	Li
Pd	Li
Al	Hg, Ga
Fe	Hg, Hg-In
Ag	Hg, Ga

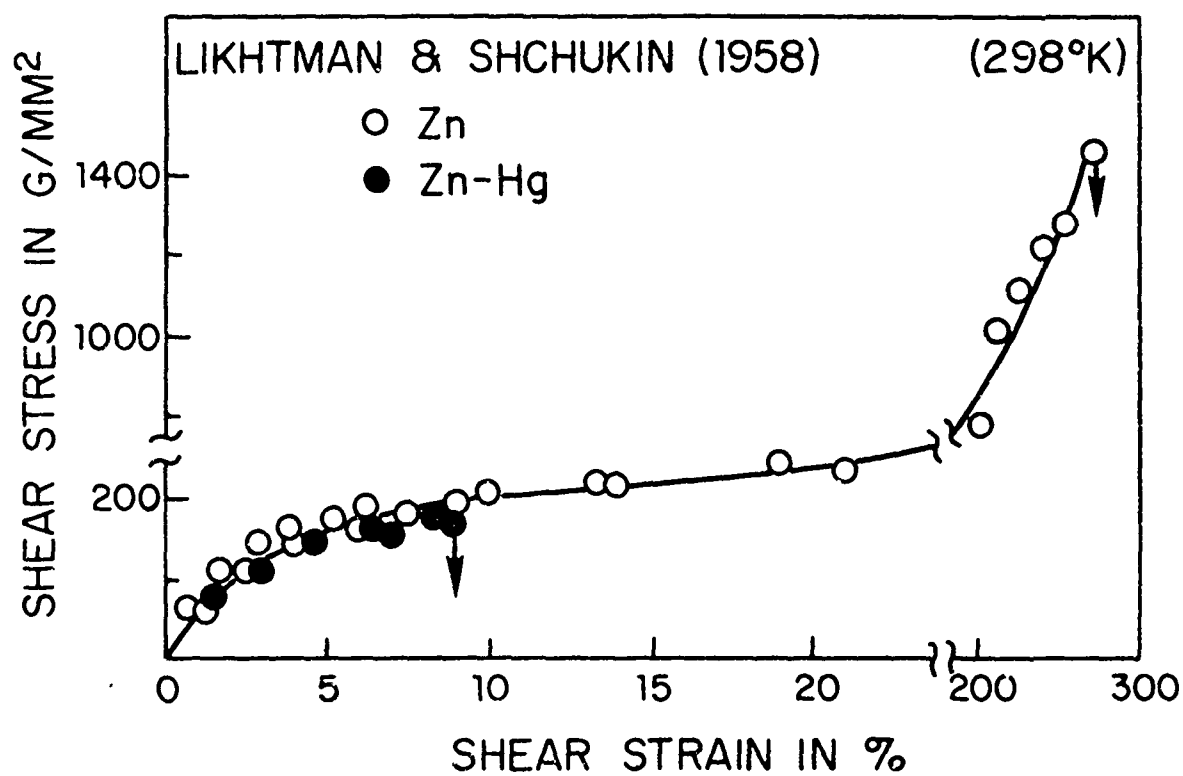


Figure 1. Stress-strain curves for (a) unamalgamated and (b) amalgamated zinc monocrystals at room temperature. $\chi_0 = 48^\circ$ (after Likhtman and Shchukin¹).

observed.² The tensile fracture stress of the solid metal coated with the liquid metal does not depend upon the time of exposure to the embrittling liquid metal prior to testing,³ or upon whether the liquid metal is pure or presaturated with the solid metal. Severe embrittlement of the solid metal occurs near the freezing temperatures of the liquid metal environments.⁴ The presence of a grain boundary is not a prerequisite for the occurrence of embrittlement, since monocrystals of ductile metals such as zinc⁵ and cadmium^{5,6} are known to fracture by cleavage in liquid gallium and other liquid metal environments. Accordingly, this paper will not be concerned with embrittlement effects by liquid metals which are caused by corrosion or diffusion controlled processes, it will instead concentrate on those examples of liquid metal embrittlement of a solid metal presently considered to result from liquid metal adsorption induced brittle fracture.

Two reviews of liquid metal embrittlement have appeared, one by Rostoker et al.,² in 1960 and the other by Lichtman et al.,⁵ in 1962. The former is an excellent book which deals extensively with various aspects of the liquid metal embrittlement of useful industrial alloys. The later review reports work performed in the Soviet Union and is particularly concerned with the embrittlement of zinc monocrystals and other metals in various liquid metal environments. A recent review by Westwood et al.⁷ summarizes the work performed prior to 1967. Subsequent to the writing of these reviews, many investigations of liquid metal embrittlement have appeared in the literature. These investigations have utilized model well characterized embrittlement systems, (e.g. embrittlement of mono and bi-crystals by liquid metals, such as zinc in liquid mercury and gallium), and

they have studied the effects of one variable at a time under controlled experimental conditions. This approach has resulted in a significantly better understanding of the phenomenon of liquid metal embrittlement.

It is considered that embrittlement results from a liquid metal chemisorption-induced reduction in the strength of atomic bonds at the regions of stress concentrations in a solid metal such as at the tip of a crack^{4,8} or at the head of a dislocation pile up near an obstacle in the surface of the solid.⁹ Embrittlement in liquid metal environments may be considered as a special case of brittle fracture, and that the effects of mechanical, metallurgical, physical and chemical factors on embrittlement may be explained rationally in terms of the principles of brittle fracture.⁹ The important problem of the specificity of liquid metal embrittlement, i.e., only a certain liquid metal embrittles a certain solid metal still remains primarily unsolved. Nevertheless, experiments with simple well characterized embrittlement couples and the development of the concept of the "Inert-carrier," i.e., embrittling species being dissolved in a nonembrittling liquid carrier metal have provided fracture data which indicate an interesting correlation between the severity of embrittlement and the electronegativities of the participating solid and the liquid metal.^{7,10} The purpose of this paper is to document advances made in the understanding of the phenomenon of liquid metal embrittlement and also to discuss these by considering embrittlement as a special case of brittle fracture and in terms of the prevalent "adsorption-induced reduction in cohesion" mechanism of embrittlement.^{4,8,9}

2. OCCURANCE OF LIQUID METAL EMBRITTLEMENT

2.1 Embrittlement by Liquid Metals

One of the most intriguing aspects of liquid metal embrittlement is its apparent specificity. It is often stated that only certain liquid metals embrittle certain solid metals (Table 2). For example, liquid gallium embrittles aluminum but not magnesium; liquid mercury embrittles zinc

Table 2

Occurrence of Embrittlement

(After Rostoker, et al.² and Stoloff, N.S.¹¹)

	Hg	Ga	Cd	Zn	Sn	Pb	Bi	Li	Na	Cs	In
Aluminum	x	x		x	x				x		x
Bismuth	x										
Cadmium		x			x					x	x
Copper	x						x	x	x		x
Iron	x	x	x	x				x			x
Magnesium				x					x		
Silver	x	x									
Tin	x	x									
Titanium	x		x								
Zinc	x	x			x	x					

x denotes occurrence of embrittlement.

but not cadmium. An inspection of the equilibrium phase diagrams of most known embrittlement couples has revealed following empirical rules which permits one to guess possible embrittlement systems:^{2,5} (1) If two metals involved form stable high melting point intermetallic compounds in the solid state, then it is unlikely that they will constitute an embrittlement couple, (2) embrittlement rarely occurs in systems in which the two metals exhibit

Preceding page blank

significant mutual solubility. It is not known, however, whether limited mutual solubility represents a genuine chemical prerequisite. It could be related merely to the difficulty of propagating a brittle crack in a solvent environment because dissolution processes will tend to blunt the crack. Such effects are called "Joiffe Effects" and have been observed in brittle ionic crystals tested in a solvent environment. Alternatively, embrittlement may not be observed in a possible embrittlement couple because the solid is quite ductile at or near the freezing temperature of the liquid such that a brittle crack cannot be initiated or propagated in the solid. For example, consideration of the empirical rules suggests that solid cadmium (m.p. 329°C) may be embrittled by liquid indium (m.p. 165°C). However cadmium is quite ductile at the melting temperature of indium and hence embrittlement is not observed in this couple. It is sometimes stated that a very limited amount of solubility of a liquid metal in a solid metal is required to facilitate "wetting".^{2,12} On the other hand embrittlement occasionally occurs in systems in which two component metals are so mutually incompatible in the equilibrium state that they form immiscible liquids on melting (e.g. cadmium in liquid gallium and iron in liquid cadmium). Nevertheless, the liquid must be in intimate contact with the surface of the solid* to initiate

*One of the most critical conditions which must be achieved to obtain embrittlement is good intimate contact between the surface of the solid and the liquid phase. For this purpose, first the surface of the solid should be cleaned by chemical, ultrasonic or some such means to remove the thin oxide film which invariably intervenes between the solid substrate and the liquid phase. Secondly, if the pure liquid metal does not spread readily on the solid substrate, then small additions of certain elements may be made to the liquid phase which are known to promote good wetting and spreading of the liquid without affecting the embrittling effects of the base liquid metal. The specific details of cleaning and wetting techniques differ for various embrittlement couples and are described in greater detail elsewhere.² In addition to good wetting, some measure of plastic flow, tensile stress and a barrier to plastic flow in the surface of the solid at some point of contact with the liquid are also required for the occurrence of embrittlement in a solid by liquid metal. Besides these initial conditions, factors that induce brittle behavior in a solid such as the presence of a stress raiser or a sharp notch, increase in strain rate, large grain size, alloying additions, microstructure of the solid and test temperature are known to promote or increase the susceptibility of a solid to embrittlement by a liquid metal or liquid metal solutions.

embrittlement and subsequently be present at the tip of the crack to cause failure. Liquid usually spreads quite readily on a clean metal surface such as the fracture surfaces of the solid. Thus, although absence of mutual solubility between the solid and the liquid metal suggests no chemical affinity apparently some measure of affinity or chemical interaction must exist between the solid and the liquid metal. It is possible that stress or lattice strain plays a role in inducing chemisorption in such systems.⁴

Furthermore, the importance of chemical interactions in the embrittlement process is also suggested by the observation that the severity of embrittlement of a solid is related to the chemical nature of the embrittling species (Table 2). For example, zinc is more severely embrittled by liquid gallium than by liquid mercury.¹⁰ Attempts have been made to relate the severity of embrittlement of a solid by various liquid metals with the relative position of the liquid metals in the electromotive force series, with atomic diameters of the liquid metal atoms, and with the dihedral contact angle that the liquid makes with the surface of a solid. None of these parameters have been found to provide a satisfactory correlation with the occurrence or the severity of embrittlement of a solid by liquid metals.¹³ Thus, neither the fundamental factors which determine whether or not a given liquid metal will embrittle a particular solid metal, nor the severity of embrittlement that will be induced are clearly understood.

2.2 Embrittlement by Vapor Phase

A relatively new phenomenon of embrittlement has been observed in which when two solid metals are in intimate contact with each other, presumably the vapor phase of the solid metal with the lower melting temperature

causes severe embrittlement of the other solid. Specific examples are the embrittlement by solid cadmium of titanium¹⁴ and steel alloys.¹⁵ The fracture mode in a tension test changes from ductile in air to brittle intergranular or transgranular cleavage in the presence of solid cadmium. A rapid change from no embrittlement to maximum embrittlement occurs as the strength level of the alloys is increased. Furthermore, the susceptibility to embrittlement increases with an increase in temperature (below the m.p. of the embrittling solid). An investigation with a microprobe revealed that the embrittling phase namely, cadmium was present at the crack tip located within the bulk of the embrittled solid. This indicates that embrittlement is caused by the vapor phase and is limited by the surface diffusion to the crack tip of the cadmium vapor. It should be noted that both steel and titanium alloys are known to be severely embrittled by liquid cadmium^{2,16} (See Table 2). This and the above observations suggest that the phenomenon of embrittlement of steel and titanium alloys by solid cadmium is similar to the embrittlement of these alloys by liquid cadmium and occurs by the same "adsorption-induced reduction in cohesion" mechanism of liquid metal embrittlement.^{4,8,9} The principal difference is that embrittlement by vapor phase is temperature dependent whereas embrittlement by the liquid phase is relatively temperature insensitive.

Another example of embrittlement occurring below the freezing temperature of the embrittling liquid metal is the iron-liquid lead couple. In this case, steels containing 0.3 w/o lead in the matrix becomes embrittled at temperatures 200°F below the freezing temperature of lead.²³ It is suggested that this constitutes evidence for the embrittlement of steels by

lead vapor. While this is possible, it is also conceivable that impurities in the steel may lower the melting temperature of lead. Thus, the low temperature embrittlement of steels may be caused by impure liquid lead rather than by the lead vapor. For example, when solid zinc is in contact with solid gallium (m.p. 30°C), impure liquid gallium appears at the interface at temperatures below the melting temperature of gallium with the consequence that zinc is severely embrittled by impure liquid gallium at 20°C . The embrittlement by vapor phase and the mechanism of embrittlement could be better evaluated if one investigates crack propagation in these metals in the presence of the vapor phase.

Embrittlement of steel by gaseous hydrogen is a well-known example of embrittlement of a solid metal by a gaseous phase. The hydrogen embrittlement of steel may also occur by the "adsorption-induced reduction in cohesion" mechanism proposed for liquid metal embrittlement. In this case, however, the embrittlement process could be controlled either by the rate of diffusion of hydrogen to the crack tip or by the rate of reaction of hydrogen at the crack tip. The embrittlement of a solid metal in liquid metal or gaseous or vapor phase environment may be considered to occur by the "adsorption-induced reduction in cohesion" mechanism which will be described in greater detail in the next section. The embrittlement may be a temperature sensitive time dependent reaction rate controlled or a temperature insensitive process depending upon the specific embrittlement system under consideration. In this regard, a systematic study of the embrittlement of titanium or steel in liquid cadmium and cadmium vapor environments with temperature would be most interesting.

3. MECHANISMS OF LIQUID METAL EMBRITTLEMENT

3.1 Reduction in Surface Energy Model

Several workers have proposed that liquid metal embrittlement is associated with a reduction in the surface free energy of the solid metal by the adsorbing liquid metal species.^{1,2,17,5} This is obvious since embrittlement effects must originate at the solid-liquid metal interface and hence energy considerations of the interface must be important. It is unlikely, however, that effects of adsorptions and associated energy considerations which are short range in nature will be important at depths greater than a few atomic layers below the surface of the solid. Therefore it is by no means clear how reductions in the energy of few surface atomic layers of the solid will cause catastrophic embrittlement to occur through the bulk of the solid. Moreover, experimentally determined values of total energy involved in crack propagation, ϕ_p , are frequently several orders of magnitude^{18,19} greater than the surface energy of the solid. The above hypothesis does not suggest any manner by which ϕ_p (i.e. plastic contribution) can be reduced, so that brittle crack propagation may be accomplished in a liquid metal environment. In other words, such a thermodynamic approach is not particularly informative because it does not provide insights into the mechanism of embrittlement on an atomic or electronic scale.

3.2 Adsorption-Induced Reduction in Cohesion Model

In view of the limitation of the above approach, it is suggested that one should focus attention at the crack tip and consider the effects of the

adsorption of the liquid metal species at or in the vicinity of the tip before attempting to understand the mechanism of the embrittlement process.⁷ In this regard, it has been suggested that embrittlement is associated with a localized reduction in the strength of atomic bonds at the crack tip or at the surface of the solid metal by certain chemisorbed species.^{4,8} With this possibility in mind, consider the crack shown in Figure 2. Crack propagation will occur by repeatedly breaking of bonds of the type A-A₀, A-A₁, etc. Such bonds might be expected to have potential energy-separation distance curves of the form U(a) indicated in Figure 3, a₀ being the equilibrium distance between atoms across the fracture plane. The resulting stress, σ, between atoms A and A₀ as they are separated, varies as (dU/da) from σ = 0 at a = a₀, to a maximum value of σ = σ_m at the point of inflection U₁ of the curve U(a). It follows that a tensile stress of magnitude σ_m acting at the crack tip would cause the bond A-A₀ to break. Assuming that the actual σ(a) curve can be approximated by one-half of a sine curve, and that its half wavelength, λ, represents the effective range of the interatomic forces, it can be shown that²⁰

$$\sigma_m = (E\lambda/\pi a_0) . \quad (1)$$

If the work done in breaking A-A₀ bonds is then equated to the surface free energy of the subsequently created fracture surfaces, γ, it can also be shown that²⁰

$$\sigma_m = (E\gamma/a_0)^{1/2} . \quad (2)$$

Next assume that the liquid metal atom B* at the crack tip reduces the strength of the bond A-A₀. The chemisorption reaction presumably

* A vapor phase or an elemental gas such as atomic or molecular hydrogen may also provide the embrittling atom B.

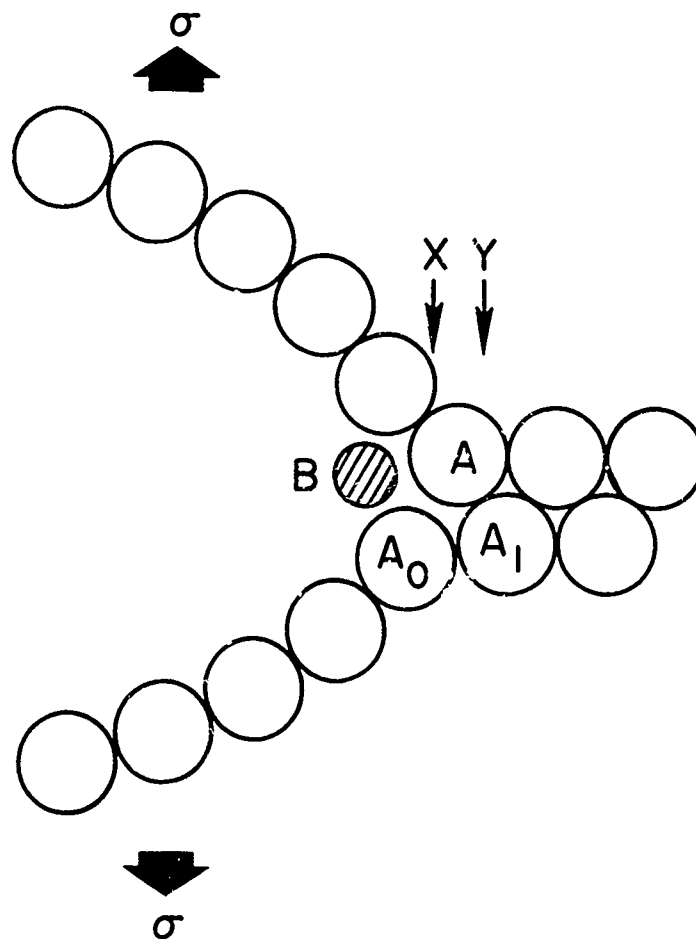


Figure 2. Illustrating (schematic) displacement of atoms at the tip of a crack. The bond $A-A_0$ constitutes the crack tip and B is a liquid metal atom.

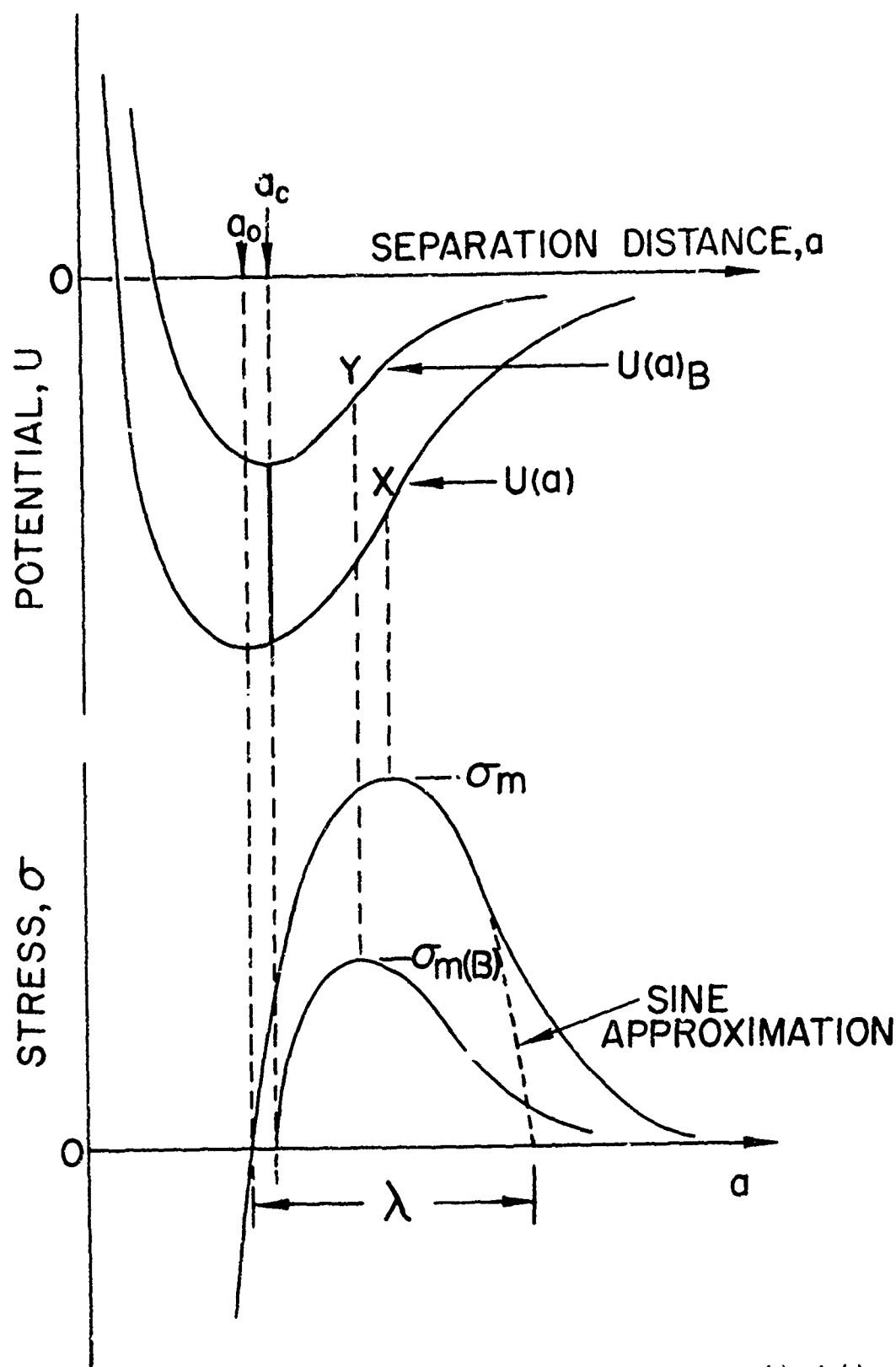


Figure 3. Schematic potential energy, $U(a)$ and $U(a)_B$, and resulting stress, $\sigma(a)$ and $\sigma(a)_B$, versus separation distance curves for bonds of type A-A₀ (Fig. 2) in the absence and presence of chemisorbed atom B. For spontaneous chemisorption of B, $a_c = a_0$. For strain-activated chemisorption, $a_c > a_0$ (after Westwood and Kamdar⁴).

involved in such a process may occur spontaneously (i.e. in time less than that required in a mechanical test), or only after atoms A and A_0 have been strained to some critical separation distance, a_c . In any event, as a result of the electronic rearrangement involved in this process the bond A- A_0 becomes inherently weaker, and thus the form and displacement of its potential energy-separation curve may now be considered similar to $U(a)_B$, Figure 3. As the applied stress is increased, the stress acting on bond A- A_0 eventually exceeds its now reduced breaking stress, $\sigma_m(B)$, the bond breaks, the crack propagates to Y, Figure 2, and atom B becomes stably chemisorbed on the freshly created surface. This procedure is then repeated until the specimen fails. The cracking process is limited by the arrival of liquid metal atoms at the crack tip and it is assumed that liquid is able to keep up with the propagating crack tip.

According to this hypothesis, crack initiation at the surface will also be facilitated by the adsorption of liquid metal B atoms. Moreover, if chemisorption is strain-activated, it will occur preferentially at sites of stress concentration, such as in the vicinity of piled-up groups of dislocations at high angle grain boundaries.

Theoretical studies of the interactions between single adsorbed atoms and metal surfaces,^{21,22} and experimental investigations of the nature of the bonding (i.e. ionic, covalent, etc.) between adsorbed alkali metals and such refractory metals as tungsten,²⁴ are now being undertaken. Unfortunately, however, these studies are not yet sufficiently advanced to provide predictions of specific embrittlement behavior. An alternative left is to devise experimental techniques to determine the bond strength at the

crack tip of the solid in the presence of adsorbed liquid metal species. Ideally, the experimental technique should be capable of detecting any adsorption-induced variation in electron distribution in the surface bonds which may lead to weakening without applying a stress; but since any such effect would be confined to the immediate surface layer of atoms, it would not be readily observed in studies involving some variation in the physical properties of the specimen as a whole. Recent studies of variations in electrical conductance, ferromagnetic moment and ferromagnetic anisotropy of W, Fe and Ni with chemisorption of oxygen, carbon monoxide and nitrogen have nevertheless been interpreted as indicating that these species weaken the binding of the metal surface atoms.²⁵ It is possible, therefore, that these or similar techniques could be applied advantageously to the problem of liquid-metal embrittlement in certain systems.

An alternative approach is first to determine the true fracture surface energy for the cleavage plane of a particular solid metal, γ , which is directly related to σ ($\sigma = \sigma_m$ in Equation (2)), and then show that γ is reduced in the presence of an active liquid metal. With this in mind, consider the propagation of a semielliptical crack of length c in a thin plate under the action of tensile stress σ_a acting perpendicular to the length of the crack.^{26,27} The maximum tensile stress acting at the crack tip, σ_c , is

$$\sigma_c = 2\sigma_a (c/R)^{1/2} \quad (3)$$

where R is the radius of curvature at the tip. The minimum radius of curvature having physical significance is given by $R = a_o$.²⁸ For such an

'atomically sharp' crack to propagate, σ_c must exceed σ_m (Equation (2) and Figure 3), and the applied stress necessary to achieve this, $\sigma_a = \sigma_p$, from Equations (2) and (3) is

$$\sigma_p = (E\gamma/4c)^{1/2} . \quad (4)$$

In practice, most cracks are not atomically sharp, but are blunted by plastic relaxation in the vicinity of the crack tip. Thus the radius of curvature at the tip becomes increased from $R = a_0$ to some larger value, $R = R_1$. Nevertheless, to propagate a plastically blunted crack the stress acting on the bond A-A₀ at the tip must exceed σ_m . Now, if $R_1/a_0 = \rho$, then from Equations (3) and (4) it can be shown that

$$\sigma_p(\text{blunted crack}) = (E\rho\gamma/4c)^{1/2} . \quad (5)$$

In other words, the energy ϕ_p involved in propagating a blunted crack is simply $(\rho\gamma)$, where ρ is a dimensionless, variable ratio (R_1/a_0) dependent upon the amount of plastic relaxation at the crack tip, and therefore upon temperature, propagation rate, yield stress, metallurgical composition and structure, etc.

Note that this analysis^{*} suggests that the crack propagation energy, ϕ_p , is related directly to the surface free energy, γ , and should not be thought of as the sum of the surface free energy plus a plastic relaxation energy term, p . It will be appreciated that if ϕ_p is equated to $(\gamma + p)$, and $p \gg \gamma$ - as is ordinarily the case for ductile metals - it is difficult to see how the magnitude of ϕ_p could be significantly affected by the testing environment.

^{*} Also presented by Gilman²⁰ and Stoloff and Johnston.⁸

Consider next the situation depicted in Figure 2. It will be noted that to propagate the crack from X to Y under a reduced stress, because of the presence of embrittling liquid-metal atom B, it is only necessary that the strength of the bond A-A₀ be affected. In other words, the embrittling action of B is independent of the radius of the crack tip. This possibility leads to the suggestion that it might be useful to define a coefficient of embrittlement for crack propagation, η_p , relating the energy adsorbed in breaking bonds at the crack tip in the presence and absence of an embrittling phase. A convenient definition is

$$\eta_p = \phi_{pA(B)} / \phi_{pA}, \quad \rho = 1 = \gamma_{A(B)} / \gamma_A \quad (6)$$

The total energy involved in the propagation of a crack in a metal, ϕ_p , can then be written as:

$$\phi_p = (\eta \rho \gamma) \quad (7)$$

where η and ρ are simple and independent ratios, η being an environmental variable, and ρ a plastic relaxation variable.

Equations (6) and (7) suggest that embrittlement may occur by "liquid-metal adsorption-induced reduction in cohesion mechanism" if the coefficient of embrittlement, η_p , determined for both atomically sharp and plastically blunted cracks is less than unity, i.e. $\gamma_{A(B)} < \gamma_A$, or $\phi_{pA(B)} < \phi_{pA}$.

A double cantilever cleavage technique has been used by Gilman²⁹ and others^{4,30} to introduce cleavage cracks in crystals and to determine the energy to propagate cracks on the cleavage plane of ionic monocrystals, CaCo₃, KCl, LiF, MgO, etc., covalent monocrystals namely germanium and silicon and metallic monocrystals such as zinc⁴ and beryllium.³¹ For these

crystals, the experimentally determined values of ϕ_p are in good agreement with the values of the cleavage surface energies derived from theoretical considerations.³² This experimental technique therefore provides a possible method for determining cleavage surface energies of metal single crystals when the liquid metal environment is present at the crack tip. Accordingly, Westwood and Kamdar have used this technique to examine the validity of the above approach by studying cleavage crack propagation on the basal plane of zinc monocrystals in liquid mercury, liquid gallium and inert environments.

3.3 Crack Propagation in the Zinc-Mercury and Zinc-Gallium System

3.3.1 Determination of Cleavage Fracture Energies

Westwood and Kamdar⁴ used the double cantilever cleavage technique to determine values of ϕ_p for zinc from liquid nitrogen temperature to 60°C, and for the zinc-liquid mercury embrittlement couple from the melting point of mercury, -39°C, to 60°C. A diagram of the type of specimens used is included in the inset in Figure 4. Following Gilman,²⁹ the cleavage fracture energy, ϕ_p , was computed from the relationship

$$\phi_p = (6F^2L_o^2/Ewt^3) \quad (8)$$

where F is the load to propagate a pre-existing crack of length L_o (introduced at -196°C), and w and t are the specimen dimensions designated in the figure. The results are presented in Figure 4. It can be seen that the value of ϕ_p for zinc, 90 ± 10 ergs/cm², is essentially independent of temperature. This value is in fair agreement with that of ~ 185 ergs/cm² for the cleavage energy of the basal plane in zinc derived by Gilman³² from theoretical considerations. This value is therefore regarded as the true fracture surface energy for cleavage on the basal plane of zinc, i.e. $\gamma(\text{Zn})$.

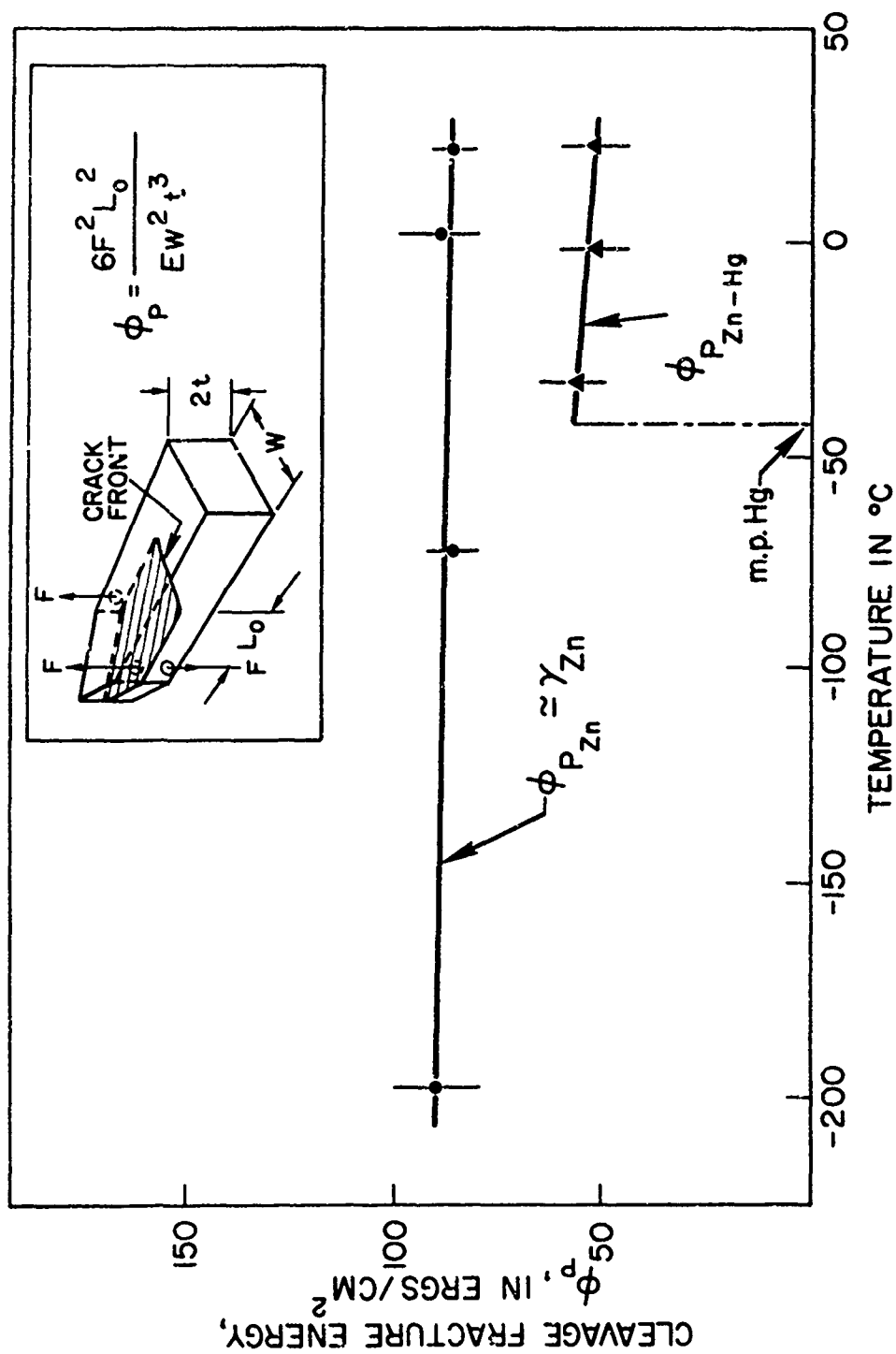


Figure 4. Effects of temperature and liquid mercury environment on the cleavage crack propagation energy, ϕ_p , for the (0001) planes of zinc. The inset shows the formula and type of specimens used to determine ϕ_p (after Westwood and Kamdar⁴).

When liquid mercury was present at the crack tip, however, ϕ_p was reduced to $53 \pm 8 \text{ ergs/cm}^2$. The coefficient of embrittlement of zinc mercury couple, $\eta_p(\text{Zn-Hg}) = \phi_p(\text{Zn-Hg})/\phi_p(\text{Zn})$, $\rho = 1$ is 0.61 ± 12 . It will be shown in Section 4.5 that this value is identical with that for the energy to initiate a crack in zinc in the presence of liquid mercury ($50 \pm 3 \text{ ergs/cm}^2$) as is to be expected since both crack initiation and propagation occur in the basal plane and involve the breaking of zinc-zinc bonds across the fracture plane.

Similar experiments were also performed using liquid gallium as the embrittling liquid metal for zinc. In this case, $\phi_p(\text{Zn-Ga})$ was $42 \pm 13 \text{ ergs/cm}^2$ and $\eta_p = 0.48 \pm 0.17$, indicating that liquid gallium is more embrittling than is liquid mercury for zinc. Several tests were made in which liquid mercury presaturated with zinc was used as the embrittling environment. Again ϕ_p was $\sim 53 \text{ ergs/cm}^2$, thus providing support for the view that liquid metal embrittlement does not involve a simple dissolution effect.²

It may be concluded from this work that the values of ϕ_p observed in the presence of liquid mercury or gallium, which are less than γ for the basal plane of zinc, provide support for the reduction-in-bond-strength model for liquid metal embrittlement. The theoretical estimates of the reduction in cohesion of zinc in liquid mercury and gallium environments are not available at the present time. The variation in the values of η_p observed in liquid mercury and gallium suggest, nevertheless, that the severity of embrittlement is probably related to the chemical nature of these species.

3.3.2 Effects of Plastic Deformation and Environment on ϕ_p

In studies similar to those described above, Westwood and Kamdar⁴ also

investigated the effects of plastic blunting of the crack tip on crack propagation and determined ϕ_p and η_p for zinc in liquid mercury and inert environments. Following double-propagation technique was adopted for most of the experiments. A long crack was initiated in zinc monocrystals at room temperature in air, and the load to propagate this crack a small distance was determined. Following propagation of the crack the specimen was unloaded and a drop of mercury introduced in the crack. The specimen was reloaded and fracture was completed. The values of $\phi_p(\text{Zn}, 298^\circ\text{K})$ and $\phi_p(\text{Zn-Hg}, 298^\circ\text{C})$ were computed using Equation (8). The experimental data are presented in Figure 5. It was observed that $\phi_p(\text{Zn-Hg})/\phi_p(\text{Zn}) = 0.61 \pm .07$, and a line of slope 0.61 drawn in Figure 5 illustrates a good fit to the data. Thus, for plastically blunted cracks $\eta_p(\text{Zn-Hg})$ at 298°K is 0.61 and is the same as that determined for atomically sharp cracks. The results provide support for the validity of Equation (6) when $\rho > 1$ and in addition indicates that in the case of plastically blunted cracks, embrittlement may also be considered to occur by the adsorption-induced reduction in cohesion mechanism. Thus, due to the reduction in cohesion of atomic bonds at the crack tip, a lower stress concentration at the tip is required to propagate a blunted crack in a liquid metal than that in an inert environment. Similar reasoning can readily be applied to most embrittlement couples where plastic flow invariably precedes embrittlement.

Effects of plastic blunting on crack propagation in zinc also provide a rational explanation for the considerably high values ($\sim 575 \text{ ergs/cm}^2$ for $\gamma(\text{Zn})$ and $\sim 245 \text{ ergs/cm}^2$ for $\gamma(\text{Zn-Hg})$) for the cleavage surface energies of zinc in an inert and liquid mercury environment determined by Maitland and

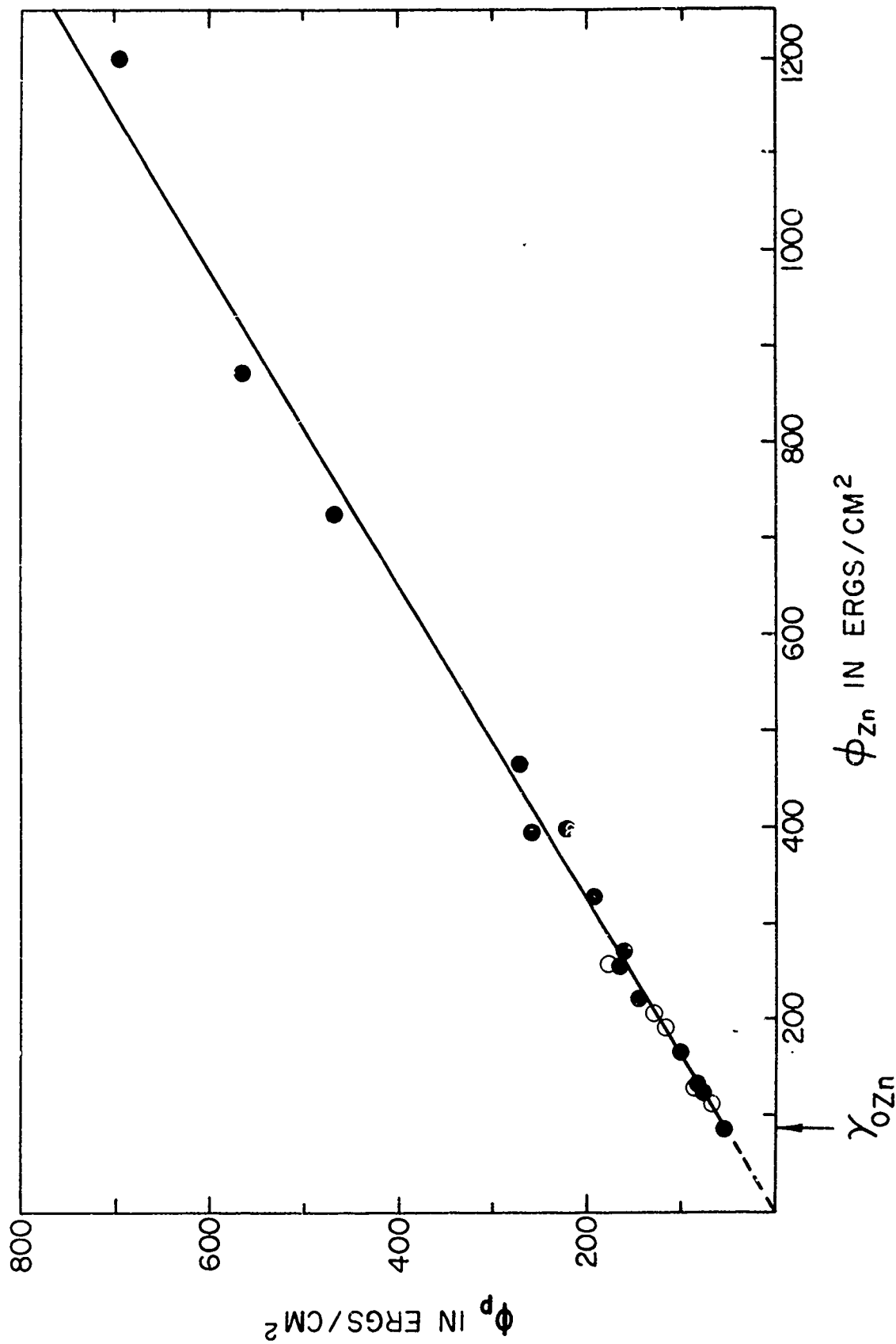


Figure 5. A comparison of the fracture energy involved in the propagation of a plastically blunted cleavage crack in air, ϕ_p , and in mercury, ϕ_p , from a double propagation experiments. A line of slope 0.61 is drawn through the data (after Westwood and Kamdar⁴).

Chadwick^{33,34} using the spark discharge technique of Hull.³⁵ Figure 5 shows that when ϕ_p (Zn-Hg) is ~ 250 ergs/cm², the corresponding value of ϕ_p (Zn) in air is about the same as that reported by Maitland et al.³³ This concurrence is not surprising since these workers used the Hull technique to introduce cracks in zinc at low temperature (i.e. 77°K). However, the crack repropagation test to determine ϕ_p was carried out at room temperature, i.e. 298°K. Thus, $\gamma(\text{Zn})$ should correspond to that for room temperature. In zinc plastic flow occurs readily at 298°K. Also, the fracture stress to repropagate cracks introduced by Hull technique were (3000 gm/mm² or more) an order of magnitude greater than that (~ 300 gm/mm²) required to repropagate cracks introduced by the double cantilever cleavage technique. At these high applied stresses, zinc is known to deform by secondary-prismatic slip.³⁶ This suggests that cracks introduced at low temperature by the Hull technique probably become blunted by plastic flow at the tip and give values higher than the true lower values for the surface energies of zinc.

Effects of plastic blunting are most important when one considers embrittlement of most solid-liquid metal couples where plastic flow invariably precedes embrittlement. In this instance, one should consider the effects of liquid at the tip of a notch-insensitive and a notch-sensitive solid. For notch-sensitive solids, e.g. the face centered cubic metals or ductile hexagonal closed packed metals such as cadmium, the liquid must continuously migrate to the crack tip to maintain crack propagation at reduced stress levels. This may occur by a second monolayer diffusion⁴ or capillarity.³⁷ If the crack advances a short distance ahead of the liquid, it becomes blunted and stops as observed in polycrystalline cadmium

tested in liquid gallium.⁸ On the other hand, a crack nucleated in notch-sensitive metals such as body centered cubic metals, may propagate one or two grain diameters in the presence of liquid metal when it becomes sufficiently long so that it is mechanically unstable (i.e. brittle under applied load), it then propagates across the specimen in the absence of liquid at the tip. The latter behavior is manifested by zinc in liquid mercury^{13,39} and by iron -3% Si monocrystals in mercury, gallium, mercury-indium solutions and in liquid indium³⁸ and by polycrystalline iron base solid solution alloys in mercury and mercury-indium solutions.³⁹

3.4 Stress-Assisted Dissolution Model

In addition to the models involving reductions in surface energy or cohesive strength, an obvious possibility is that embrittlement may be due to very rapid stress-assisted localized dissolution process occurring at the crack tip. Robertson⁴⁰ has presented detailed analyses of crack propagation through a solid in the presence of a liquid. The crack is assumed to propagate by solution of the solid in the liquid under the influence of an applied stress, with volume diffusion of the dissolved solute through the liquid controlling the propagation. He concludes that crack velocities in the order of tens of centimeter per second could be achieved simply by the increased solubility of the solid at the tip caused by the increased chemical potential at the stressed crack tip. Such a kinetic process should be thermally activated. While it is conceivable that stress could aid the dissolution of a solid metal into a "solvent" liquid metal environment, it is difficult to see how it could affect dissolution into a "nonsolvent" liquid metal, since stress is unlikely to affect the solvating ability of the liquid environment. In addition, there is

overwhelming evidence against the time and temperature dependent dissolution or diffusion controlled process envisioned in this mechanism. It is well known that most embrittlement couples exhibit very limited mutual or no solubility, while solids which are highly soluble tend to be immune.^{2,5} For example, the solubility of iron in liquid cadmium is only 2×10^{-4} w/o at 400°C but iron is severely embrittled by cadmium. Also cadmium is severely embrittled by gallium in which it is insoluble in both the solid and the liquid state while it is unaffected by liquid mercury in which it is highly soluble. The severity of embrittlement of most solid liquid metal couples is unaffected either by testing in liquid presaturated with the host solid or by testing near the freezing temperature of the liquid. A particular example is that described previously (see Section 3.2.1) in which the energy to propagate cracks in zinc monocrystals at -32°C was found to be the same whether one uses liquid mercury or mercury presaturated with zinc.⁴ The Robertson model also leads to the expectation that embrittlement will increase with increase in test temperature due to higher diffusion rate of the solid from the crack tip into the liquid. Contrary to this deduction, the observed behavior of most embrittlement couples is that the susceptibility to embrittlement decreases with increasing temperature, for example: iron-aluminum,³⁹ zinc⁴¹ and alpha brass tested in mercury.² Rostoker et al.² have reported that aluminum undergoes brittle to ductile transition with increasing temperature when tested in indium, lead-tin or mercury. Similar transitions have also been observed for iron-aluminum alloys³⁹ tested in mercury and commercial titanium alloys tested in liquid cadmium.¹⁶ Time dependent kinetic processes are also unimportant in the embrittlement process since a solid stressed at an appropriate high stress

fails in an instantaneous and catastrophic manner when contacted with a suitable embrittling liquid metal, e.g. zinc in liquid mercury⁴² and cadmium in gallium¹³ or cadmium and silver in mercury-indium solutions.^{38,43,7} Furthermore, embrittlement by liquid metal environments appears to be a special case of brittle fracture and occurs in accord with the principles of brittle fracture.⁹ The above mentioned observations are untenable with a dissolution dependent mechanism for liquid metal embrittlement. Thus, the mechanism of liquid metal embrittlement involving stress assisted dissolution dependent processes appears an unlikely possibility.

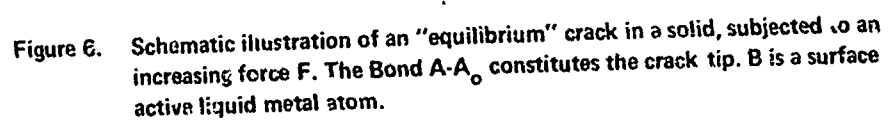
4. BRITTLE FRACTURE IN LIQUID METAL ENVIRONMENTS

4.1 A Criterion for Ductile-Brittle Fracture and Embrittlement

At the present time, it is considered that the phenomenon of liquid metal embrittlement and effects of various factors (mechanical, metallurgical, physical and chemical) on embrittlement can be interpreted rationally by considering the interaction of the embrittling species at or in the vicinity of the crack tip. We have discussed embrittlement as a consequence of the chemisorption induced reduction in cohesion (actually reduction in the tensile stress) at a crack tip. This assumption together with consideration of the effects of the short range nature of the interaction between the adsorbed species and metallic surfaces on shear strength (actually plastic deformation or stress to move or multiply dislocations) at the crack tip, suggests that liquid metal embrittlement may be considered a special case of a general criterion for predicting the ductile or brittle behavior of solids presented earlier by Gilman²⁰ and discussed in detail recently by Kelly et al.⁴⁴ The argument presented by the latter is essentially as follows: An equilibrium crack in a solid subjected to an increasing force F , Figure 6, will propagate in a fully brittle manner by cleavage,* if the ratio of the largest tensile fracture stress, σ , in the

* It is suggested here that the term "cleavage" may be used in connection with brittle crack propagation by either transcrystalline or intercrystalline paths. In the latter case, the bond $A-A_0$ under discussion would be oriented across a grain boundary, but the arguments presented are equally applicable. In practice, failure in liquid metal environments frequently occurs in an intercrystalline manner — presumably because less energy is required than for transcrystalline cleavage in most ductile metals. For anisotropic metals such as zinc, however, failure of polycrystalline specimens occurs predominantly by cleavage on basal planes.

Preceding page blank



vicinity of the crack tip to the largest shear stress, τ , on the most favorable oriented slip plane S-P near the tip is greater than the ratio of the ideal cleavage stress, σ_{\max} , to the ideal shear stress τ_{\max} . If the converse is the case, then the crack propagation will be accompanied with some plastic flow. As a rough approximation, for metals, if the ratio $\sigma_{\max}/\tau_{\max}$ is ≤ 10 , then failure will be predominantly by cleavage. If $\sigma_{\max}/\tau_{\max}$ is > 10 failure will be predominantly by shear. The appropriate values of these ratios are determined by the type of bonding in the solid (i.e. ionic, metallic etc.), by its crystal structure and the Poisson's ratio, ν . The values of these ratios for some typical solid metals which are embrittled by liquid metals are given in Table 3.

Table 3*

Values of ratios of σ/τ for some typical solid metals
which are embrittled by liquid metals

Material	σ/τ	$\sigma_{\max}/\tau_{\max}$
Cu	12.6	28.2
Ag	14.4	30.2
Au	24.7	33.8
Ni	7.9	22.1
Fe	8.5	6.75

* After Kelly et al.⁴⁴

Consider now the effect of a surface-active liquid metal atom B at the crack tip of A-A₀ in Figure 6. As a consequence of the chemisorption of this atom, and for reasons discussed earlier, it is suggested that some variation in the strength of the bond between the atoms A and A₀ will result, and hence the magnitude of σ_{\max} will be changed. On the other hand, because of free electron screening effects in a metal caused by the presence

of high concentration of mobile conduction electrons,^{45,46} the effects of such a chemisorbed liquid-metal atom will not be felt at depths greater than a few atom diameters from the crack tip, S. Thus the chemisorbed atom will be unlikely to influence the strength of bonds across the slip plane S-P for a distance from S sufficient to significantly affect the ease of dislocation motion in the vicinity of the crack tip. As far as plastic deformation in the vicinity of the crack tip is concerned, it follows that the magnitude of τ_{\max} should be considered unaffected by the presence of atom B.

If the adsorption of liquid-metal atom B leads to a reduction in σ_{\max} while τ_{\max} is unaffected, then the ratio $\sigma_{\max}/\tau_{\max}$ will be decreased. This effect will be manifested as an increased tendency to cleavage, i.e. as some degree of liquid-metal embrittlement,* the severity of which will be related to the magnitude of the reduction of σ . Alternatively, the ratio $\sigma_{\max}/\tau_{\max}$ could be increased by adsorbing some liquid-metal species which interacts at the bond A-A₀ Figure 6, to produce an increase in σ_{\max} . An element known to form high melting point (strongly bonded) intermetallic compounds with the solid metal element might be expected to act in this way.

The above reasoning may be used to explain liquid metal embrittlement of normally ductile face centered cubic metals such as copper, silver, gold and aluminum. For most embrittlement couples, the yield stress and stress-strain or flow behavior of the solid metal tested in air or in an inert environment remains unaffected when tested in an embrittling liquid metal

* Providing there is an adequate supply of liquid metal atoms, and their diffusion rate is sufficient to allow them to keep up with the propagating crack tip.

environment,^{1,2,9,39,10,16} Figure 1. This indicates that as postulated τ_{\max} and τ are not affected by the adsorption of the liquid metal on the surface of the solid. However, experimental determination of the cleavage fracture energy of zinc, $\gamma(\text{Zn})$ in an inert and liquid mercury or gallium environment indicate that in liquid metal environments, σ_{\max} may decrease by some 40 to 50%. Such measurements are difficult to make for most metals, because they are ductile and difficult to cleave. Nevertheless, let us assume that for these metals, liquid metal adsorption may reduce σ_{\max} by about 40 to 50%. Since τ_{\max} is not affected, the value of the ratio $\sigma_{\max}/\tau_{\max}$ for Cu, Ag, and Au in liquid metal environments will be about half of the values listed in Table 3 for these metals in inert environments. Note that the decreased values are about the same as the value of the ratio, σ/τ given in the same Table 3. Thus, in accord with Kelly et al's. criterion, in liquid metal environments one would predict a transition from ductile to brittle behavior for these metals. Similar reasoning may be used in a qualitative manner to explain the transition from pure shear type failure in inert environment at liquid helium temperature to brittle cleavage in liquid metal environments at elevated temperatures observed in aluminum and cadmium monocrystals.^{5,10,47} Aluminum monocrystals failed by (001) type cleavage in liquid gallium at 30°C⁴⁷ where as cadmium monocrystals failed by basal cleavage in liquid gallium⁵ and in mercury-indium solutions at 30°C,¹⁰ Figure 7.

From the foregoing, it may be suggested that while considering the phenomenon of liquid metal embrittlement, it is a convenient first approximation to think of σ as the environment-sensitive parameter, and τ as the

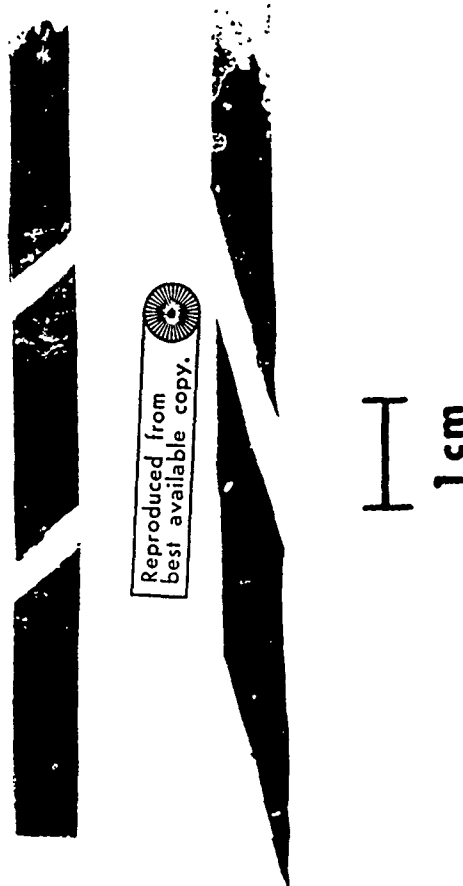


Figure 7. Demonstrating cleavage of cadmium monocrystals at 25°C following coating with mercury ~ 60 at. pct indium solution (after Kamdar and Westwood¹⁰⁸ and Kamdar¹⁰).

metallurgical structure-sensitive parameter. These parameters are not always independent, alloying can affect both σ and τ , but where appropriate, this simple approach will be adopted in the present paper.

Only pure liquid metals thus far have been mentioned, but apparently substantial variations in the severity of embrittlement can be induced by changing the chemical composition of the embrittling liquid metal environment by adding minor quantities (less than 5%) of other elements in solution.^{2,48,49,50} It is not yet clear whether effects due to minor additions are caused by changes in "wetting"^{2,12} characteristics or rates of surface diffusion of the liquid metal,⁵¹ or whether these effects can be related to some fundamental interaction parameter between the solute element and the solid metal. However, systematic variation in the susceptibility to embrittlement of a solid over a wide range of variation in the composition of a liquid metal has been observed (i) by dissolving a possible embrittling phase in a nonembrittling carrier liquid metal¹⁰ and (ii) by dissolving a possible inhibiting phase (i.e. reducing embrittlement) in an embrittling carrier liquid metal.⁴³ From a consideration of such studies, one would anticipate that if embrittlement does involve chemisorption, then the severity of embrittlement should be related to some electronic parameter of the solid metal-liquid metal system. This possibility is under active consideration,⁵² but as far as the author is aware, no such correlation has yet been confirmed. A possible correlation with electronegativity will be discussed later in this paper.

The severity of embrittlement observed is also dependent upon the metallurgical-structure dependent factors which determine τ . Thus embrittlement observed in a solid in a pure liquid metal depends also upon

factors that affect the solid e.g., alloying additions, cold work, temperature, grain size, the microstructure and the mechanical variables. The effects of these factors on embrittlement may be interpreted by considering the ease or the difficulty with which relaxation of stress concentrations via plastic deformation may occur at the tip of the crack during crack nucleation or crack propagation. The effects of these factors on embrittlement therefore are related to the magnitude of the structure-sensitive parameter, τ . Increase in τ will decrease the ratio, σ/τ , thus causing an increase in the susceptibility to embrittlement conversely a decrease in τ (e.g. by an increase in temperature or grain size and decrease in strain rate) may increase the ratio, σ/τ , and thus causing a decrease in the susceptibility to embrittlement.

In addition to the above considerations, there should also be a sufficient supply of the active liquid to ensure adsorption at a crack nucleation site, and subsequently at the propagating crack tip. It is possible however that if fracture in a liquid metal environment is nucleation controlled, then once initiated the crack may propagate to failure regardless of the presence of the liquid at the tip as for example was noted in the case of Fe-3% Si monocrystals tested in Hg-In solutions. On the other hand, if fracture in a liquid metal environment is propagation controlled, a crack may not nucleate in a liquid metal environment in a smooth specimen, (i.e. embrittlement will not be observed). But in a notched specimen a sharp crack will propagate to failure in the presence of the liquid at the tip, i.e. embrittlement will be noted if a stress raiser is present. Such a behavior was observed in Iron-Nickel alloys tested in a liquid mercury environment.⁵³

It is realized that certain factors such as alloying, temperature, etc. may vary the magnitude of both σ and τ , and that various mechanical, physical and chemical factors not only operate simultaneously but are interrelated. Nevertheless, the above simple approach appears to provide a rational interpretation for embrittlement effects that have been observed when one variable was investigated in a simple well characterized system. Some of the important factors on the severity of liquid metal embrittlement will be considered in more detail in other sections utilizing examples of well characterized simple embrittlement couples taken from the extensive but unfortunately not always reliable literature on liquid metal embrittlement. The above considerations and available experimental evidence do in fact suggest that embrittlement in a liquid metal environment may be considered a special case of the general criterion which Kelly et al.⁴⁴ have developed for predicting the ductile-brittle behavior of solids.

Concerning brittle fracture however, Kamdar and Westwood⁹ have used liquid metal environments to demonstrate that the prerequisites for liquid metal adsorption-induced brittle fracture are the same as that for brittle fracture in inert environments and that such environments may be used instead of low temperatures and inert environments to test the validity of several fracture criteria. The objective of such investigations was to show that adsorption induced embrittlement is truly a special case of brittle fracture and is not a corrosion or dissolution dependant phenomena. With this in mind, in the next few sections we will present and discuss the extensive investigations by Kamdar and Westwood⁹ on brittle fracture in the zinc in liquid mercury environments.

4.2 Prerequisites for Embrittlement

Certain prerequisites must be fulfilled before fracture can initiate in a crystalline solid in liquid metal environment. For a ductile, unpre-cracked metal specimen these are (i) an applied tensile stress, (ii) some measure of plastic deformation, and (iii) the existence in the specimen of some stable obstacle to dislocation motion, capable of serving as a stress concentrator; this obstacle can be either pre-existing (e.g. a grain boundary) or created during deformation (e.g. a kink band). In addition, there should also be a sufficient supply of the active liquid metal to ensure adsorption at this obstacle, and subsequently at the propagating crack tip. A specimen which is normally brittle when tested in tension in a liquid metal environment is found to be immune when tested in compression or pure shear, e.g. zinc in mercury. Also, fracture in an amalgamated specimen tested in a three point bend test invariably initiates in the face under tensile stress¹³ but not in the face which was under compressive stress. These observations are in accord with prerequisite (i). Also, in accord with prerequisite (ii), fracture in most embrittlement couples is invariably preceded by yielding.^{2,9,39,48} However, fracture initiated below the flow stress in coarse grain polycrystalline zinc, tested in liquid mercury environment.⁵⁴ Nevertheless upon examination, the apparently undamaged specimen loaded just below the fracture stress revealed the presence of microcracks only in the grains in which local yielding had occurred.¹³ Thus in some instances, local yielding can be a sufficient prerequisite for the initiation of fracture. If the specimen contains a pre-existing crack, the prerequisites (ii) and (iii) are no longer necessary. If the solid is

notch brittle, it may not be necessary for the liquid metal to keep up with the propagating crack once it is greater than critical size. The presence of a stress concentrator in a solid, such as a grain or a twin boundary, or a kink band, etc. from which the crack may initiate in a liquid metal environment is an important prerequisite for the initiation of brittle fracture. Since most fractures occur by intergranular mode, a possibility exists that diffusion, penetration or corrosion of liquid into the boundaries may be responsible for embrittlement. We will accordingly discuss in greater detail the validity of this prerequisite for fracture in the following section.

4.3 The Stress Concentrator Requirement

The necessity for the presence of some stable obstacles to dislocation motion in order to observe liquid metal embrittlement in a ductile, unpre-cracked metal has been demonstrated by a number of workers, e.g. for α -brass in liquid mercury by Nichols and Rostoker,¹⁷ and Rosenberg and Cadoff⁴⁸ and for copper in liquid bismuth by Morgan.⁵⁵ A good example of such an obstacle is zinc monocrystals which are known to deform by basal slip only and consequently do not contain any pre-existing obstacles to slip. In these crystals, indented to introduce obstacles such as a twin or a kink band and subsequently chemically polished to remove surface damage, fracture in liquid mercury invariably initiated from the twin or the kink band.⁹ Nevertheless, Likhtman and Shchukin et al.^{1,56} have reported that undamaged zinc monocrystals, oriented for a single slip, can be significantly embrittled by liquid mercury or gallium. According to Likhtman and Shchukin,¹ the room temperature stress and strain at fracture of 1mm dia. crystals of orientation $\chi = 48^\circ$ * were respectively reduced from $\sim 1400 \text{ gm/mm}^2$

* χ is the angle between the (0001) basal plane and the tensile axis of the specimen before testing, and χ_0 is this angle at fracture.

and 260% in air, to 200 gm/mm^2 and 10% in liquid mercury Figure 1. This result is unexpected because the existence or nature of any stable obstacle to dislocation motion in monocrystals of pure zinc oriented for single slip is not evident, either from this work or that of Garber and Gindin.⁵⁷ Kamdar and Westwood⁹ have recently investigated this apparent anomaly using considerably larger zinc monocrystals, 6mm square in section. These were handled with extreme care to prevent accidental bending or surface damage. Moreover, since it is known that deformation in zinc occurs in a markedly inhomogeneous fashion in the vicinity of the grips, usually with the formation of kink bands,⁵⁸ the crystals were coated with liquid mercury over the center portion of their length only, and not within a region approximately 1.5 cm long in the vicinity of the grips ("partially-coated" specimens). Thus for specimens of orientation $15^\circ < \chi_0 < 70^\circ$, the embrittling liquid metal was confined to that portion of the crystal for which slip might be expected to occur predominantly on the basal plane.

Some of the results obtained in this work are presented in Figure 8(b). The difference between this data and that of Shchukin et al.⁵⁶ (Figure 8(a)) is readily apparent. In direct contrast to the previous work, it was found that crystals of orientation $15^\circ < \chi_0 < 70^\circ$, for which deformation occurs predominantly by single slip in the basal plane, are not significantly embrittled by liquid mercury. However, crystals of orientation $\chi_0 > 75^\circ$ were embrittled; values of the resolved shear stress and strain at fracture were respectively some 5 and 25 times lower than those for similar but uncoated specimens. Fracture always occurred in these specimens at a kink band formed during deformation in the amalgamated gauge section, Figures 9,10. Likewise, crystals of $15^\circ < \chi_0 < 70^\circ$ which were amalgamated

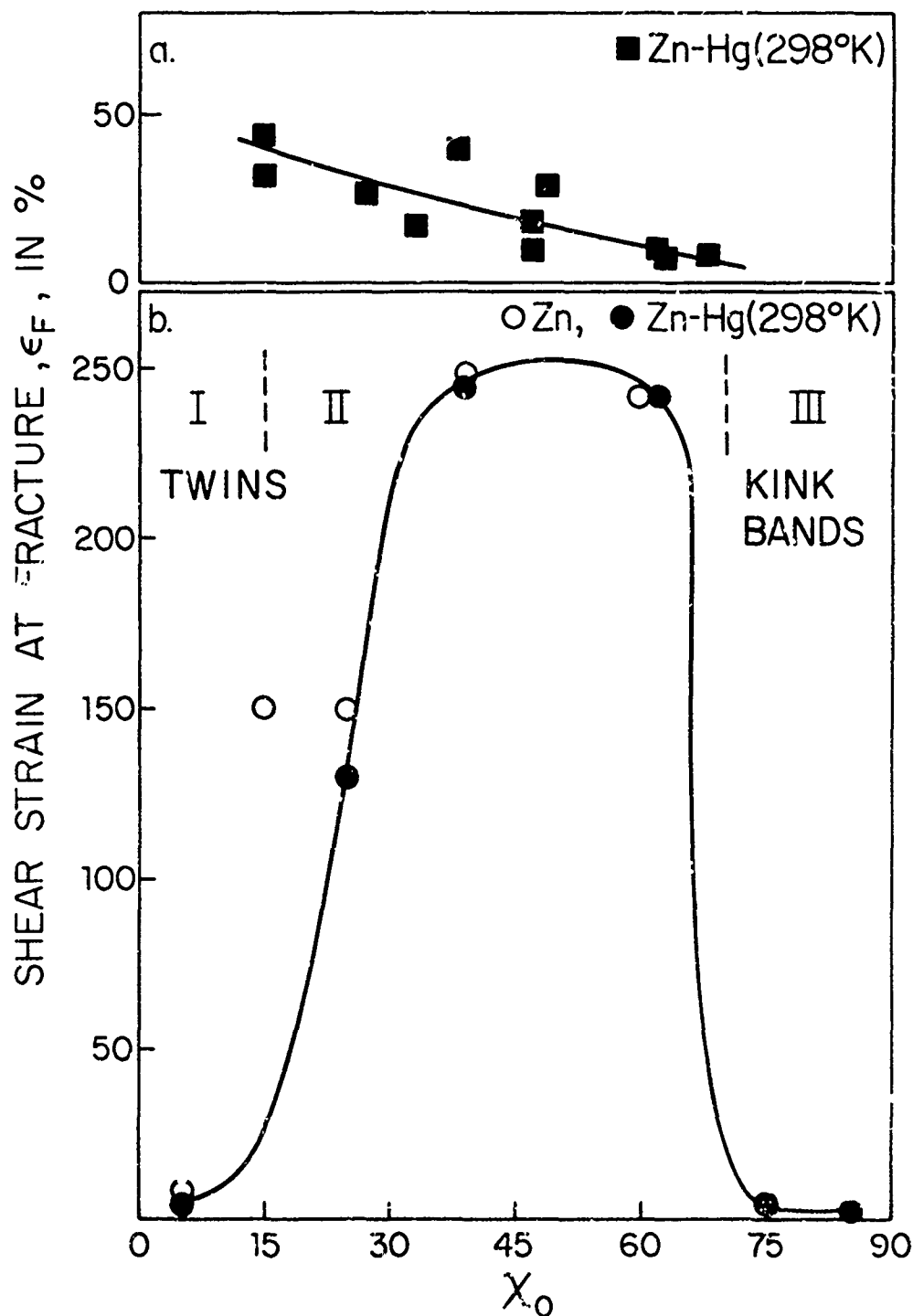


Figure 8. Orientation dependence of shear strain at fracture for (a) amalgamated 1mm dia. zinc monocrystals (after Shchukin et al.⁷¹) (b) uncoated or partially amalgamated 6mm square zinc monocrystals (Kamdar and Westwood⁹).



Figure 9. The cleavage step pattern reveals that failure of this amalgamated zinc monocrystal was initiated at one of the dislocation walls which constitute the boundaries of the kink band K. Twins are visible at T (after Kamdar and Westwood⁹).

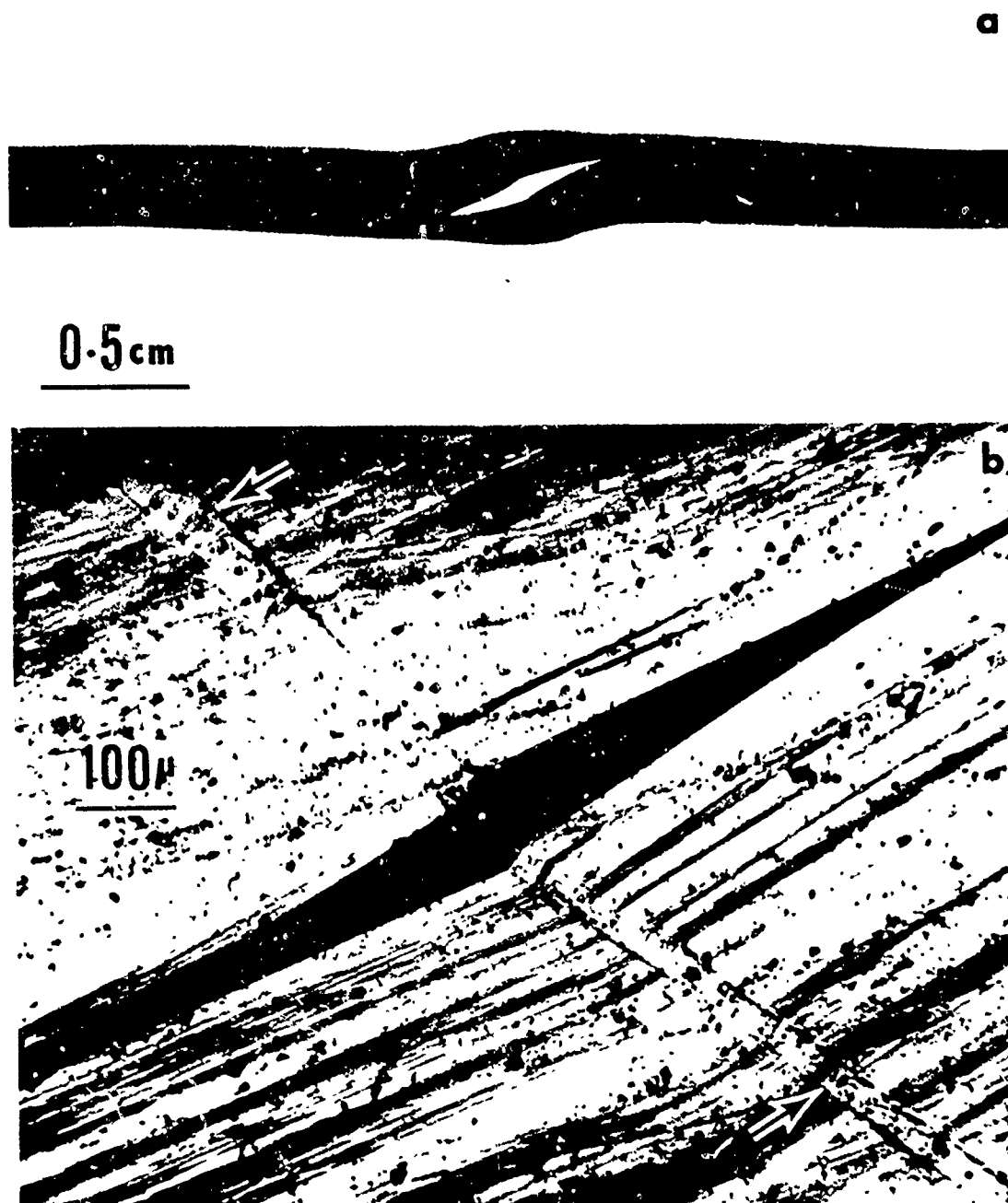


Figure 10. Illustrating the formation of cleavage cracks at kink bands in amalgamated zinc monocrystals $\lambda_0 = 25^\circ$. The kink band is denoted by arrows in (b) (after Kamdar and Westwood⁹).

overall, failed by cleavage nucleated at a kink boundary located in the vicinity of the grips. Crystals having $\chi_0 < 5^\circ$, on the other hand, deform predominantly by twinning, and both amalgamated and unamalgamated crystals failed after only a few percent strain by secondary cleavage on the (0001) planes of a twin.

It is apparent from these studies that the experiments performed by earlier workers with zinc had utilized either accidentally deformed crystals, or specimens amalgamated in the vicinity of the grips where deformation is not homogeneous and kink bands provide the necessary obstacle for crack initiation.

4.4 Criteria for Crack Initiation

Several criteria have been proposed for crack initiation in solids which slip and cleave on the same plane, and also contain a suitable obstacle to slip. Such criteria, of course, apply to brittle failure in general. However, by optimizing the conditions for brittle behavior, deformation in active liquid metal environments has proved to be a very convenient method of examining both their qualitative and quantitative validity. The various criteria are summarized below, and are then compared with experimental data obtained from studies on the zinc-liquid mercury system.

The first criterion is that due to Likhtman and Shchukin,¹ namely

$$\sigma_{NF} \tau_F L = k^2 G \gamma \quad (9)$$

where σ_{NF} and τ_F are normal and the shear stress at fracture, respectively, k is a dimensionless coefficient of order unity, G is the shear modulus, and γ is the fracture surface energy. In several published applications of this criterion to fracture in zinc.^{56,5,42} L is equated

to the crystal diameter. However, in the original derivation of Equation (9), L is the maximum dimension of the slip plane along a slip direction. If the angle between the slip direction and the tensile axis, $\lambda = \chi$, then $L = D_0 / \sin \chi$, where D_0 is the crystal diameter or side dimension and is assumed constant for a given set of experiments. If only a limited amount of deformation occurs in the material before fracture, so that χ can be taken as equal to χ_0 , then Equation (9) becomes

$$\sigma_{NF} \tau_F = (k^2 G \gamma / D_0) \sin \chi_0 = K_1^2 \sin \chi_0. \quad (10)$$

Thus the product of the normal stress and shear stress at fracture is not constant, as is often stated in the Russian literature, but instead is orientation dependent.

Gilman⁵⁹ has proposed that the condition for cleavage fracture in the basal plane of zinc is given by

$$n = 4\gamma[E(1-\nu)/G]^{1/2} / \sigma_{NF} b \quad (11)$$

where n is the number of edge dislocations held up at some stable obstacle and b is their Burgers vector, γ is the surface energy of the (0001) plane in zinc, E is Young's modulus and ν is Poisson's ratio.

Now the shear stress required to hold n blocked edge dislocations in a slip plane of length L is given by Eshelby, Frank and Nabarro.⁶⁰

$$\tau = Gbn/\pi(1-\nu)L \quad (12)$$

and if such a pile-up nucleates a crack, τ can be regarded as τ_F . When

Equations (11) and (12) are combined, the following criterion for fracture is obtained:*

$$\sigma_{NF} \tau_F L = 4\gamma[EG/(1-\nu)]^{1/2}/\pi. \quad (13)$$

Putting $L = D_0/\sin\chi_0$ as before, Equation (13) can be written

$$\sigma_{NF} \tau_F = K_2^2 \sin\chi_0 \quad (14)$$

where $K_2^2 = 4\gamma[EG/(1-\nu)]^{1/2}/\pi D_0$. Equation (13) is of the same form as Equation (9) derived by Likhtman and Shchukin,¹ and similarly Equation (14) may be compared with Equation (10).

Stroh's⁶¹ analysis of this problem is based upon the consideration that large local tensile stresses exist at the end of any dislocation tilt boundary terminating within a crystal. It is postulated that fracture is initiated when a complete tilt boundary is converted into a pair of terminating tilt boundaries by basal slip. Assuming that the original tilt boundary lay perpendicular to the slip planes, and that the length of the longer of the created pair is W , then $W_{\max} \simeq D_0/\cos\chi_0 = L \tan\chi_0$. Stroh's criterion for fracture by this mechanism is then

$$\sigma_{NF} \tau_F = K_3^2 \cos\chi_0 \quad (15)$$

where $K_3 = (4G\gamma/\pi D_0)^{1/2}$. Alternatively, Equation (15) may be written

$$\sigma_{NF} \tau_F L = (4G\gamma/\pi) \cot\chi_0 \quad (16)$$

* In an earlier derivation of this criterion,⁹ Equation (12) was taken as $\tau = 3Gnb/2\pi L$, which is valid if $\nu = 0.33$. This led to the following version of Equation (13): $\sigma_{NF} \tau_F L = 6\gamma[EG(1-\nu)]^{1/2}/\pi$. However, ν for zinc is actually 0.26,⁵⁹ and as a result, the values of the fracture surface energy of zinc in liquid mercury previously published by Kamdar and Westwood are in error by about -9%. Equation (13) represents a generalized version of the Kamdar-Westwood criterion.

Bullough⁶² has criticized the Stroh model on the grounds that it seems unlikely that such a maximum length sub-boundary would exist in every crystal. Instead, he has proposed an alternative criterion based on the Bullough⁶³-Gilman⁵⁹-Rozhanskii⁶⁴ model for the formation of cracks in the slip plane, as follows:

$$P_F = 4\gamma[(1-\cos\chi_0)/\sin^3\chi_0]/nb \quad (17)$$

where P_F is the tensile fracture stress.

From Equation (17), he derives

$$\begin{aligned} \sigma_{NF} &= K_4[(1-\cos\chi_0)/\sin\chi_0] = K_4/\tan(\chi_0/2) \\ \tau_F &= K_4[(1-\cos\chi_0)\cos\chi_0/\sin^2\chi_0] = K_4[\cos\chi_0/(1+\cos\chi_0)] \end{aligned} \quad (18)$$

where $K_4 = 4\gamma/nb$.*

Smith and Barnby⁶⁵ have recently proposed a shear stress criterion for crack initiation in a plane containing a pile-up of edge dislocations.

They suggest

$$\tau_F = [G\pi\gamma/2L(1-\nu)]^{1/2} \quad (19)$$

Again putting $L = D_0/\sin\chi_0$, Equation (19) may be written

* Recently Heald⁶⁶ has suggested that Equation (13) derived by Kamdar and Westwood is in error. He suggested that the appropriate fracture criterion is γ or $\phi_I = (\tau_F - \tau_0)\sigma_{NF} \cdot L_F(1+\cos\chi_0)\pi(1-\nu)/4G \sin\chi_0$ which following Kamdar and Westwood he derived as a modification of Equation (17) of Bullough. Here ϕ_I , the energy to initiate a crack is used instead of γ , the surface energy. It should be noted that the criterion suggested by Heald is identical to Equation (18) derived by Kamdar and Westwood as a modification of Equation (17) by Bullough. Since the fracture data are found to be in good agreement with the curves represented by Equations (18) and (13), compare Figures 11 with 12, it is apparent that the improvement to Equation (13) suggested by Heald is marginal and within the scatter of the experimental fracture data.

$$\tau_F = K_5 [\sin \chi_0]^{1/2} \quad (20)$$

where

$$K_5 = [G\pi\gamma/2D_0(1-\nu)]^{1/2}.$$

The variations of the theoretically derived values of τ_F and σ_{NF} with crystal orientation can also be simply derived for the criteria of Likhtman-Shchukin, Kamdar-Westwood and Stroh. For the small deformations expected to occur in a brittle or embrittled material, it can be assumed that $\chi \approx \chi_0$, and thus

$$\tau_F = P_F \sin \chi_0 \cos \chi_0,$$

and

$$\sigma_{NF} = P_F \sin^2 \chi_0,$$

so that

$$\sigma_{NF}/\tau_F = \tan \chi_0. \quad (21)$$

Combining Equation (21) with Equations (10), (14), and (15), and assuming D_0 constant throughout, one obtains

(i) For the Likhtman-Shchukin and Kamdar-Westwood criteria:

$$\begin{aligned} \tau_F &= (K_1 \text{ or } K_2) (\cos \chi_0)^{1/2} \\ \sigma_{NF} &= (K_1 \text{ or } K_2) (\sin^2 \chi_0 / \cos \chi_0)^{1/2}. \end{aligned} \quad (22)$$

(ii) For the Stroh criterion:

$$\begin{aligned} \tau_F &= K_3 (\cos^2 \chi_0 / \sin \chi_0)^{1/2} \\ \sigma_{NF} &= K_3 (\sin \chi_0)^{1/2} \end{aligned} \quad (23)$$

Equations (16), (20), (22), and (23) may be used to examine the validity of proposed fracture criteria, provided that the comparative experiments are performed on specimens of constant D_0 , and that fracture occurs after only a small amount of deformation such that the approximation $\chi = \chi_0$ is valid. When specimens of constant D_0 are not available, however, then the Likhtman-Shchukin and Kamdar-Westwood criteria can be examined by means of Equations (6) and (13), where L is taken as L_F , the length of the fractured slip plane as determined after failure. If these criteria are valid, then the product $(\sigma_{NF} \tau_F L_F)$ should be constant. For the Stroh criterion to be valid, the product $(\sigma_{NF} \tau_F L_F \tan \chi_0)$ must be constant; for the Smith-Barnby criterion to be valid, the term $[\tau_F / (\sin \chi_0)^{1/2}]$ must be constant.

4.5 Crack Initiation in Pure Zinc

Studies of the fracture behavior of asymmetric bicrystals of zinc in liquid mercury at room temperature have provided a convenient means of evaluating the above criteria.⁹ The boundary in such crystals (see insert in Figure 11) provides a strong barrier to the emergence of edge dislocations from one of the component crystals,⁵⁹ and failure occurs after only 0.5-4% strain. Tensile experiments were performed with two types of asymmetric zinc bicrystals: Type I was grown by electron beam welding two monocrystals together (D_0 constant). Type II was grown by seeding (D_0 not constant). Both types were 5mm x 10mm in section and 7-9 cm in length, and were amalgamated over the center part of the gauge section only. On testing, cleavage cracks were initiated at the grain boundary, and these propagated completely through the crystals of orientation such as B in Figure 11.

Experimental data points presented in Figures 11 and 12 are from crystals of Type I. The solid curves drawn in Figure 11 correspond to

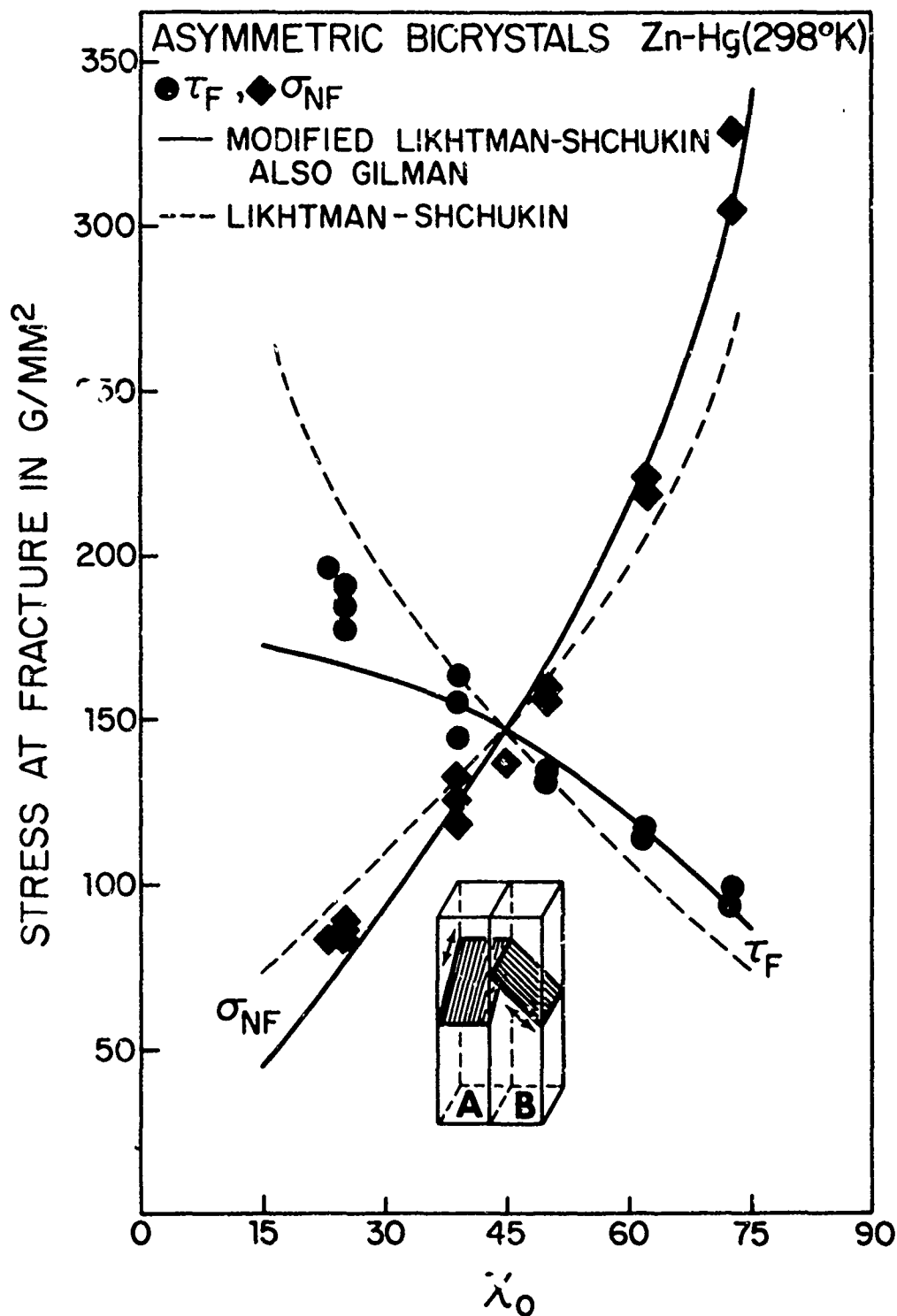


Figure 11. Orientation dependence of the normal stress, σ_{NF} , and shear stress, τ_F , at fracture for Type 1 asymmetric zinc bicrystals in the partially amalgamated condition. For comparison, the theoretically constructed curves correspond to Eqs. (22) (solid lines — Likhtman-Shchukin or Kamdar-Westwood criteria) or Eqs. (24), (dashed lines) when $K_1 = K_2 = 178 \text{ gm/mm}^2$ and $K = 148 \text{ gm/mm}^2$ (after Kamdar and Westwood⁹).

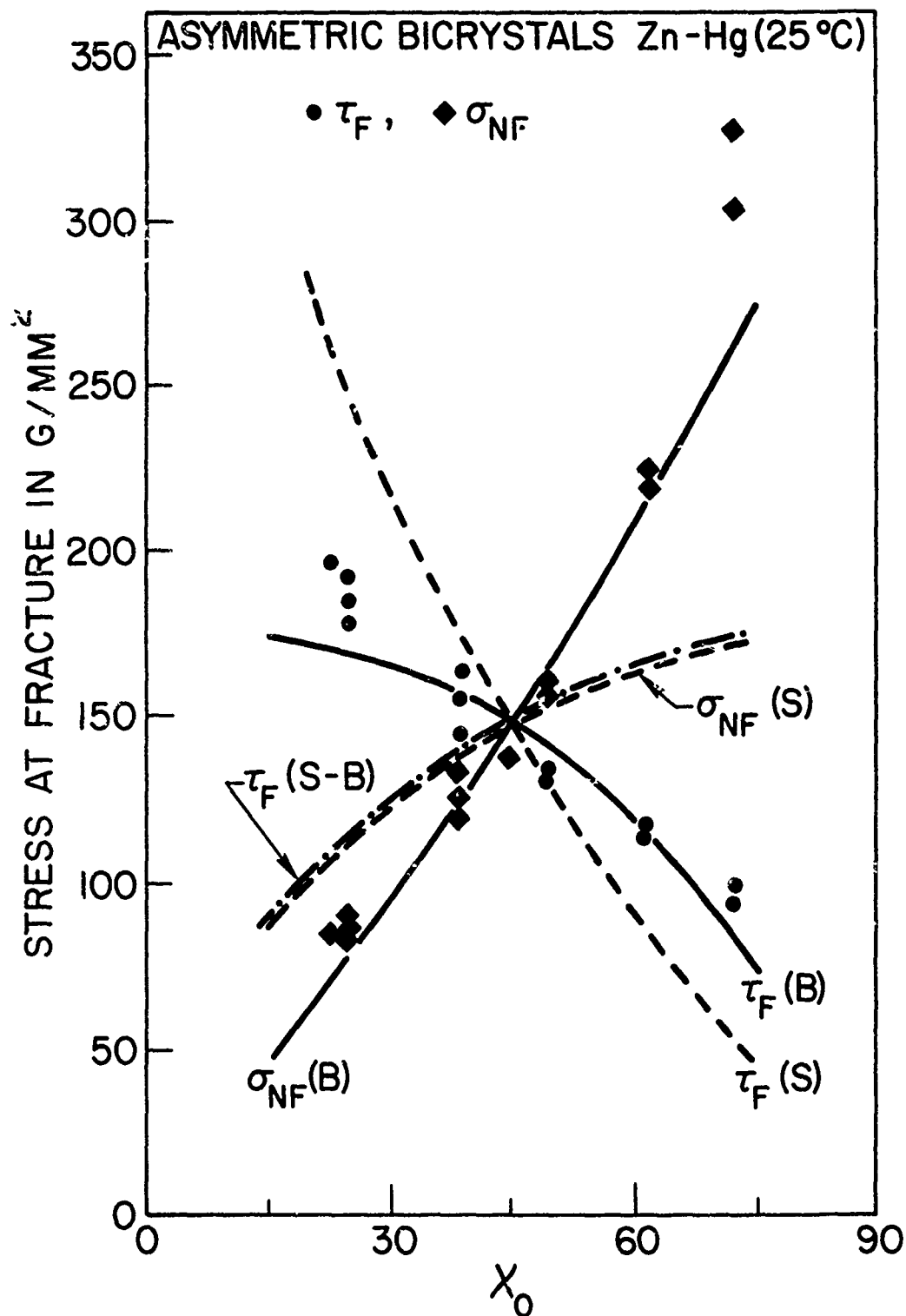


Figure 12. Same data as Fig. 11. The solid lines, B, correspond to Eqs. (18) (Bu'lough's⁶² analysis); the dashed lines, S, to Eqs. (23) (Stroin's⁶¹ analysis), and the other line, S-B, to Eq. (20) (Smith-Bernby's⁶⁵ analysis) when $K_3 = K_5 = 178 \text{ gm/mm}^2$ and $K_4 = 359 \text{ gm/mm}^2$ (after Kamdar and Westwood⁹).

Equation (22), assuming $\chi = \chi_0$ and putting $K_1 = K_2 = 178 \text{ gm/mm}^2$. It can be seen that the theoretical values of τ_F and σ_{NF} calculated from Equation (22) are in good agreement with experimentally determined values, with the exception of those from crystals of $\chi_0 = 25^\circ$ for which a relatively large amount of plastic deformation occurred before failure ($\sim 4\%$ compared with $\sim 0.5\%$ for crystals of $\chi_0 = 60^\circ$).

Now if L in Equation (9) is equated to the specimen diameter (width) D_0 , and this is assumed constant, and if $\lambda = \chi$, and $\chi = \chi_0$ then

$$\begin{aligned}\sigma_{NF} &= K(\tan \chi_0)^{1/2} \\ \tau_F &= K(\cot \chi_0)^{1/2}.\end{aligned}\tag{24}$$

The dashed curves in Figure 11 correspond to Equations (24), putting $K = 148 \text{ gm/mm}^2$. It can be seen that if L is equated to D_0 , the analysis does not fit the data quite as well as when L is taken as the slip plane length.

Figure 12 presents the data again in order to compare it with the Stroh⁶¹ (S), Bullough⁶² (B), and Smith-Barnby⁶⁵ (S-B) theoretical estimates of τ_F or σ_{NF} , obtained by means of Equations (23), (18), and (20), and with $K_3 = K_5 = 179 \text{ gm/mm}^2$ and $K_4 = 358 \text{ gm/mm}^2$. Bullough's estimates are in fair agreement with the experimentally determined values except for crystals having $\chi_0 > \sim 70^\circ$. However, neither Stroh's nor that of Smith and Barnby's analysis are in accord with the data.

For bicrystals of Type II, grown by seeding, D_0 was not constant from specimen to specimen, so that it is not possible to analyze the test data in the manner just presented. Accordingly, it was examined in terms of the product $(\sigma_{NF} \tau_F L_F)$, Equations (9), (13), and (16), for specimens of various

orientations. The data are shown in Figure 13. It can be seen that the strain at fracture for these specimens remained essentially constant at 0.5%, regardless of orientation, Figure 13. Moreover, in accord with the fracture criteria of Likhtman-Shchukin and Kamdar-Westwood, Equations (9) and (13), the product of $(\sigma_{NF}\tau_F L_F)$ was constant over the range of orientations for which slip might be expected to occur predominantly on the basal plane, and failure by a Bullough-Gilman-Rozhanskii type mechanism. Since the product of $(\sigma_{NF}\tau_F L_F)$ was independent of orientation, it is apparent that the Stroh criterion, Equation (16) is not valid for these experiments. Taking $(\sigma_{NF}\tau_F L_F) = 30,350 \pm 2,000 \text{ gm}^2/\text{mm}^3$ from Figure 13, $E = 2.54 \times 10^{11} \text{ dynes/cm}^2$, $G = 3.84 \times 10^{11} \text{ dynes/cm}^2$,⁶⁷ and $\nu = 0.26$,⁵⁹ the cleavage fracture surface energy for the basal plane of zinc in the presence of liquid mercury was calculated from Equation (13) to be $53 \pm 3 \text{ ergs/cm}^2$.

4.6 Crack Initiation in Zinc Alloys

Small alloying additions (less than 0.5 a/o gold) increase the critical resolved shear stress of zinc monocrystals by an order of magnitude to about 100 g/mm^2 . Figure 14, which is of the same magnitude as the fracture stress of unalloyed zinc in liquid mercury, $\tau_F \sim 95 \text{ g/mm}^2$, Table 4.⁵⁴ In such alloys the fracture stress and hence σ_{NF} and τ_F will be

Table 4
Summary of Test Data on Amalgamated Asymmetric Zinc Bicrystals*

Material	χ	τ_C (g/mm^2)	τ_F (g/mm^2)	ϕ_1 in ergs/cm^2 via Equation (25)
Zinc	22°-75°	10 ± 3	35-95	45 ± 5
Zn-0.05 at % Cu	40° or 70°	61 ± 7	80-105	61 ± 5
Zn-0.2 at % Cu	16°-80°	95 ± 10	120-180	60 ± 7

*After Kamdar and Westwood.^{9,54}

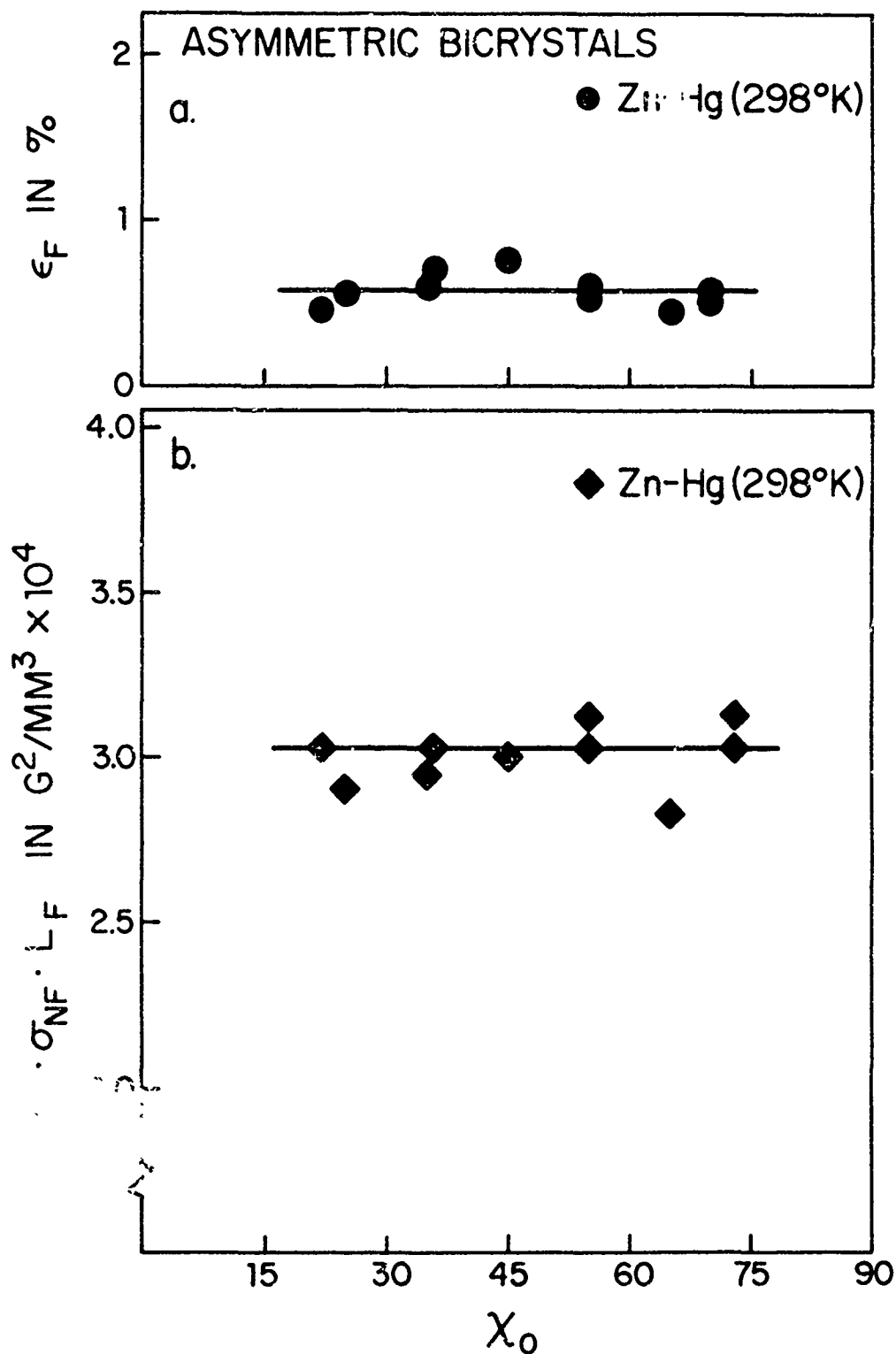


Figure 13. Orientation dependence of (a) the strain at fracture, and (b) the product of the normal stress, σ_{NF} , shear stress, τ_F , and slip plane length, L_F , at fracture for asymmetric zinc bicrystals grown by the seeding technique, and tested in the partially amalgamated condition (after Kamdar and Westwood⁹).

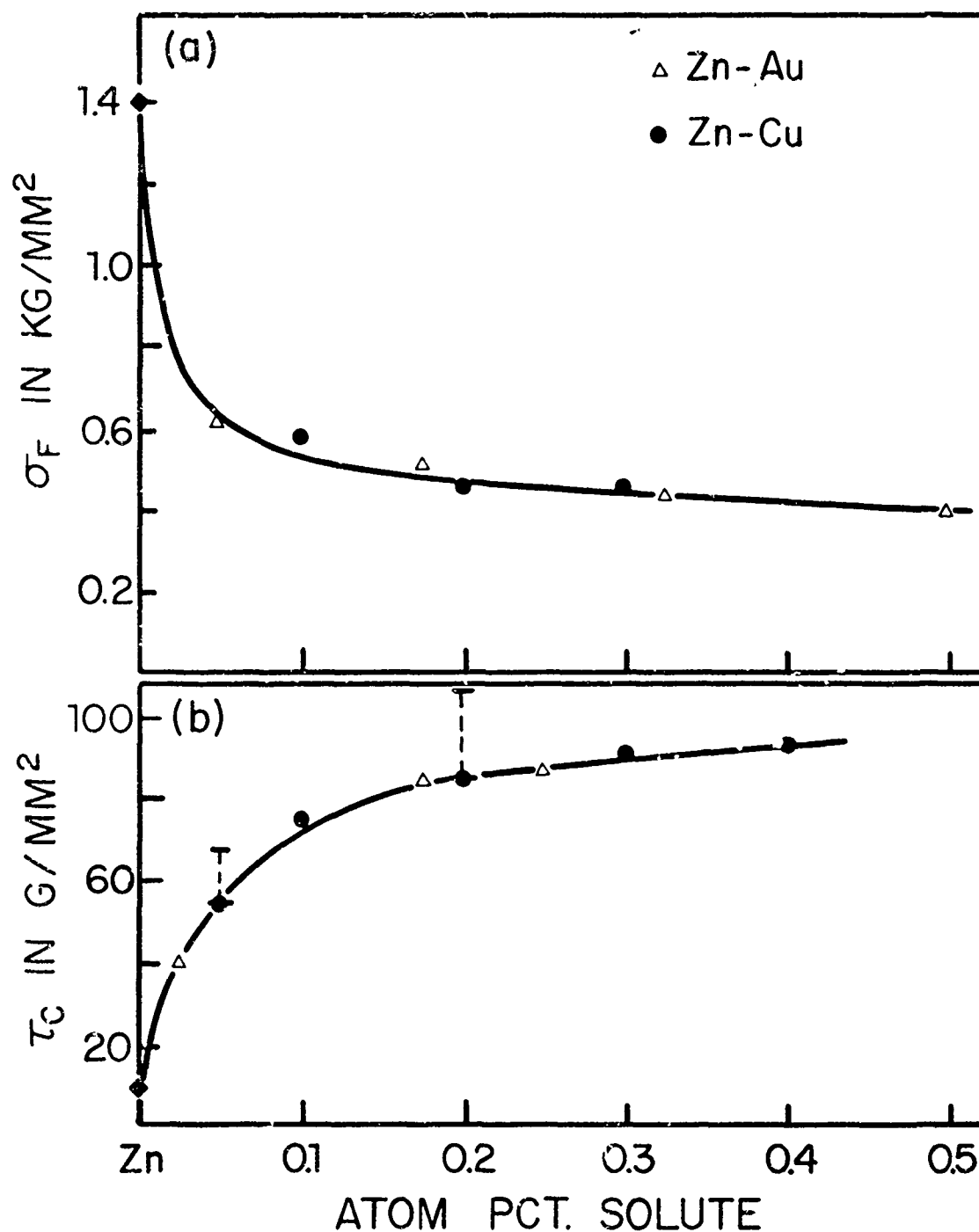


Figure 14 (a). Effect of solute content on the room temperature fracture stress, σ_F , of polycrystalline zinc in liquid mercury. The grain diameter of the zinc was ~ 1 mm, and its engineering flow stress ~ 1.9 kg/mm². The strain rate was 4×10^{-5} per sec. (b). Variation of critical resolved shear stress, τ_C , with solute content for zinc monocrystals. Range of values for asymmetric bicrystals of Zn-0.05 at. % Cu and Zn-0.2 at. % Cu are given by bars (after Kamdar and Westwood⁵⁴).

higher than the c.r.s.s. Since flow must precede fracture,¹⁹ it can be readily seen that using such high values of σ_{NF} and τ_F , the values of γ derived from Equation (13) for zinc alloys will be unreasonably (several times) higher than that for pure zinc. It is reasonable to expect that for additions of less than 0.5 at/o of solute fracture initiation in zinc alloys on the average should involve the breaking of zinc-zinc bonds across the fracture plane rather than the zinc-solute atom bonds. Thus, γ for zinc alloys should be about the same as for pure zinc. In order to resolve this question, the variables in Equation (13) were re-examined. In the derivation of Equation (13) it was assumed that τ_F truly represented the stress acting on the piled up group of dislocations which nucleated the crack. In fact, however, the effective stress acting on the dislocations in the pile up at fracture is somewhat less than τ_F , namely $(\tau_F - \tau_0)^{60}$ and this term should replace τ_F in Equation (13). There then arises the problem of deciding what value of stress to assign to τ_0 . On this point the work of Ku and Johnston⁶⁸ on crack initiation in MgO bicrystals is relevant. These workers found that their fracture data was capable of rational interpretation if τ_0 was equated with the dislocation multiplication stress, τ_C , but not if τ_0 was equated with the much smaller stress at which dislocations first become mobile. These workers suggested that the plastically induced stress concentrations which lead to crack initiation arise only after a slip band is formed. Thus the critical threshold event is dislocation multiplication, not merely dislocation motion.

For pure zinc $\tau_C \gg \tau_F$, so that τ_C may be neglected without serious error. However, for alloyed crystals, τ_C is a significant fraction of τ_F .

For example, for Zn-0.2 a/o Cu crystals, the ratio $\tau_C/\tau_F = 0.7$, (Table 4) and in this case, τ_C must be taken into account if meaningful values of γ are to be derived. Accordingly, in their studies of the embrittlement behavior of asymmetric bicrystals of dilute zinc alloys in liquid mercury, Kamdar and Westwood⁵⁴ have equated τ_0 to τ_C , the critical resolved shear stress (c.r.s.s.) for monocrystals of the appropriate alloy. The value of τ_C was taken as that stress at which the first deviation from linearity occurred in the tensile stress-strain curve. The modified form of Equation (13) is then

$$\sigma_{NF} \cdot (\tau_F - \tau_C) \cdot L_F = 4\gamma[EG/(1-\nu)]^{1/2}/\pi$$

or

$$\sigma_{NF} \cdot (\tau_F - \tau_C) \cdot L_F = 4\phi_I[EG/(1-\nu)]^{1/2}/\pi^* \quad (25)$$

This equation has been used to analyze the fracture data from Zn-0.05 a/o Cu, Zn-0.2 a/o Cu crystals ($20^\circ < \chi_0 < 80^\circ$) and the earlier data from unalloyed zinc bicrystals, Figure 13. The value of ϕ_I obtained for both alloys was 60 ± 7 ergs/cm², (Figure 15); that is, about 25% greater than the value obtained for pure zinc bicrystals tested in liquid mercury (~ 48 ergs/cm²), Table 4. It is not yet clear whether this is a significant increase. The important conclusion to be drawn, however, is that although the solute element additions raised the c.r.s.s. some 6-9 times and, as a consequence raised the fracture stress some four to five times (since flow is a prerequisite for fracture), the cleavage fracture energy remained approximately

* Here, ϕ_I is the energy to initiate a cleavage crack and includes the energy expended by plastic relaxation processes during crack nucleation, i.e. when the radius of curvature of the crack tip, $\rho \gg 1$. However, $\phi_I = \gamma$, when $\rho = 1$.

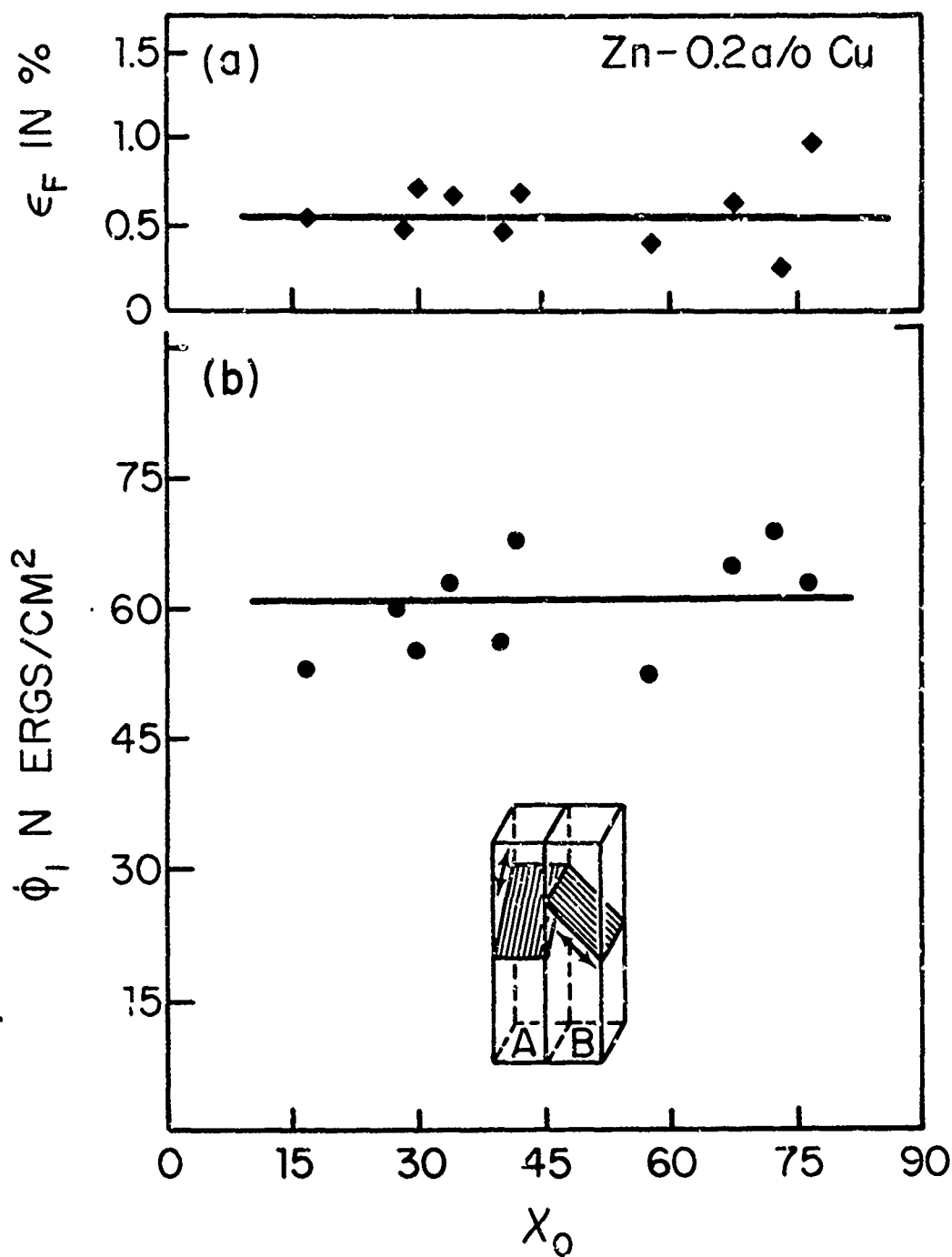


Figure 15. Orientation dependence of (a) the shear strain at failure, ϵ_F , and (b) the energy to initiate cleavage failure on the basal plane, ϕ_1 , for asymmetric bicrystal of Zn-0.2 at. % Cu in the partially amalgamated condition at 298° K (after Kamdar and Westwood⁴).

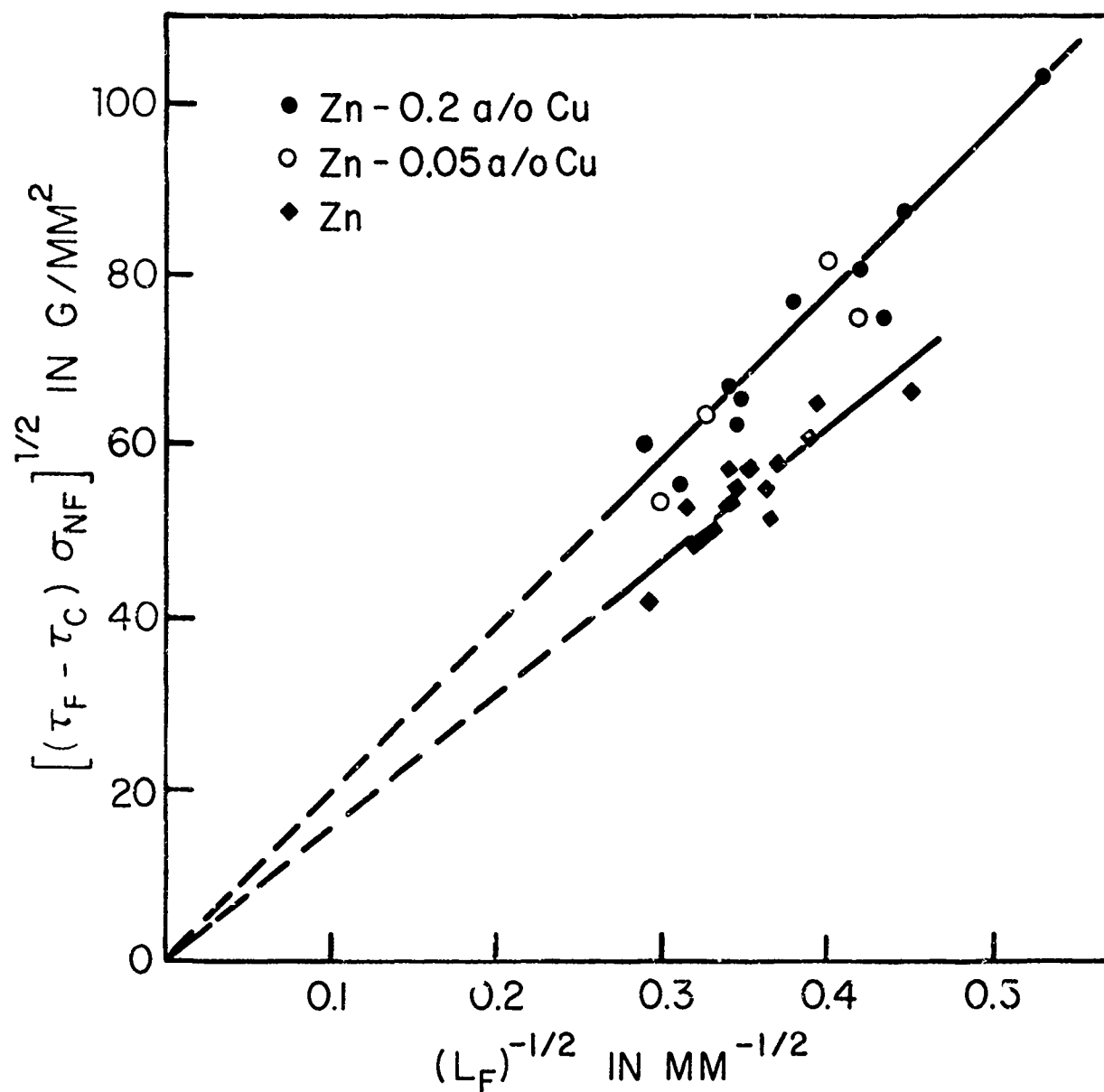


Figure 16. Illustrating linear relationship between the product $[(\tau_F - \tau_C) \sigma_{NF}]^{1/2}$ and $(L_F)^{-1/2}$ for partially amalgamated asymmetric bicrystals of zinc and its alloys tested in tension at 298°K. The correlation shown is equivalent to the Petch fracture stress-grain size relationship (after Kamdar and Westwood^{54, 9}).

constant and about the same as that for unalloyed zinc, Table 4. In other words, the fracture process for these dilute alloys remained effectively controlled by the energy required to break zinc-zinc bonds across the basal plane. It should be noted that the data presented in Table 4 and Figure 16 provide support for the validity of Equation (25) when various additions (0.05% and 0.2 a/o) of copper are made to zinc.

Geometric considerations dictate that the value of L , the slip plane length, should vary considerably with orientation χ_0 . For example, for a 6 mm square crystal, L varies from about 6 to 18 mm as χ_0 varies from 80° to 20° . From Equation (25) the product $[(\tau_F - \tau_C) \cdot \sigma_{NF}]^{1/2}$, in unit of stress, should be inversely related to the square root of the fracture slip plane length, L_F , and the curve should pass through the origin. Data from fracture studies with amalgamed alloyed zinc bicrystals and from earlier studies with pure zinc⁹ are presented in this form in Figure 16, and are seen to be in accord with the predictions. Such a relationship is equivalent to the well known Petch fracture stress-grain size relationship commonly observed for polycrystalline solids. Examples of the validity of the Petch relationship for values of L_F as large as 12 mm ($L_F = 0.29$) and for single or bicrystals are uncommon.

4.7 The Coefficient of Embrittlement for Crack Initiation in the Zn-Hg System

In Section 3.2, a coefficient of embrittlement for crack propagation η_p was defined as the ratio $\phi_{P,A(B)}/\phi_{P(A)}$, $\rho = 1 = \gamma_{A(B)}/\gamma_{(A)}$. For zinc-mercury embrittlement couple, $\eta_p = \phi_p(\text{Zn-Hg}, 298^\circ\text{K})/\phi_p(\text{Zn}, 77^\circ\text{K or } 298^\circ\text{K}) = \gamma(\text{Zn-Hg}, 298^\circ\text{K})/\gamma(\text{Zn}, 77^\circ\text{K})$ was 0.61 ± 0.12 . This value which is

less than unity was taken to indicate that crack propagation in zinc on the basal plane occurs in accord with the adsorption induced reduction in cohesion mechanism. Since crack nucleation and propagation both occur in the same plane (0001) over the temperature 77°K to 298°K , above observation and a consideration of the mechanism of crack nucleation in the presence and in the absence of an adsorption active liquid metal atoms at or near the obstacle suggested that a coefficient of embrittlement for crack initiation, η_I for a zinc-mercury embrittlement couple may also be defined as the ratio of the energy to break atomic bonds across the fracture plane to initiate a cleavage crack in liquid mercury environments, $\phi_I(\text{Zn-Hg}, 298^{\circ}\text{K})$ to that in the absence of mercury in an inert environment (e.g. liquid nitrogen) at low temperatures, $\phi_I(\text{Zn}, 77^{\circ}\text{K})$.^{6,9} Thus, $\eta_I = \phi_I(\text{Zn-Hg}, 298^{\circ}\text{K})/\phi_I(\text{Zn}, 77^{\circ}\text{K})$. If crack initiation in liquid mercury and in inert environments at 77°K occurs in a truly brittle manner such that plastic relaxation processes during crack nucleation are minimized; then η_I should be equivalent to the value of the ratio of the cleavage surface energies, $\gamma(\text{Zn-Hg}, 298^{\circ}\text{K})/\gamma(\text{Zn}, 77^{\circ}\text{K})$. In this case, η_I would be less than unity. Crack nucleation in zinc in liquid mercury therefore may be considered to occur in accord with the "adsorption-induced reduction in cohesion" mechanism of liquid metal embrittlement. Also, $\eta_I \approx \eta_P$, since cleavage in zinc is known to initiate and propagate in the same basal (0001) plane.⁹ It is generally agreed that fracture in liquid metal environments initiates in most cases by the adsorption-induced reduction in cohesion mechanism^{4,8} (Section 3.2 and 3.3). However, no quantitative evidence is yet available in support of the possibility that fracture in these environments may be initiation controlled. Recently,

Kamdar⁶⁹ has made a quantitative evaluation of the coefficient of embrittlement for crack initiation, η_I , in a zinc-mercury couple by determining reliable values of $\phi_I(\text{Zn}, 77^\circ\text{K})$, the fracture initiation energies of zinc in an inert environment at 77°K and $\phi_I(\text{Zn-Hg}, 298^\circ\text{K})$ by reanalyzing the fracture data from amalgamated zinc bicrystal presented in Figure 13. Since fracture nucleation in zinc in liquid mercury and in an inert environment at 77°K occurs by basal cleavage and presumably by the same Bullough⁶³-Gilman⁵⁹-Rozhanskii⁶⁴ mechanism, it is appropriate to use Equation (25), which is a modified version of Equation (13) to derive values of the fracture initiation energies. Accordingly, the tensile cleavage fracture data of Deruyetere and Greenough⁷⁰ and Shchukin and Likhtman⁷¹ for zinc monocrystals and of Kamdar^{72,73} for asymmetric bicrystals of various orientations, χ_0 (where χ_0 is the angle between the tensile axis and (0001) cleavage plane at fracture) and different diameters in conjunction with Equation (25) were used to derive reliable values of $\phi_I(\text{Zn}, 77^\circ\text{K})$ and provide support for the validity of Equation (25).

In agreement with the prediction from Equation (25), it is seen that ϕ_I does not vary significantly with χ_0 or a sixfold change in crystal diameter, Figure 17, the fracture data is represented by a Petch type fracture stress-grain size relationship, Figure 18, (note that similar relationship was also observed for zinc in mercury environments, Figure 16) and that $\phi_I(\text{Zn}, 77^\circ\text{K}) = 100 \pm 20 \text{ ergs/cm}^2$, Figure 17. Using Equation (25) and fracture data from Reference 9 and Figure 13, $\phi_I(\text{Zn-Hg}, 298^\circ\text{K})$ and its variation with χ_0 was redetermined. $\phi_I(\text{Zn-Hg}, 298^\circ\text{K})$ was $\sim 48 \text{ ergs/cm}^2$, Figure 19. This value is about the same as the $(\sim 53 \text{ ergs/cm}^2)$ determined

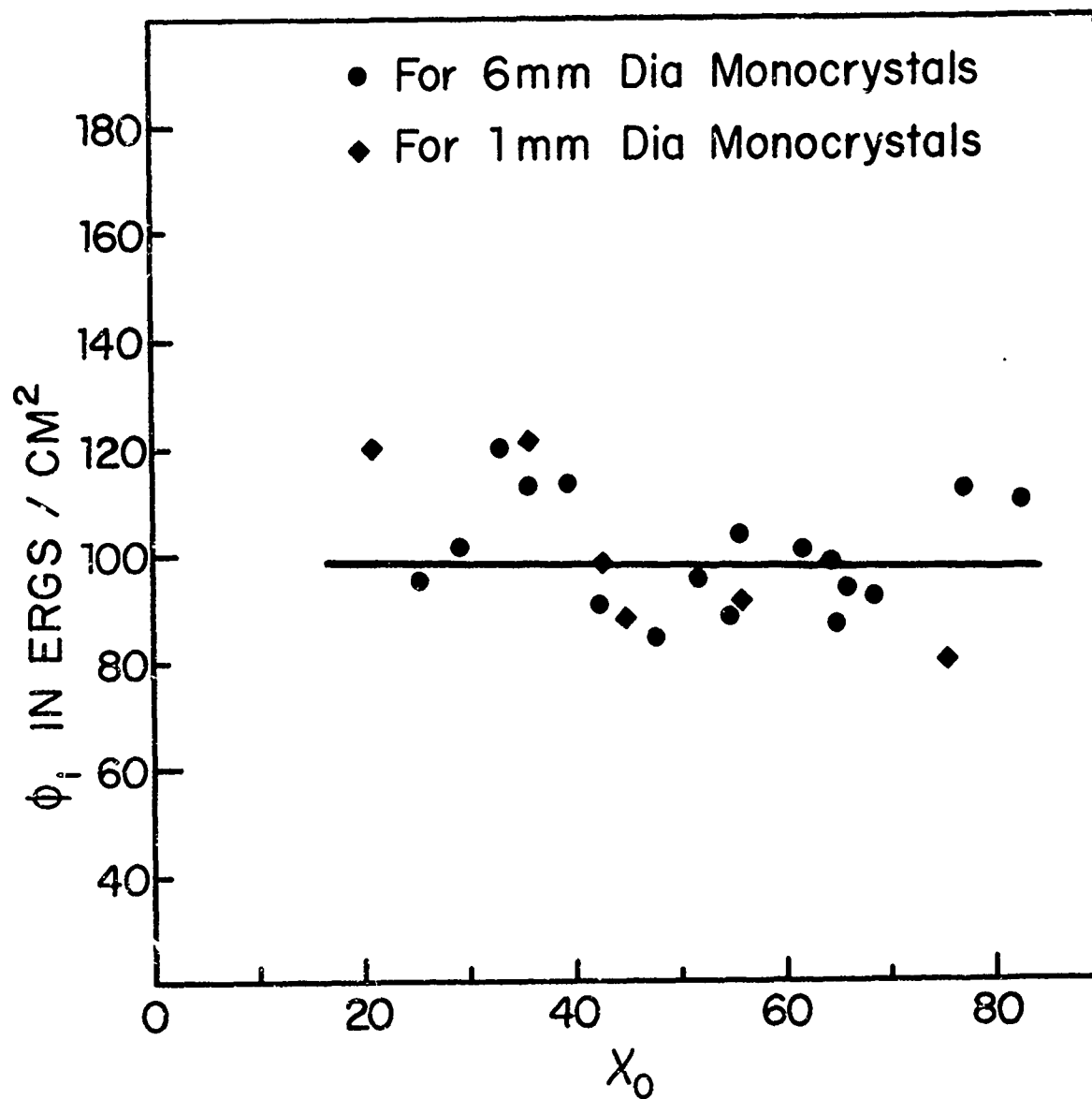


Figure 17. Illustrating the variation of the energy to initiate basal cracks in zinc monocrystals at 77°K with χ_0 and crystal diameter (after Kamdar^{69, 72}).

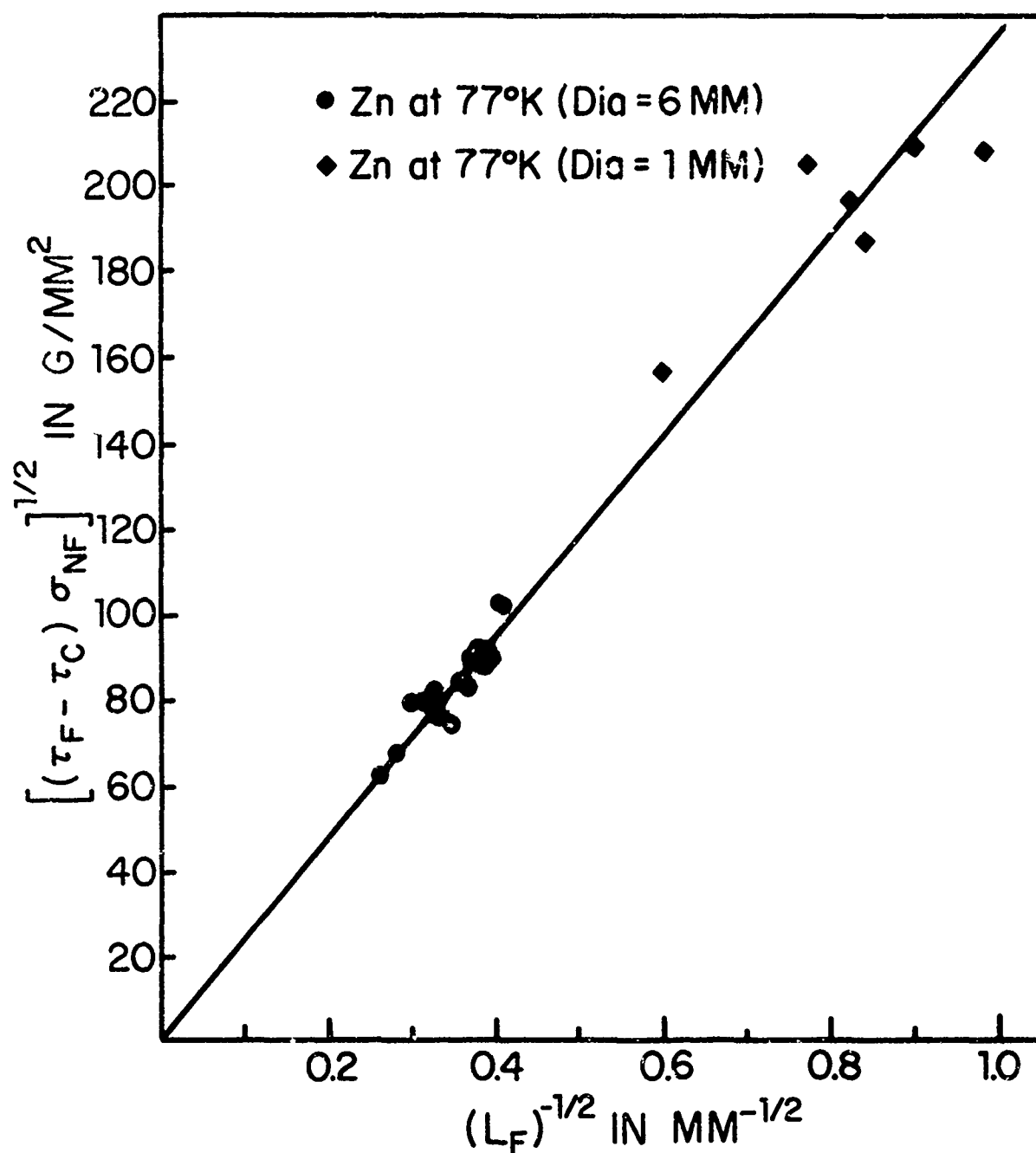


Figure 18. Illustrating linear relationship between the product $[(\tau_F - \tau_C)\sigma_{NF}]^{1/2}$ and $(L_F)^{-1/2}$ for zinc monocystals of 1mm and 6mm dia. tested in tension at 77°K. The correlation shown is equivalent to Petch fracture-stress grain size relationship when L_F varied from 6.02 to 14mm (after Kamdar⁷²).

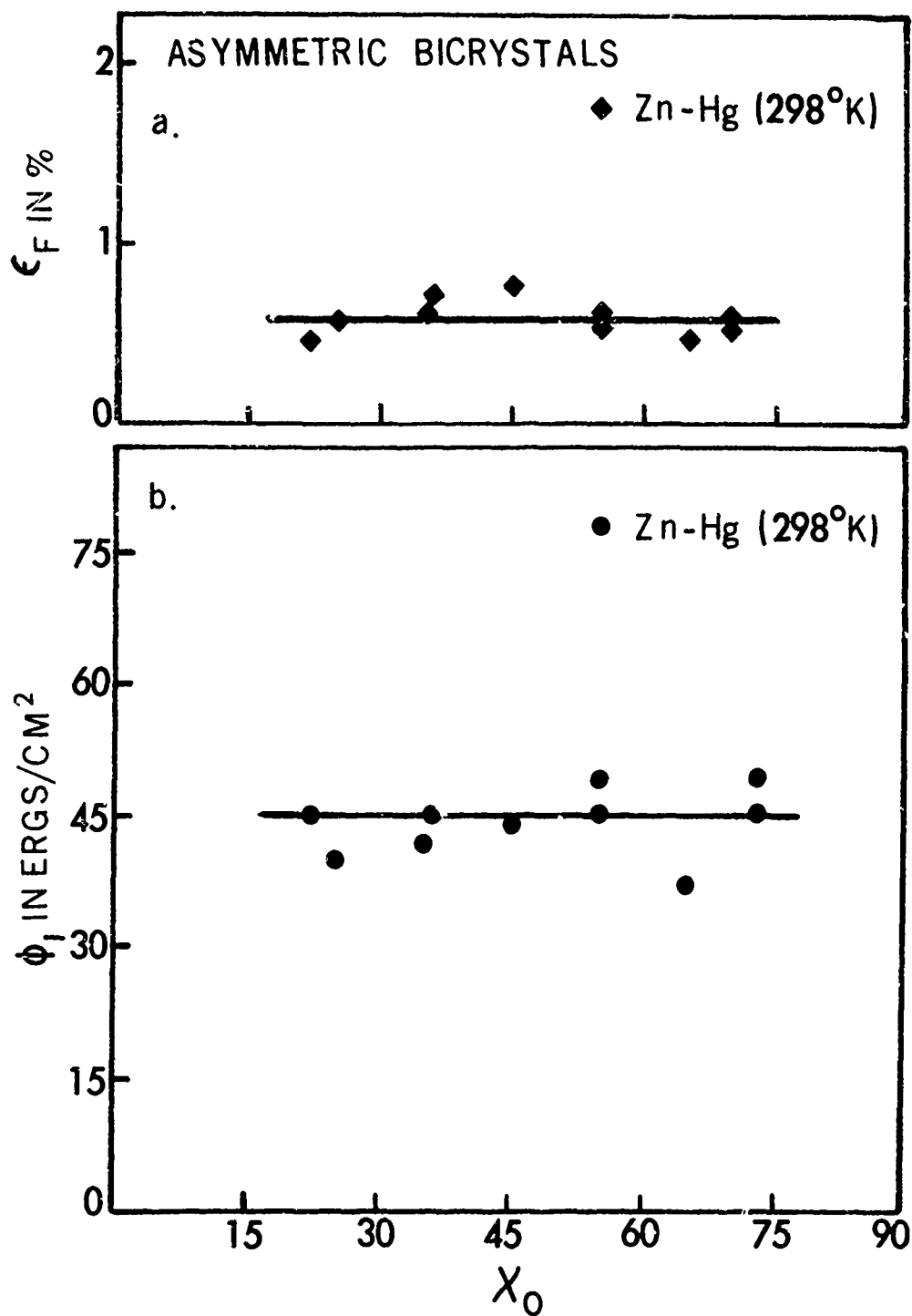


Figure 19. Orientation dependence of i) the shear strain at fracture, ϵ_F , Fig. 19(a) and ii) the energy to initiate cleavage fracture on the basal plane, ϕ_1 , for asymmetric bicrystals of zinc, Fig. 19(b) in liquid mercury at 298°K (after Kamdar⁶⁹).

earlier in Section 4.5. The value of η_I , the ratio $\phi_I(\text{Zn-Hg}, 298^\circ\text{K})/\phi_I(\text{Zn}, 77^\circ\text{K})$ is ~ 0.50 in agreement with that of 0.61 ± 0.12 for η_P , the coefficient of embrittlement determined by Westwood and Kamdar,⁴ (Section 3.3.1). Thus $\eta_I \simeq \eta_P$.

The values $\sim 48 \text{ ergs/cm}^2$ derived for $\phi_I(\text{Zn-Hg}, 298^\circ\text{K})^*$ and $\sim 100 \text{ ergs/cm}^2$ for $\phi_I(\text{Zn}, 77^\circ\text{K})$ are in good agreement with those of ~ 53 and 90 ergs/cm^2 for $\phi_P(\text{Zn-Hg}, 298^\circ\text{K})$ and $\phi_P(\text{Zn}, 77^\circ\text{K})$, respectively, determined by Westwood and Kamdar⁴ using the double cantilever cleavage technique. The value of $\sim 100 \text{ ergs/cm}^2$ computed for $\phi_I(\text{Zn}, 77^\circ\text{K})$ and $\phi_P(\text{Zn}, 77^\circ\text{K})$ is in fair agreement with that of $\sim 185 \text{ ergs/cm}^2$ for $\gamma(\text{Zn})$, the cleavage surface energy of (0001) plane in zinc derived by Gilman^{29,32} from theoretical considerations. Therefore, both $\phi_I(\text{Zn}, 77^\circ\text{K})$ and $\phi_P(\text{Zn}, 77^\circ\text{K})$ are considered to be equivalent to $\gamma(\text{Zn}, 77^\circ\text{K})$, the cleavage surface energy of the basal plane in zinc in inert environments at 77°K .⁷² This suggests that crack initiation in zinc in liquid nitrogen environments (i.e., at 77°K) occurs at energies which are equivalent to that required to break atomic bonds across the fracture plane, and that only small amount of energy is absorbed by plastic deformation processes which cause relaxation of stress concentrations at a barrier during crack initiation. The significant observations, however, are that $\phi_I(\text{Zn-Hg}, 298^\circ\text{K}) < \phi_I(\text{Zn}, 77^\circ\text{K}) \simeq \gamma(\text{Zn}, 77^\circ\text{K})$ and the ratio of these energies, η_I is ~ 0.50 . Now, $\gamma(\text{Zn}, 77^\circ\text{K}) = 90 \pm 10 \text{ ergs/cm}^2$ is about the same as $\gamma(\text{Zn}, 298^\circ\text{K}) = 87 \pm 5 \text{ ergs/cm}^2$.⁴ $\gamma(\text{Zn})$ does not vary significantly with the temperature in the range 77°K to 298°K . Therefore, the energy to break bonds across the fracture plane in liquid mercury environments at 298°K

This suggests that for pure zinc since $\tau_C \ll \tau_F$ (Table 4), the values of fracture initiation energies derived by using Equation (25), a modified version of Equation (13), are essentially the same as that derived by using Equation (13) in Section 4.5.

is less than the cohesive strength of atomic bonds in an inert environment at 77°K and 298°K.⁶⁹ This suggests that adsorption of mercury atoms at the grain boundary in zinc or at the sites of high stress concentrations near a barrier causes reduction in cohesion of atomic bonds across the fracture plane, thereby facilitating crack nucleation in zinc in liquid mercury environments. Therefore, crack initiation in a zinc-mercury couple can be considered to occur by the "adsorption-induced reduction in cohesion" mechanism.

The result, $\phi_I(\text{Zn}, 77^\circ\text{K}) = \phi_p(\text{Zn}, 77^\circ\text{K}) \sim \gamma(\text{Zn}, 77^\circ\text{K})$, is in good agreement with the condition for nucleation controlled fracture, namely $\phi_I = \phi_p = \gamma$, derived by Stroh⁷⁴ and Smith⁷⁵ from theoretical considerations. Thus, fracture in zinc in an inert environment at 77°K is shown to be nucleation controlled.⁷² Theoretical estimates of $\gamma(\text{Zn-Hg}, 298^\circ\text{K})$ are not available. Nevertheless, since $\phi_I(\text{Zn-Hg}, 298^\circ\text{K}) \sim \phi_p(\text{Zn-Hg}, 298^\circ\text{K})$ and $\eta_I \approx \eta_p$, it is suggested that fracture in zinc in mercury environments may be considered to be nucleation controlled.

Extensive investigations with the model embrittlement couple, zinc and its alloys in liquid mercury environments and at low temperatures in an inert environment discussed in these sections provide convincing support for the ideas that liquid metal embrittlement is a special case of brittle fracture and that the embrittlement process occurs by the "adsorption-induced reduction in cohesion" mechanism.⁶⁹

5. EFFECTS OF METALLURGICAL AND PHYSICAL FACTORS

In the previous section, it was concluded that adsorption-induced liquid metal embrittlement can be regarded as a special case of brittle fracture. It is apparent therefore that those factors (e.g. grain size, strain rate, temperature, alloying additions etc.) which tend to induce brittle behaviour in a metal in an inert environment also increase the susceptibility of a solid to liquid metal embrittlement.^{7,39} The effects of these factors on variations in susceptibility to liquid metal embrittlement can be better appreciated by considering the significance of the observation described in the previous section that fracture in zinc-mercury system can be considered brittle and nucleation controlled as defined by $\phi_I = \phi_P = \gamma$, the theoretical condition for nucleation controlled fracture derived by Stroh⁷⁴ and Smith.⁷⁵ Under ideal experimental conditions, therefore, the relief of stress concentrations at the sites of crack nucleation or at the tip of a crack occur by the nucleation and propagation of a sharp crack to fracture rather than by plastic deformation. This suggests that maximum embrittlement has occurred. The severity of embrittlement cannot be increased further in a pure solid-pure liquid metal couple except by selecting a new liquid metal environment thereby altering the magnitude of reduction in the cohesive strength of atomic bonds at a crack tip, i.e. by changing the magnitude of the environment sensitive parameters, σ , described earlier (Section 4.1). However, it is possible to decrease the severity of embrittlement of a solid by increasing the magnitude of the ratio σ/τ by decreasing the magnitude of the structure sensitive parameter τ , without significantly affecting the magnitude of σ . As

Preceding page blank

discussed earlier in Section 4.1, an increase in the magnitude of this ratio may cause a decrease in the susceptibility to embrittlement (i.e. it may increase the stress or strain at fracture or change the fracture characteristics from being nucleation to propagation controlled). If the decrease is high enough, a brittle to ductile transition may occur in the solid with the result that inhibition of embrittlement will occur. The maximum shear stress, τ_{\max} , on a slip plane near a crack tip should be related to the yield stress, σ_y of the solid. τ increasing or decreasing with similar changes in σ_y . σ_y is known to vary with grain size, temperature, strain rate and other factors such as Taylor orientation factor m , the number of available slip systems to satisfy Von Mises criterion for ductility in polycrystals, etc. A quantitative relationship between σ_y and grain size relating to the ductile-brittle transitions in a solid can be described by the well known Cottrell⁷⁶-Petch^{77,78} equation $\sigma_y k_y d^{1/2} \geq \beta \mu \gamma$.^{*} A modification of this equation has been made by Armstrong⁷⁹-Ichinose and Robertson¹⁶ to include the effects of strain rate, temperature and other factors. Thus, the variation in σ_y and hence that in the susceptibility to embrittlement of a pure solid can be related to all these factors. In addition, to these factors, the magnitude of τ or σ_y can be significantly affected by solute additions to solid via solute locking of dislocation sources,⁵⁴ solid solution hardening,³⁹ order-disorder reactions³⁹ and the presence and dispersion of second phases. The magnitude of σ however, may also be affected when large additions of solute are made. In any event, the effects of some of these factors are simultaneous and interrelated. In

* Here k_y is the slope of the linear plot of σ_y against grain size, β , is a factor expressing state of stress, μ is the shear modulus and γ the effective fracture-surface energy.

this section. As far as possible we will use the above considerations while discussing the effects of these various metallurgical and physical factors on the susceptibility of a solid to liquid metal embrittlement.

5.1 Effects of Grain Size

Theories of fracture in metals have been based primarily on the dependence of fracture strength on grain size, d . The significance of grain boundaries is that they constitute an obstacle to plastic flow (i.e. sites for pile up of dislocations) and therefore potential sites of stress concentrations. The magnitude of stress concentrations is related to the pile up lengths or the grain size. The central feature of all pile-up models of brittle fracture is the linear dependence of fracture stress with $d^{-1/2}$. The chief results of investigations of fracture strength of polycrystals in inert environments are summarized in Figure 20. For grain sizes in range I, fracture is nucleation controlled, i.e. once initiated a microcrack propagates to final fracture. In range II, however microcracks form when the yield stress is reached, but they do not cause failure until the stress reaches a much higher value. A linear dependence of fracture stress with $d^{-1/2}$ in the liquid metal embrittlement of a solid will constitute further strong evidence that liquid metal embrittlement is a special case of brittle fracture. It is unlikely that penetration or dissolution of liquid into the grain boundary will result in a linear dependence of σ_F and vs. $d^{-1/2}$. However, such evidence will be in accord with reduction in cohesion mechanism of liquid metal embrittlement discussed earlier.

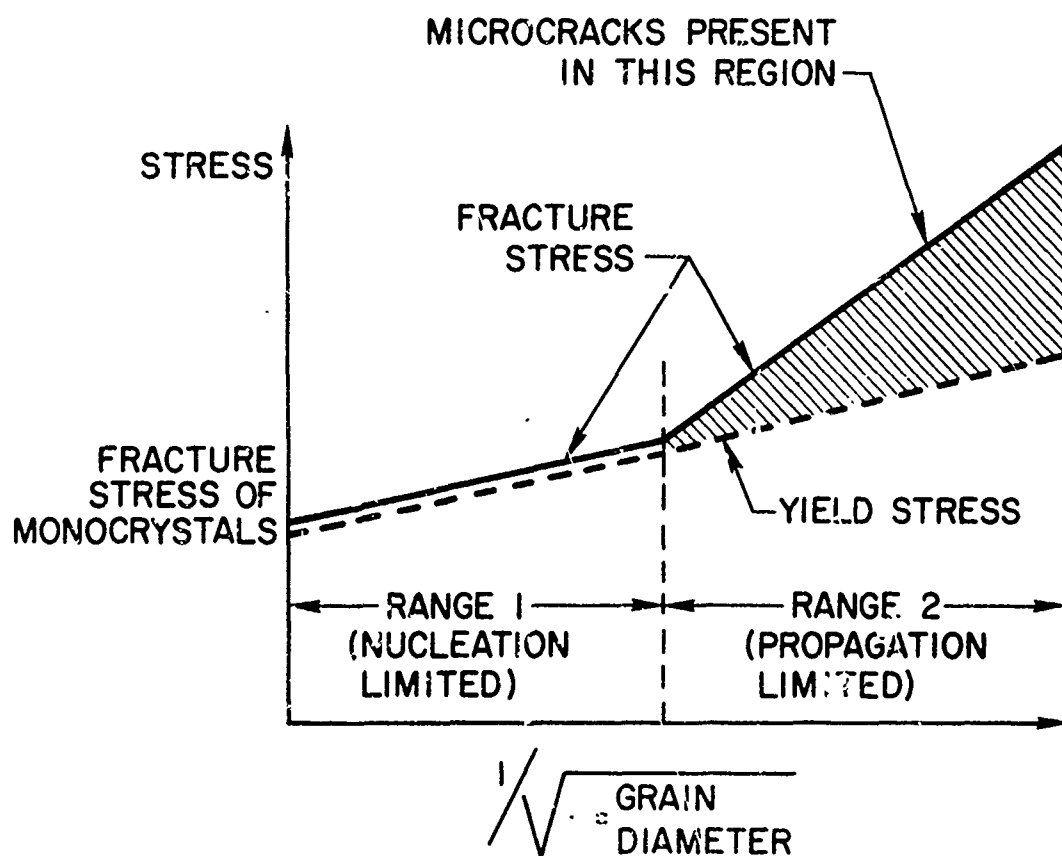


Figure 20. Summary of experimental results on fracture of polycrystals (after Gilman⁵⁹).

In agreement with results summarized in Figure 20, the fracture data from pure zinc polycrystals of various grain sizes tested in tension in a liquid mercury environment provide evidence,⁸² that σ_F did indeed vary linearly with $d^{-1/2}$, Figure 21. In addition, an examination prior to final failure of specimens having grain sizes in range II revealed the presence of unpropagated cleavage microcracks, one or two grain diameters in size, only in grains in which local yielding had occurred.¹³ Such microcracks could not be detected in specimen having grain sizes in range I.¹³ Thus, in range I, fracture is nucleation controlled whereas in range II, it is propagation controlled. From Figure 21, it is seen that the fracture stress is lower than the flow or yield stress of zinc polycrystals. The presence of microcracks only in those grains in which local yielding had occurred indicate that the prerequisite for embrittlement in this case appears to be yielding in favorably oriented isolated grains which corresponds to yielding in a monocrystal rather than general yielding of the polycrystalline material. The values of fracture surface energy derived from the σ_F vs. $d^{-1/2}$ plot was $\sim 95 \text{ ergs/cm}^2$ and that derived by using Equation (25) (assuming fracture initiated in grain oriented at 45° to tensile axis and $d = L$) was several times larger than this value. Note that these values are considerably higher than the value of ($\sim 50 \text{ ergs/cm}^2$) reported earlier for (Table 4) zinc bicrystals tested in liquid mercury environment. The significance of this value of fracture energy, and fracture occurring below the flow stress on the fracture nucleation process in zinc polycrystals, will be discussed later while discussing the effects of dilute alloying additions on the embrittlement of zinc in liquid mercury.

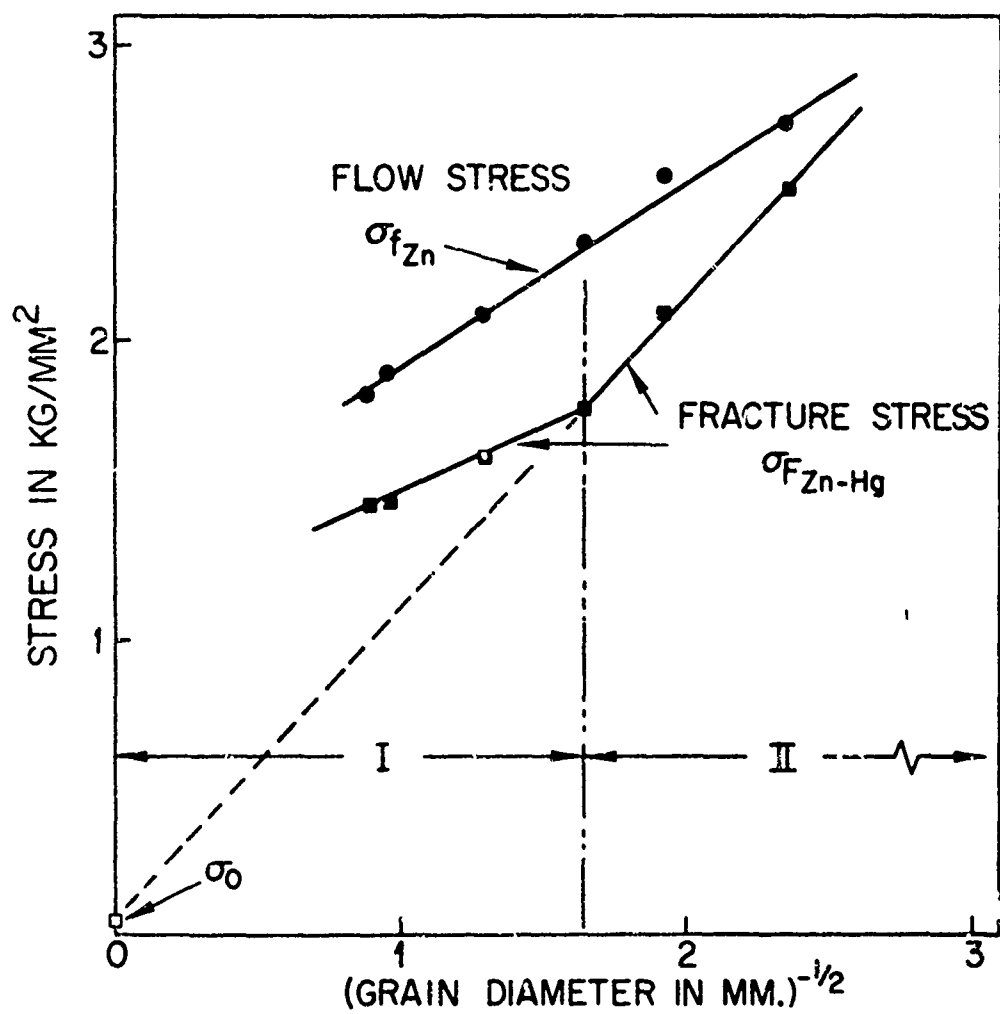


Figure 21. Variation of the flow stress of amalgamated zinc polycrystalline specimens, $\sigma_{f,Zn}$, and fracture stress of amalgamated zinc specimens, $\sigma_{F,Zn-Hg}$, with grain size at 298°K (after Westwood⁸²).

In contrast to the fracture behavior of zinc-mercury couple, Stoloff et al.⁸ observed that the fracture stress of cadmium in liquid gallium was the same or higher than the flow stress. This behavior is in agreement with the general prerequisite that yielding must precede brittle fracture (See Section 4.2). The fracture stress, however, did vary linearly with $d^{-1/2}$ and the fracture mode was predominantly transgranular supplemented by intergranular fracture.⁸ Fracture in liquid gallium environment appears to be propagation controlled. A crack initiated in liquid gallium runs ahead of the liquid, stops and becomes blunted. The blunted crack repropagates only when the liquid arrives or is present at the crack tip. These observations are taken to provide evidence in support of the adsorption-induced reduction in cohesion mechanism.⁸ Thus, adsorption of liquid at the crack tip reduces cohesion at the tip such that a lower stress concentration and hence a lower applied tensile stress is required to propagate a blunted crack in liquid metal environment than that in air.

Another example of propagation controlled fracture is that of copper - 4 w/o silver alloy tested in liquid mercury - 5% zinc solutions.⁸³ In this alloy, cracks were found to develop below the fracture stress but only after general yielding had occurred. The frequency of such cracks increased with increasing stress level and final fracture occurred by the linking up of such nonpropagating cracks.

When tested in air, many ductile metals, e.g. copper, alpha brass, cadmium, nickel, etc. reveal no grain size dependence of fracture, if indeed the latter can be measured at all. However, when each of these metals is tested in appropriate liquid metal environment (lithium or mercury on

copper, mercury on brass, gallium on cadmium and lithium on nickel) the fracture stress σ_F becomes proportional to $d^{-1/2}$ and obeys the well known Petch relation.¹¹

5.2 Effects of Temperature

Temperature can affect the susceptibility to liquid metal embrittlement of a solid (i) by causing the crack tip to become blunted at elevated temperatures either due to increased ductility (τ decreases) of solid or due to dissolution at the tip in the liquid metal environment and (ii) by controlling the rate of arrival or diffusion of the liquid metal atoms to the propagating tip. It is possible that temperature may have little effect on the susceptibility to embrittlement. The observation that susceptibility sometimes increases with decreasing temperature⁴¹ Figure 22, or that embrittlement can occur near the freezing temperature of a liquid saturated with host solid⁴ (See Section 3.3.1) is often times taken as an evidence that embrittlement does not involve thermally activated diffusion or dissolution dependent processes. It is generally considered that at low temperatures (i.e. temperatures in the vicinity of the melting point of the liquid metal) liquid metal embrittlement is a relatively temperature insensitive phenomenon and that diffusion in the conventional sense may not be an important factor. However, it is known that in many embrittlement couples the liquid metal must be present at the crack tip to sustain propagation of a brittle crack in a ductile metal, as for example, was noted in polycrystalline cadmium embrittled by liquid gallium.⁸ Thus, the effects of temperature on the transport of liquid phase to the crack tip in controlling the susceptibility to embrittlement should be important, however,

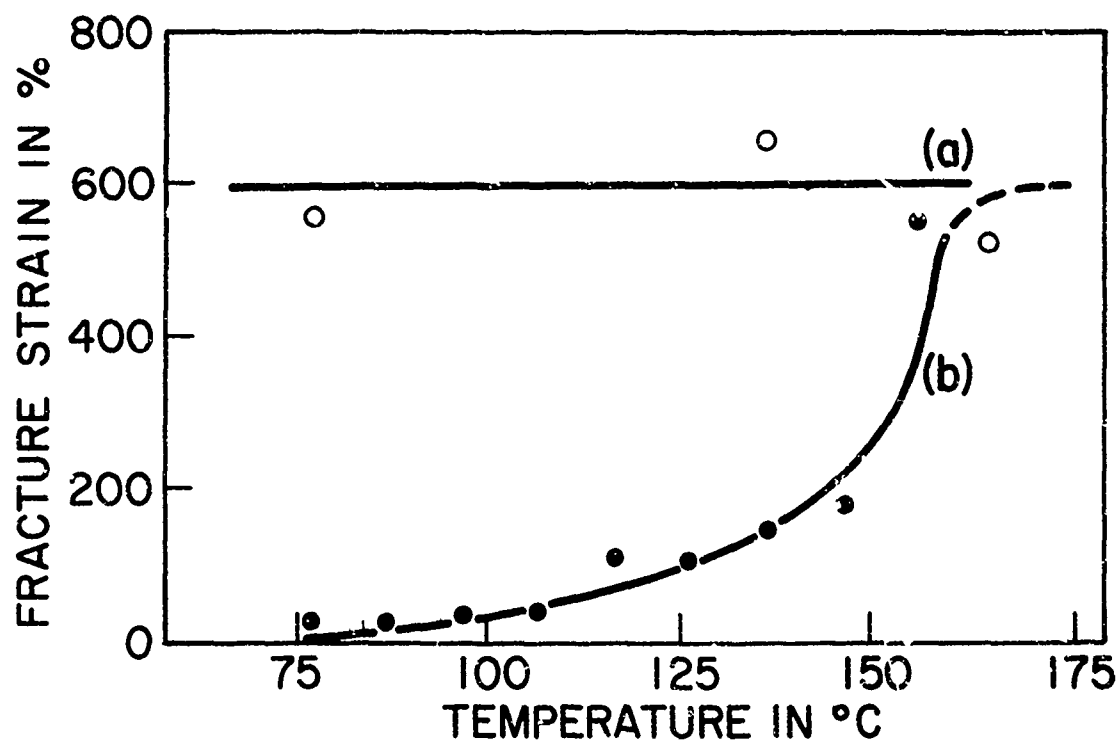


Figure 22. Dependence of strain at fracture on temperature for (a) unamalgamated, and (b) amalgamated zinc monocrystals of ~1mm diameter (after Rozhanskii et al.⁴¹).

concerning such effects little theoretical or experimental work of sufficient precision is available at the present time. In most instances, embrittlement is not observed below the freezing temperature of the liquid indicating that embrittlement by the vapor phase or atoms transport by vapor phase is not responsible for embrittlement.* In one instance, however, the embrittlement of steels containing 0.3 w/o lead in the matrix was observed at 200°F below the freezing temperature of lead. Such effects may arise due to impurities in the steel which lower the melting point of lead.

At an elevated temperature, commonly termed the transition temperature, T_C , a metal may undergo sharp transitions from brittle to ductile behavior when tested in a liquid metal environment. Metals, such as brass,⁸⁴ aluminum^{80,81,84} and titanium¹⁶ when tested in appropriate liquid metal environments are known to undergo such transitions. The example of brittle-ductile transitions occurring in aluminum tested in mercury - 3% zinc solutions is shown in Figure 23. It is seen that above T_C fracture stress in mercury is the same as that in air. Following an analysis of the effects of time and temperature, on the fracture stress of brass and aluminum both in liquid mercury and in air, the absence of variation in the fracture stress of aluminum in liquid mercury from that in air above T_C may be taken as an evidence that diffusion of liquid into the grain boundary can be neglected as the cause of embrittlement at elevated temperatures.³ The transition temperature increases with a decrease in grain size or an increase in strain rate, $\dot{\epsilon}$, Figure 23. T_C varied linearly with $-d^{-1/2}$ and $d^{-1/2}$ in tin-10% zinc and mercury-3% Zn solutions, respectively. Such changes in T_C with grain size (i.e. $T_C \propto d^{-1/2}$ or $-d^{-1/2}$) are shown to be in agreement with a

* Except for those examples of embrittlement by the vapor phase which are discussed in Section 2.2.

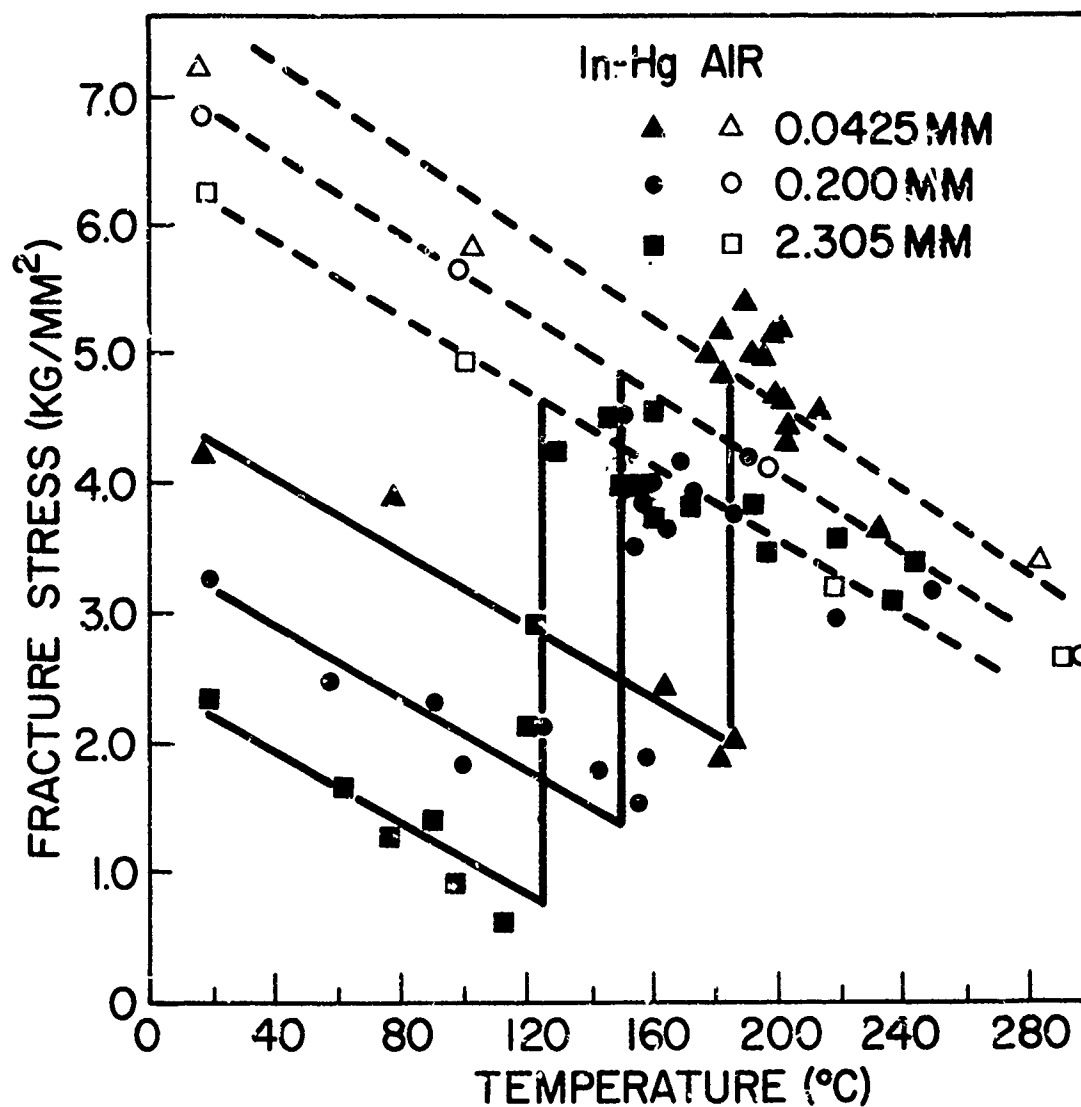


Figure 23. Fracture stress of annealed specimen of aluminum in mercury -3% zinc solution as a function of temperature and three grain sizes (after Ichinose⁸⁰).

modification of the Petch^{77,78}-Stroh⁶¹ analysis of the ductile-brittle transitions in metals. This analysis however, is not in agreement with either the Petch analysis or its modification by Armstrong⁷⁹ where it was shown that T_C should vary linearly with $\log d$ or should be invariant with grain size. In brass tested in liquid mercury, T_C did in fact vary linearly with $\log d$,⁸⁴ Figure 24. The change in T_C with $\log \dot{\epsilon}$ for aluminum tested in mercury 3.0% Zn and tin-10.0% zinc is in accord with the Petch^{77,78} analysis. Robertson¹⁶ has shown that the T_C for titanium tested in liquid cadmium varies linearly with $\log \dot{\epsilon}$, Figure 25. The slope of the line which separates brittle behavior from ductile behavior in Figure 25, is -75°C per unit change in $\log \dot{\epsilon}$. This change in T_C with $\dot{\epsilon}$ is about the same as that of -58°C per unit change in $\log \dot{\epsilon}$ observed in the variation of the yield stress of titanium with temperature and strain rate. In either case the change is about the same. This means that at T_C , if the yield stress is at a critical value — this value being achieved by selecting a proper combination of the temperature and strain rate — equal to or greater than the fracture stress, then a change in test temperature by $\sim 60^\circ\text{C}$ and a unit change in strain rate cause the yield stress to remain at the critical value necessary for the occurrence of fracture, i.e. for the transition to occur from ductile to brittle fracture. These results then support Petch's hypothesis that ductile brittle transition occur when $\sigma_F \simeq \sigma_y$, assuming of course that σ_F is relatively insensitive to variations in temperature, and that σ_y varies linearly with temperature. Such results for the brittle-ductile transitions in metals in liquid metal environments indicate that embrittlement arises due to liquid metal adsorption induced

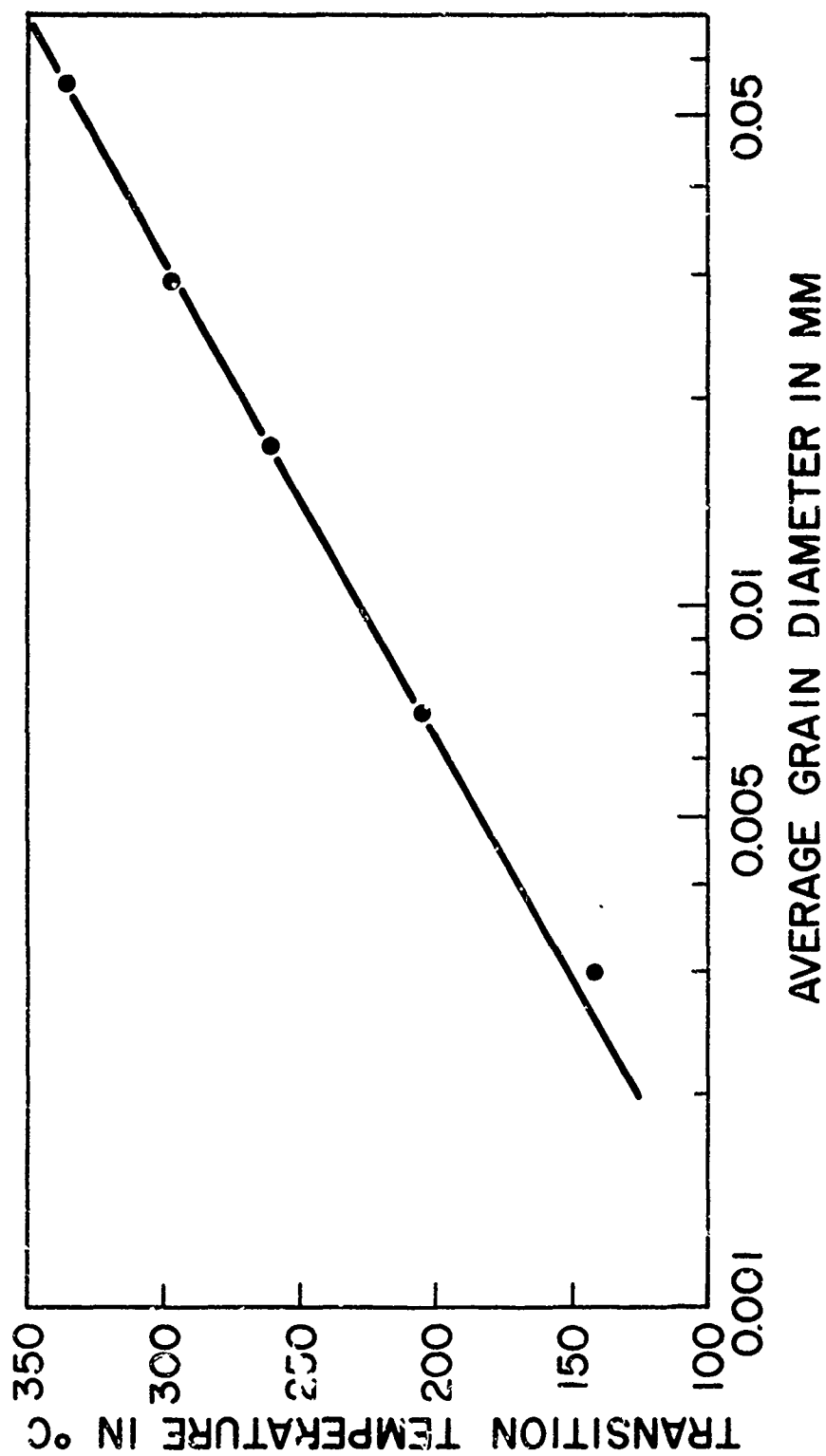


Figure 24. Correlation between brittle to ductile transition temperature for amalgamated 70-30 brass specimens and log of the grain diameter (after Nichols and Rostaker⁸⁴).

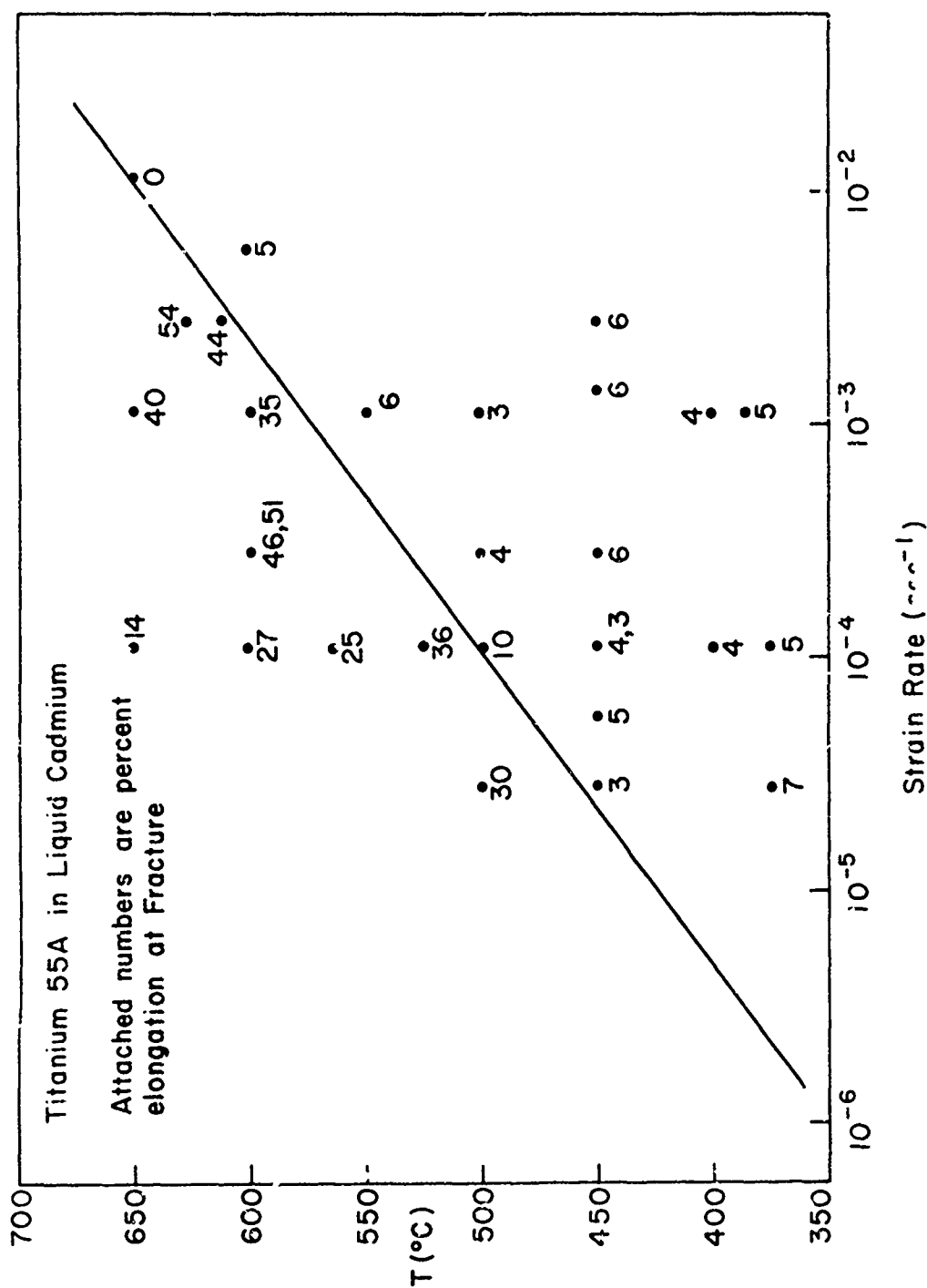


Figure 25. Temperature and strain rates at which titanium -55A was tested in liquid cadmium. The attached numbers give the elongation at fracture for each test. The line separates the region of ductile behavior from the region of brittle behavior (after Robertson¹⁶).

reduction in atomic cohesion at the crack tip. The inhibition of embrittlement at elevated temperature is caused by the fact that it is difficult to initiate or propagate a brittle crack in a solid whose yield stress had decreased significantly with increase in temperature. In some instances, it is possible that crack blunting is caused by dissolution at the crack tip at elevated temperatures and this then is responsible for the inhibition of embrittlement. Here also, the stress necessary to propagate a blunted crack is high such that yielding at the crack tip is preferred to fracture.

At temperatures between the freezing temperature and the transition temperature, however, it does appear that the severity of embrittlement is relatively insensitive to temperature, except in situations where the rate of diffusion of the liquid metal atoms to the crack tip is a controlling factor. When the liquid metal is already at the crack tip before the material is stressed, then the magnitude of the energy to propagate a crack, ϕ_p , is not markedly affected by variations in temperature of, say, 60°C, Figure 4. Studies of the rate of crack propagation through polycrystalline sheet, on the other hand, have revealed various effects.⁸⁵ For Al 2024-T4 plate wetted with liquid mercury, Figure 25, the rate of crack propagation increases with temperature. The variation is small, however, and leads to apparent activation energy of only about 0.05 eV. Rhines et al.⁸⁵ comment that it seems doubtful that this value could be associated with any chemical reaction process, but it may be associated with a change in viscosity of the mercury with temperature. An alternate possibility is that this value represents the activation energy for second monolayer diffusion of mercury

to the crack tip. For polycrystalline 70-30 brass, the cracking rate at first increases and then decreases, Figure 26. Rhines et al.¹⁵ suggest that the decrease at temperatures above 50°C in brass is associated with the formation of intermetallic compounds with components of the brass which "choke off" the mercury flow to the crack tip. However, the solubility of copper in liquid mercury is very small at 50°C, and zinc, which is soluble to about 10 a/o in liquid mercury at 50°C, does not form compounds with mercury which are stable at this temperature. An alternative possibility is that the reduced rate of crack propagation is associated with an increased rate of "sideways" intergranular penetration. Studies with bicrystals could clarify the actual cause of this effect.

One of the major points of concern in understanding the nature of liquid metal embrittlement has been to explain the high rates of cracking sometimes observed in otherwise ductile metals in view of the requirement that the liquid metal be continuously present at the propagating crack tip. There is evidence that the fluid mechanics of the system controls the rate at which the bulk liquid metal travels to the vicinity of the crack tip.⁸⁵ However, there is some discussion of how close the bulk liquid metal can get to the tip before transport by some other process, such as mono- or bi-layer diffusion, is required. Rostoker et al.² suggest that a driving force of 10^5 atmospheres would be required for "bulk" liquid metal to be present at an atomically sharp crack. However, it has been pointed out that capillarity effects could provide "negative" pressures of order $10^4 - 10^5$ atmospheres which would pull the liquid metal into very small cracks, aiding transport to the tip.^{40,37}

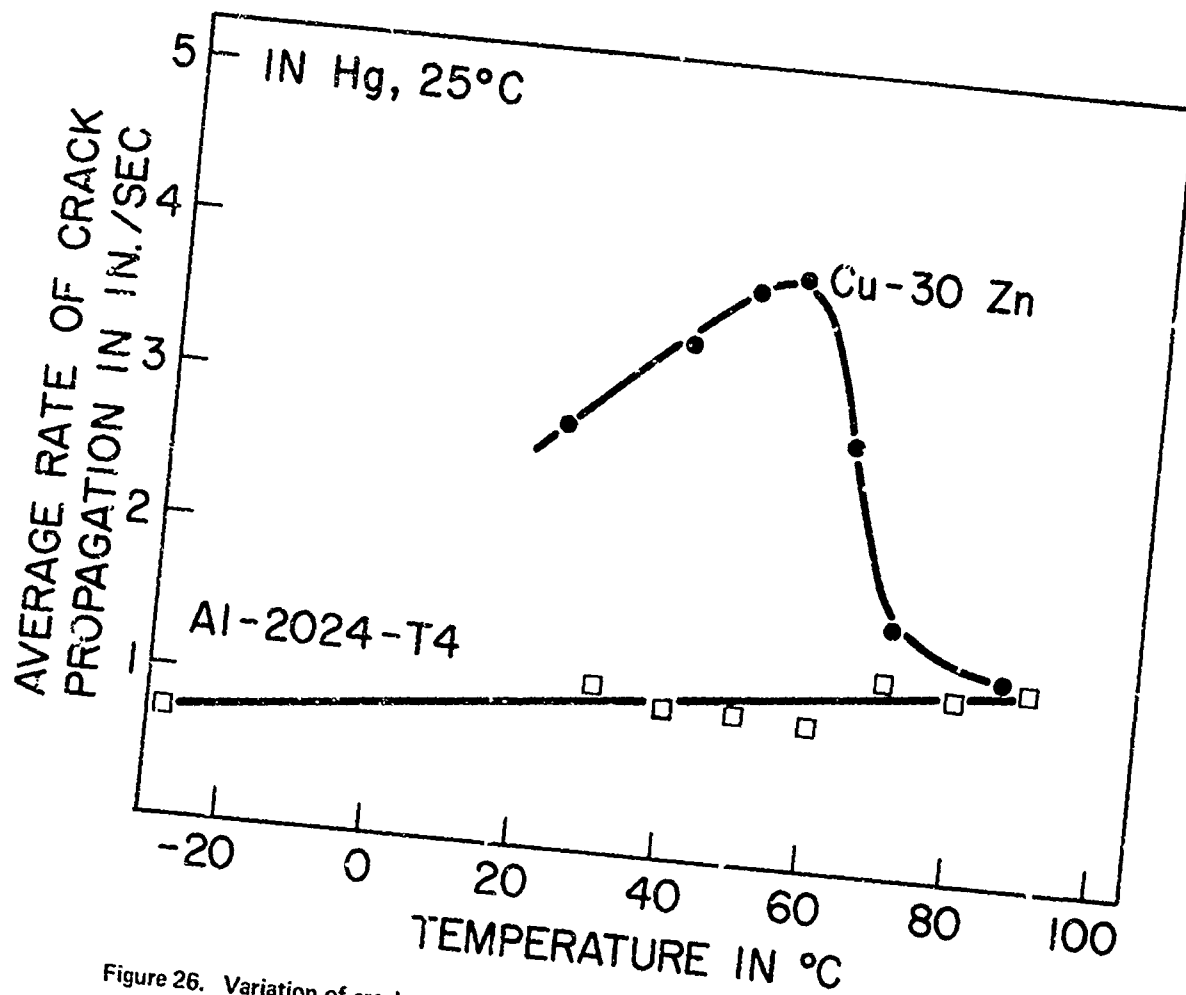


Figure 26. Variation of crack propagation rate with temperature for amalgamated polycrystalline brass or aluminum alloy specimens (after Rhines et al.⁸⁵).

If it is assumed that the liquid metal atoms proceed from the bulk liquid phase to the crack tip by monolayer diffusion, say of liquid mercury on zinc, then the observed crack propagation rates may be difficult to explain because this can be rather a slow process. On the other hand, since it is known that liquid metal atoms are expendable in the embrittlement process — presumably because they become stably adsorbed on the freshly created fracture surfaces — it can be argued that transport to a propagating crack tip probably occurs by a second monolayer process, e.g., by mercury atoms over mercury atoms, and not mercury atoms over zinc atoms.⁴ While the actual value of the activation energy, Q , for the second monolayer diffusion of mercury on mercury has not been determined, Q for cesium on cesium is ~ 0.1 eV, and $D_0 \sim 10^{-2}$ cm²/sec at about 30°C.⁸⁶ These values suggest that second monolayer diffusion should be capable of maintaining a sufficient supply of liquid metal atoms at the crack tip to explain observed rates of crack propagation.

Robertson⁴⁰ has also considered the problem of high rates of crack propagation on the basis of a dissolution model for liquid metal embrittlement. He estimates that the diffusion of solid metal atoms away from a crack tip via the liquid metal phase can occur sufficiently rapidly to produce crack propagation rates of 10-4000 cm per sec.

5.3 Effects of Alloying

Pure metals are embrittled by liquid metals, for example, zinc by liquid mercury and cadmium by liquid gallium. However, in many instances pure metals such as iron and copper* were considered immune when tested in

* Course grain copper has been shown to be embrittled by mercury.¹¹

liquid mercury although iron and copper base alloys, particularly brasses, are known to be significantly embrittled by liquid mercury and the embrittlement of brass by mercury constitutes a classic example of liquid metal embrittlement.

In general, the susceptibility of a pure metal to embrittlement increases with increasing solute content (e.g. iron and copper base alloys in liquid mercury environment^{48,39,87}) provided that grain size and external test conditions are kept fixed. An increase in the yield stress with solute content caused by solid solution hardening is considered responsible for the increased susceptibility to embrittlement.⁴⁸ This alone, however, does not constitute a sufficient condition for embrittlement. The effects of alloying on the specific factors that affect yielding are important and should be considered, while discussing the susceptibility of the solid to embrittlement.^{39,87} These factors are the ability to deform on a sufficient number of slip systems to satisfy Von Mises criterion for ductility in polycrystals, reduced tendency for cross slip caused by lowering of stacking fault energy, the occurrence of order-disorder reaction, and dislocation source locking by impurities when applicable.

5.3.1 Embrittlement of dilute zinc alloys

When polycrystalline zinc is alloyed with small amounts of copper or gold in solid solution, its susceptibility to embrittlement by liquid mercury is markedly increased.⁵⁴ Specifically, additions of 0.2 at .% of either copper or gold to polycrystalline zinc of 1 mm grain diameter do not change its flow stress significantly from 1.9 kg/mm², but reduce the tensile fracture stress of amalgamated specimens from 1.4 kg/mm² to 0.46 kg/mm²,

Figure 14; that is, to 25% of the flow stress of such alloys. The fracture stress of alloys is not sensitive to a temperature variation of $\sim 60^{\circ}\text{C}$, Figure 14, whereas the fracture stress of pure zinc in the presence of mercury is reduced from 1.4 Kg/mm^2 to 1.1 Kg/mm^2 , i.e. approximately 30% by decreasing the temperature from 298°K to 240°K .^{7,88} Since it is known that the stress to propagate a crack in zinc in the presence of mercury is not affected by temperature in this range, Figure 4, it must be the crack initiation process which is temperature sensitive for pure zinc in liquid mercury environments. Also, it can be seen from Figure 14 that the fracture stress of amalgamated polycrystalline zinc is reduced from 1.4 Kg/mm^2 to 0.46 Kg/mm^2 by the addition of 0.2 at % of solute, and that this value is not reduced further by greater additions. This suggests that 0.46 Kg/mm^2 may be the minimum stress for crack initiation in zinc alloys of $\sim 1 \text{ mm}$ grain size. It is of interest to apply Equation (25) and compute a value for the energy to initiate failure in such specimens. Assuming that fracture nucleates by cleavage on a basal plane oriented between 35° and 65° to the tensile axis, and taking τ_c to be 95 g/mm^2 the average c.r.s.s. for Zn-(0.2-0.4 at %) Cu alloys, Figure 14 and $L_F = 1 \text{ mm}$, ϕ_I (Zn-0.2 to 0.4 a/o Cu-Hg, 298°K) is computed to be between 52 and 66 ergs/cm^2 . Considering the assumptions, this value is in remarkable agreement with that of 60 ergs/cm^2 derived from the studies with alloy bicrystals (see Table 4, Section 4.6). This suggested that since fracture in alloyed bicrystals is nucleation controlled the same should be true for the polycrystalline alloys. Metallographic examinations of the alloy polycrystal specimen loaded to a stress just below the fracture stress did not reveal any microcracks indicating thereby that fracture is indeed nucleation controlled.

A possible explanation for the effects of alloying on the susceptibility to embrittlement by liquid mercury of zinc- mono-, bi-, and polycrystals described earlier in Sections 4.5, 4.6, and 5.1, may be developed, however, by considering the influence of alloying on τ_c , Figure 14. For the zinc mono- and bi-crystals, dislocation multiplication, slip band formation, and macroscopic plastic flow occur at the c.r.s.s., τ_c . Since fracture is considered to be a consequence of the piling-up of dislocations at some stable lattice barrier such as a kink band or bi-crystal boundary, fracture must be preceded by flow. Thus, the fracture stress τ_F must be greater than τ_c . It follows that since alloying increases τ_c , it must also increase τ_F as observed (Table 4).

For polycrystalline zinc, on the other hand, macroscopic plastic flow occurs at stresses considerably greater than τ_c . The flow stress of polycrystalline pure zinc of ~ 1 mm grain diameter in air, Figure 21, for example, is some 200 times the value of τ_c (~ 10 gm/mm², Table 4) for zinc monocrystals. It will thus be appreciated, nevertheless, that the initiation of yielding in a polycrystal is a localized event, occurring first in a few favorably oriented grains.⁸⁹ When a ductile polycrystal is deformed in an inert environment, the stress concentrations resulting from pile-ups formed at the boundaries of isolated yielding grains are relaxed by dislocation cross slip or climb out of the pile-up, or by plastic flow in the neighboring grain-leading to the propagation of yielding throughout the solid. In a brittle or embrittled polycrystal, on the other hand, stress concentrations at grain boundaries are more likely to be relaxed by the initiation of cleavage cracks. Stress relaxation by crack nucleation rather than plastic

flow will be facilitated (i) if cohesion across the cleavage plane is reduced by chemisorption of some surface-active species, as is considered to be the case in liquid-metal embrittlement, (ii) if dislocation cross slip or climb is inhibited, or (iii) if the generation of dislocations in neighboring grains is made more difficult. It seems likely that the increase in susceptibility of polycrystalline zinc to embrittlement on alloying is related primarily to the last effect. Specifically it may be supposed that alloying zinc with up to 0.5 at .% of copper or gold locks dislocation sources at or near grain boundaries without creating alternative "sources" in the form of second phase particles. As a consequence, the relaxation of stress concentrations at boundaries by plastic flow is inhibited, and crack initiation, leading to catastrophic failure in a mercury environment,^{7,42} is thereby facilitated.

This hypothesis is supported by the data of Figure 14. The data reveals that the initially rapid increase of τ_c with solute concentration, followed by a leveling off at ~ 0.3 at .% solute, is "mirrored" by the decrease in fracture stress of amalgamated polycrystalline zinc on alloying. This strongly indicates the existence of some correlation between these two parameters.

In pure zinc polycrystals of a grain size (~ 1 mm) comparable to that of the alloys, the effects of solute atoms locking dislocation sources will not be present. Relaxation of stress concentration at the grain boundary can therefore occur by cross-slip or by dislocations climbing out of the slip plane. The latter seems a more likely possibility since lightly deformed zinc monocrystals are known to undergo recovery effects at 298°K occasionally with the formation of kink bands.^{90,91,58,36} Due to relaxation effects,

the energy to initiate a crack in pure zinc is several times higher (see Section 5.1) than that of ~ 60 ergs/cm² for the alloys. Nevertheless, fracture in zinc of ~ 1 mm grain size is nucleation controlled, as discussed in Section 5.1. Nucleation controlled fracture does not necessarily imply that maximum embrittlement has occurred. Thus, although fracture in both pure zinc and its alloys is nucleation controlled the susceptibility to embrittlement of zinc and its alloys are significantly different, Figure 14. Thus, nucleation controlled fracture does not necessarily imply that maximum embrittlement has occurred.

5.3.2 Embrittlement of solid-solution and age-hardenable alloys

The addition to copper of the solid solution elements (i.e. zinc, aluminum, germanium and silicon) drastically increases its tendency for brittle failure in mercury. Rosenberg and Cadoff⁴⁸ attributed this behavior to the solid solution strengthening influence of these elements. Thus it can be shown, as in Figure 27, that the ratio σ_F/σ_Y (σ_F is the fracture stress, σ_Y is the yield stress) decreases with increasing yield stress of the alloy system. The yield stress of copper-base alloys, however, is in turn a function of the stacking-fault-energy, (SFE), with yield stress increasing as SFE decreases.^{39,87} Therefore, Stoloff et al.³⁹ suggested that the latter is the fundamental parameter controlling the degree of embrittlement for fcc solid solution alloys. Figure 28(a) shows that σ_F/σ_Y increases linearly with increasing SFE over the range 0 to 20 ergs, the latter being the limit of experimentally determinable energies by means of direct observation in the electron microscope. In a similar manner, the ductility at fracture increases as SFE increases. Since the points for different solute species fall on a common line, Stoloff et al.³⁹ suggested

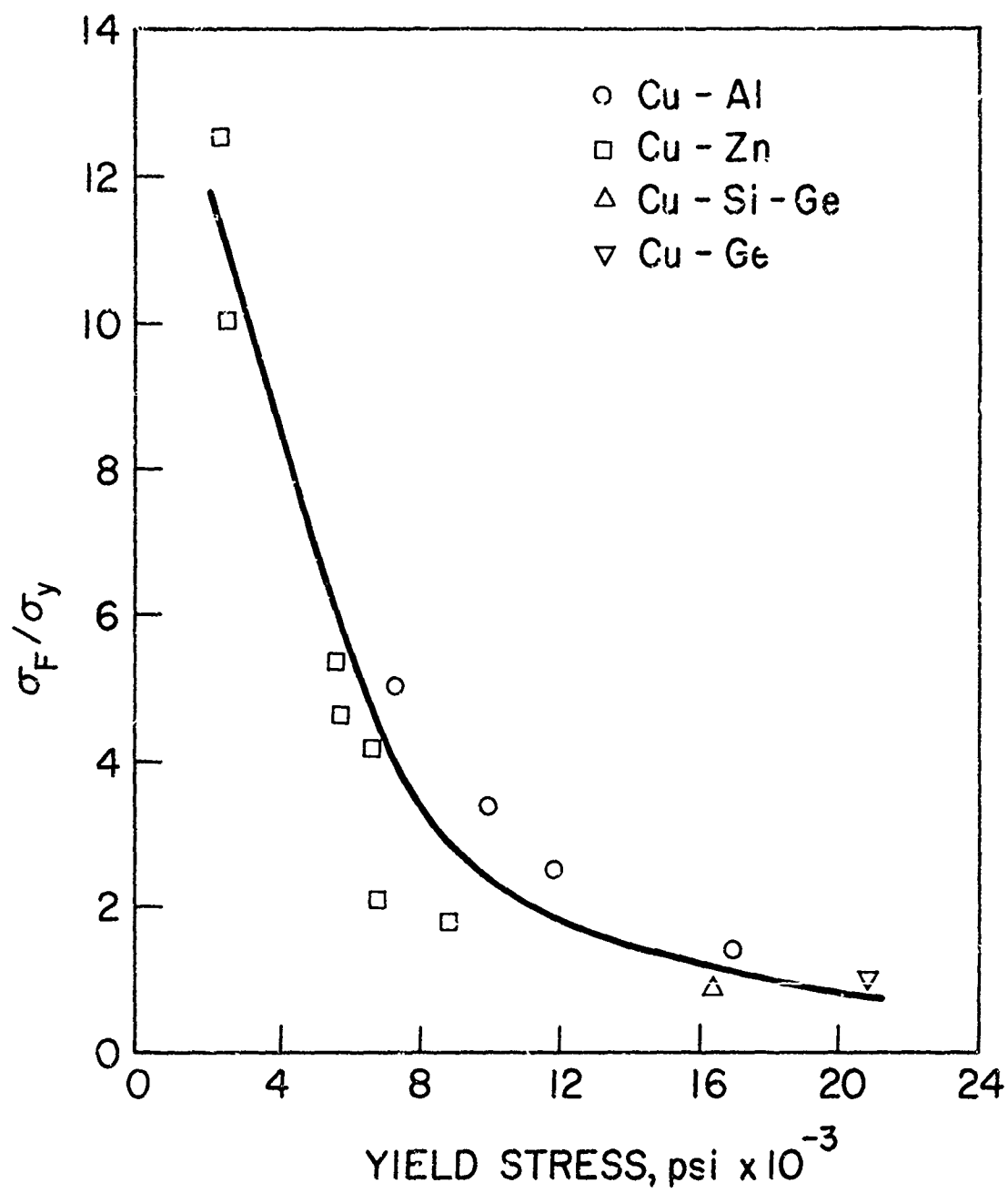


Figure 27. The effect of yield stress, σ_y , on the ratio of fracture-stress, σ_F , to yield stress in copper base alloys tested in mercury at 298°K (after Rosenberg and Cadoff⁴⁸).

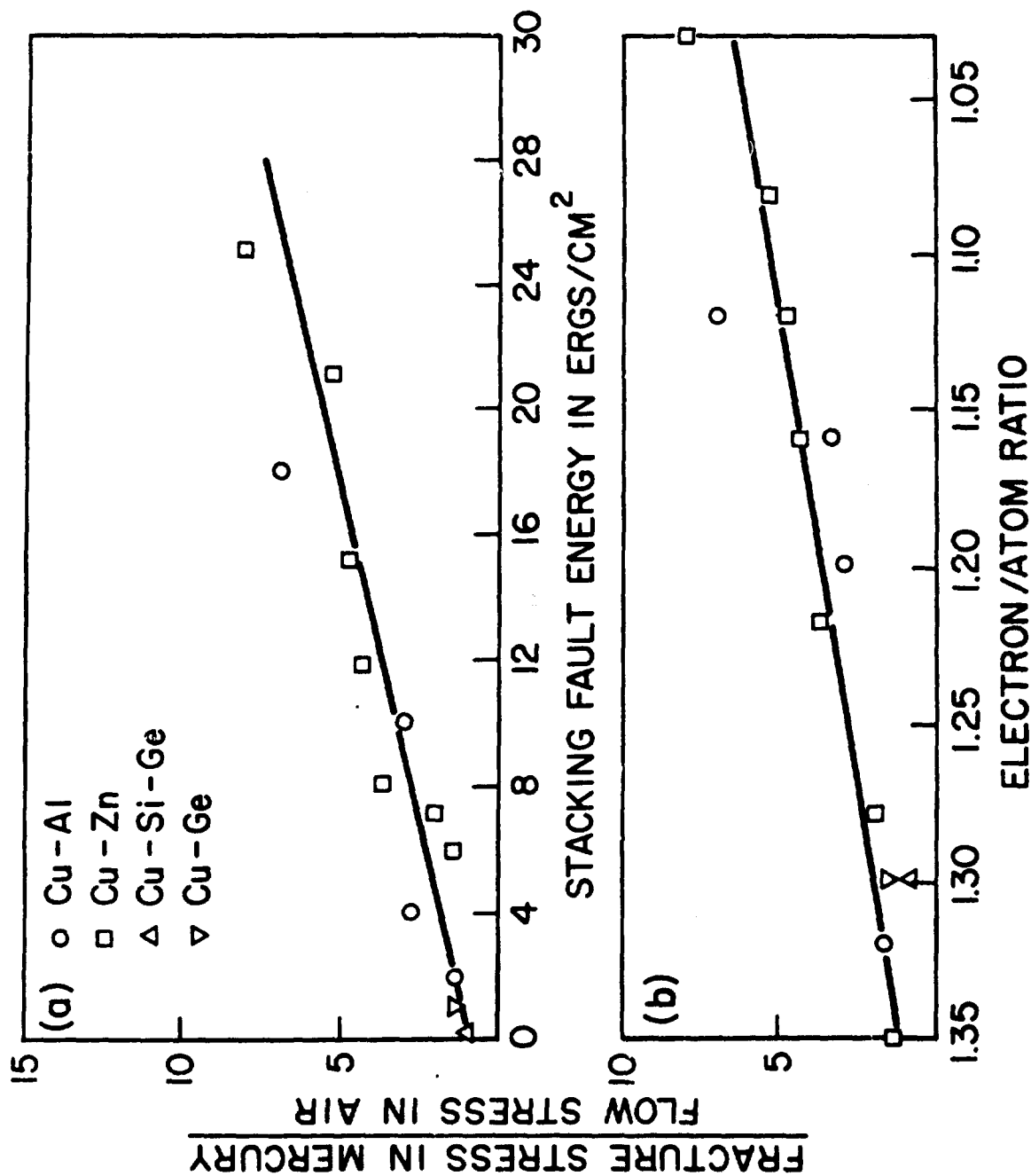


Figure 28. Embrittlement of copper base alloys as a function of (a) stacking fault energy (after Stoloff et al.³⁸), and (b) electron/atom ratio (after Westwood et al.⁷).

that the nature of the chemical species added to copper was immaterial so long as a particular SFE was reached.

The significance of a low SFE is that dislocations piled-up behind an obstacle (grain boundary, tilt boundary or precipitate particle) cannot cross-slip readily in a low SFE material. Hence stress concentrations in the latter quickly build up with strain, to levels capable of nucleating cracks.

In view of the observed relationship in these copper base alloys, between stacking fault energy and susceptibility to embrittlement, it might at first be thought that alloying additions control embrittlement simply via the metallurgical parameter, τ , and that, as Rosenberg and Cadoff⁴⁸ and Stoloff et al.^{39,87} have suggested, the chemical nature of solute species has no pronounced effect. It is known, however, that the electron/atom ratio determines the stacking fault energy of Cu-Zn, -Al, -Si or -Ge alloys (Smallman and Westmacott,⁹⁴ Howie and Swann,⁹² Foley et al.⁹³), and also affects their elastic constants. For example, the observed decreases in $[(c_{11} - c_{12})/2]$ with additions of solutes of valency higher than that of copper are related to the electron/atom ratio of the alloys.⁹⁵ It is apparent, then, that alloying can also affect the bond strength of an alloy, so that in some instances, it may be this factor which actually controls susceptibility to embrittlement. With this possibility in mind, it is of interest to note that the data of Stoloff et al.³⁹ shown plotted against stacking fault energy in Figure 28(a), exhibits an equally good relationship with electron/atom ratio, Figure 28(b). It may be suggested therefore, that the chemical nature of the solute species does play a role in the embrittlement of certain copper alloys because it determines the electron/atom ratio of these materials

and hence (i) their stacking fault energy and the factor τ , and (ii) their elastic properties and hence the parameter σ .

Iron-base alloys also exhibit enhanced susceptibility when certain elements, particularly silicon,³⁹ aluminum³⁹ and nickel,⁵³ are present in solid solution, see Figures 29,30,31. Unalloyed iron is immune to mercury embrittlement, but alloys containing more than 2 at %Si or 4 a/o Al or 8 w/o nickel are increasingly susceptible, Figures 29,30.

The dominant feature of the solute addition appears related to restrictions in the number of slip systems or ease of cross-slip. Transmission electron microscopy and surface observations have revealed that both silicon and aluminum are very effective in suppressing cell formation or wavy glide, and consequently incidence of secondary slip in iron.³⁹ Optical microscopy of deformed iron-nickel alloys revealed that up to 8 w% nickel content, the structure was ferritic with wavy slip lines whereas at higher nickel content the structure was martensitic with coarse slip lines.⁵³ Straight or coarse slip leads to increased likelihood of high stress concentration at grain boundaries with enhanced possibility of crack nucleation.

The change in slip character on alloying may not always represent a necessary condition in determining the effects of solute additions on the susceptibility of a solid to liquid metal embrittlement. It is conceivable that the absence of embrittlement in a mercury environment (noted in a tension test with a smooth specimen having nickel contents of up to 7% w/o Figure 31, or aluminum contents of up to 4%, Figure 29), is due to the fact that fracture is nucleation limited. Thus, although embrittlement may be anticipated for these alloys, the stress concentrations at the surface of the

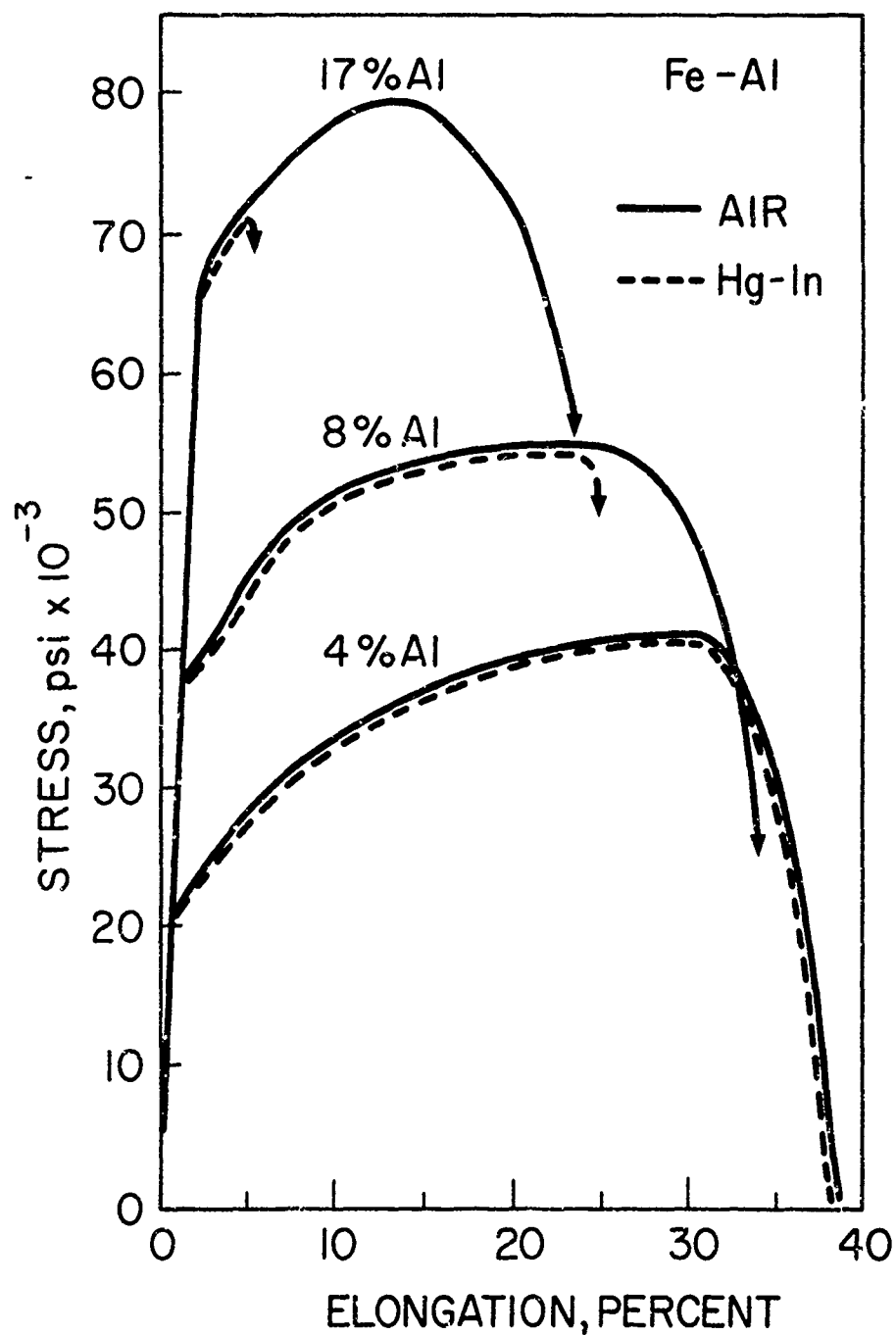


Figure 29. Illustrating the absence of the effect of environment on the yield stress and strain hardening rate on various iron-aluminum alloys tested in mercury-indium solutions (after Szoloff et al.³⁹).

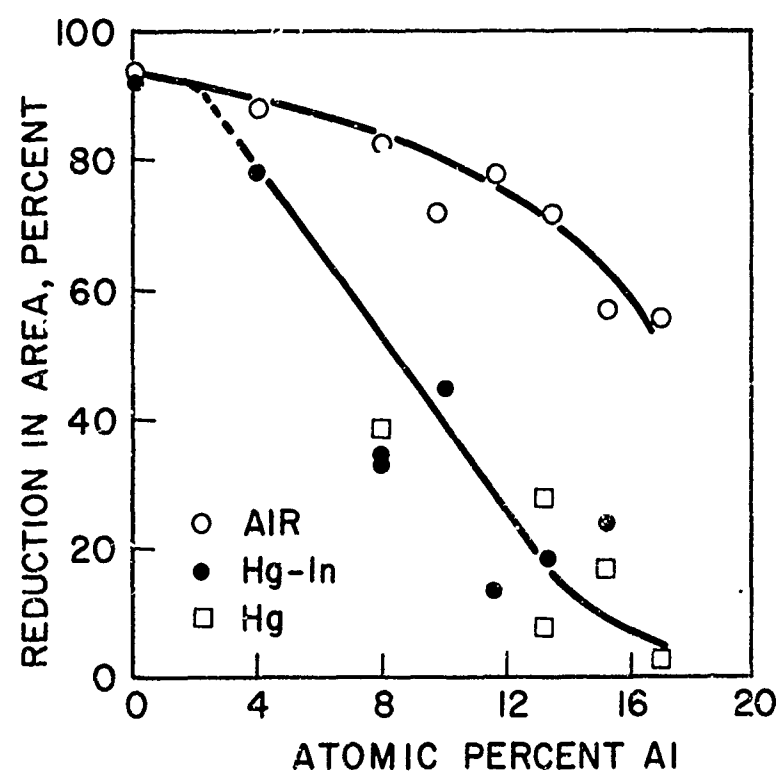


Figure 30. Illustrating the effects of aluminum additions to iron on its susceptibility to embrittlement in mercury and mercury-indium solution (after Stoloff et al.³⁹).

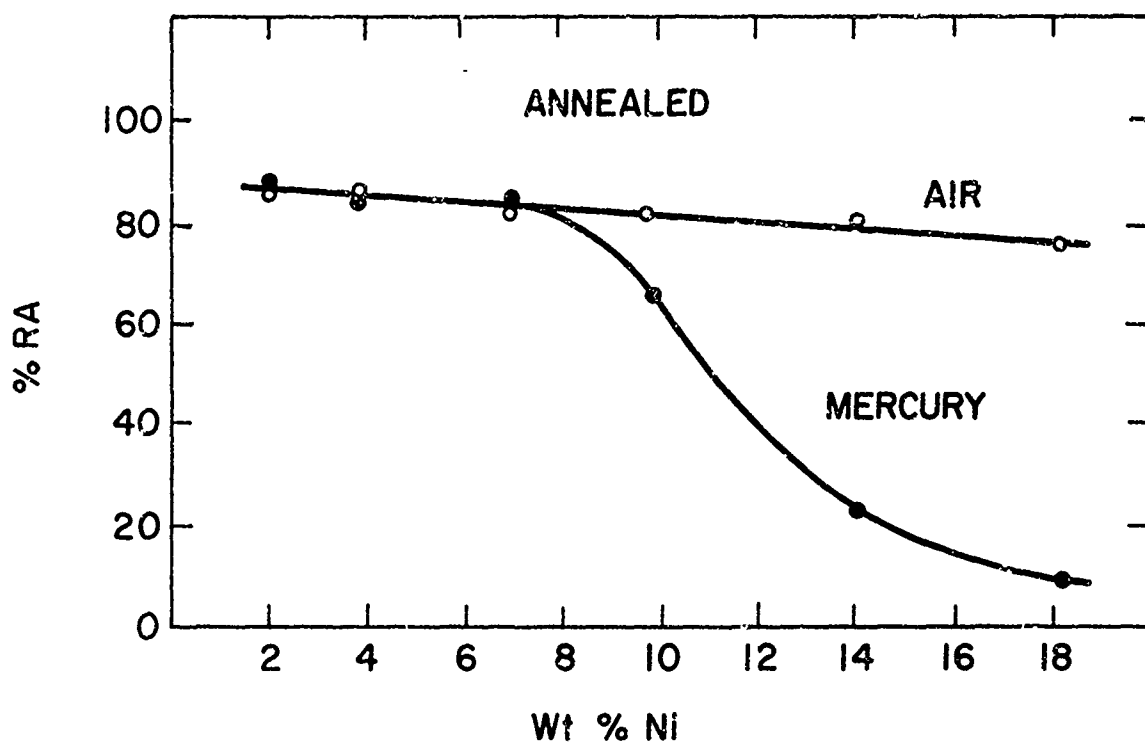


Figure 31. Illustrating the effects of nickel additions to iron on the susceptibility (reduction in area, RA) of smooth tensile specimens tested in liquid mercury environments (after Hayden et al.⁵³).

solid are not sufficient to nucleate a crack in the presence of mercury. If a stress raiser, such as a notch or a sharp crack is present in the specimen, however, then the presence of mercury at the crack tip may cause brittle crack propagation or embrittlement in these alloys. A study of crack propagation in notched specimen demonstrated that mercury will embrittle iron-nickel alloys at all composition levels, i.e. from 2 to 8% nickel and up.⁵³ Specifically it was found that for all alloys the plain stress crack opening force, G_c , calculated from the measurements of the crack opening displacement in mercury environments was about one order of magnitude lower than that calculated from the energy absorbed in a charpy impact test carried out in air, Figure 32. In addition to the presence of a notch, the strain rate of the test also may be an important factor. In aluminum monocrystals tested in liquid gallium at the crack tip, embrittlement was not observed when test was carried out at a low strain rate (e.g. 10^{-4} cm/sec.). But, when the strain rate was increased by several orders of magnitudes (e.g. 5 in/min), the monocrystal failed in a brittle manner and the fracture surfaces were identified as (001) cleavages.⁴⁷ The results with iron-nickel alloys and aluminum monocrystals indicate that slip character alone may not represent a sufficient condition for determining the effects of alloying on embrittlement. Consequently other factors which enhance or increase brittleness in a solid—such as the presence of a stress raiser or a notch, strain rate of test, grain size, etc. — must be taken into consideration.

When slip character does not change significantly with alloy composition, or for very dilute alloys, it appears that flow stress determines the severity of embrittlement. For example, commercially pure aluminum extends

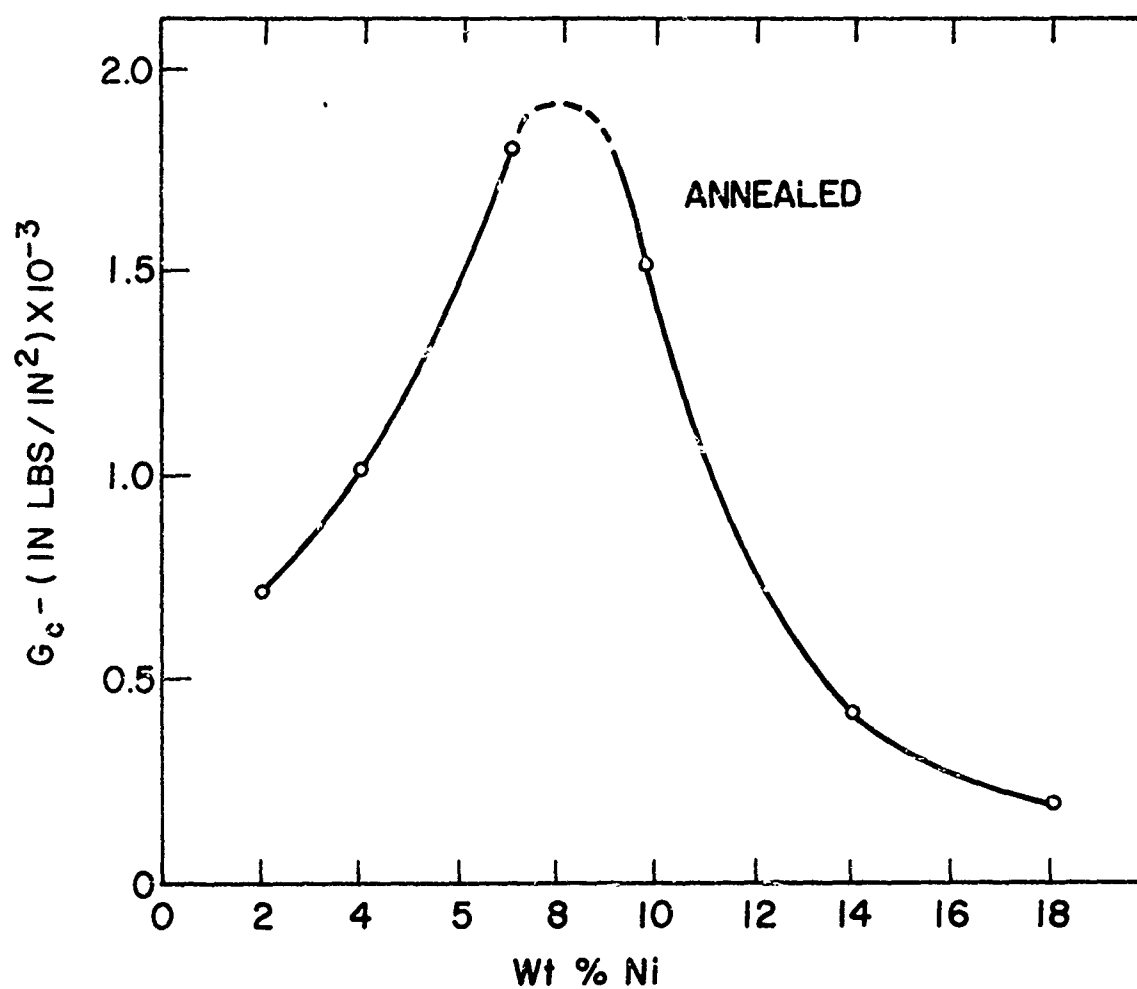


Figure 32. Fracture toughness parameter, G_c of doubly notched annealed specimens broken in mercury versus nickel content (after Hayden et al.⁵²).

some 25% in air, and this strain at fracture is reduced to about 12% when the specimen is amalgamated. Nevertheless, an Al 2024 alloy specimen (4.5% Cu, 1.5% Mg, 0.6% Mn) in the solution treated and in a naturally aged condition, and normally exhibiting some 17% elongation, breaks below its flow stress when amalgamated.⁹⁶

It is generally observed that high-strength alloys are more severely embrittled than low strength alloys based on the same metal. Rostoker et al.² have demonstrated this for both steels and a wide variety of aluminum alloys. For the latter materials, a comparison was made between the fracture stress in air and that in mercury containing 3% zinc in solution, these data are shown replotted in Figure 33. Below about 65 kpsi, the fracture strength in this solution and in air is not significantly different. Above this critical stress, however, the liquid mercury environment causes increasingly severe embrittlement. That is, the greater the intrinsic strength of the alloy, the weaker it becomes when exposed to mercury -3.0% zinc solution. The data also indicate, however, that this environment has significant effect on the ductility of even the weakest alloys. For materials of strength greater than 65 kpsi, failure occurs below the flow stress. The effects of precipitation hardening on embrittlement has been studied in a number of fcc systems, notably 2024 aluminum,² Al-4% Cu,¹⁷ Cu-4% Ag^{53,97} and Cu-2% Be.⁹⁸ In all cases the maximum susceptibility to liquid metal embrittlement coincides with peak strength of the alloys. Tests involving various combinations of prestrain and aging show that fracture can be induced at stress levels well below the yield stress.

One of the more interesting aspects of embrittlement in age hardenable alloys is that a change from the characteristic intergranular failure to

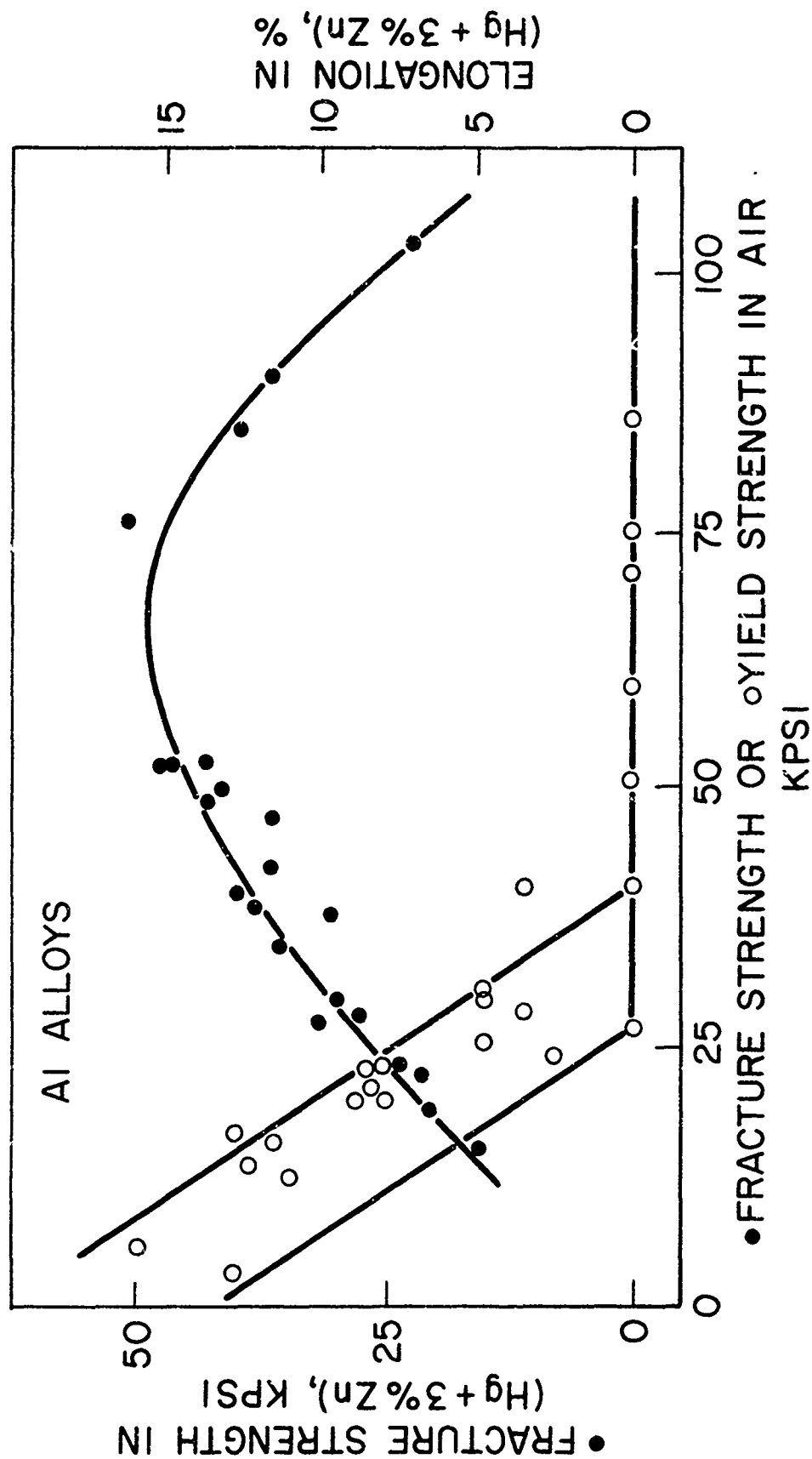


Figure 33. Correlation for aluminum alloys between (dark circles fracture strength in air and in (Hg + 3% Zn) amalgam, and (open circle) yield strength in air and elongation at failure in (Hg + 3% Zn) amalgam (after Rostoker et al. 1960).

transgranular failure is observed in the hardened condition for 2024 Al, Cu-4% Ag and Al-4% Cu. When tested in solution treated condition, the fracture mode reverts to intergranular.

5.4 Effects of Prestrain and Cold Work

For ductile pure metals or nonstrain aging alloys, the fracture stress usually increases approximately linearly with prestrain, while strain at fracture is decreased (Rosenberg and Cadoff,⁴⁸ Pargeter and Ives⁹⁹). For fine grained material, or strain aging alloys, however, the effects of prestraining are not always those anticipated. For example, note the peculiar variation in fracture stress of amalgamated, fine grained 70-30 brass with prestrain in Figure 34. Figure 35 presents some data obtained with a strain-aging aluminum alloy, Al 5083 containing 4.5% Mg, 0.7% Mn; Rostoker.¹⁰⁰ It is apparent that the data for the prestrained and amalgamated aluminum alloy specimens do not conform to a Petch-type relationship, unless the fracture energy is actually negative. Figure 36 illustrates the effect of prestrain on the fracture stress of Al 2024 alloy specimens in the aged and amalgamated condition (Nichols and Rostoker).¹⁰¹ Once again an unexpected variation is observed. Nichols and Rostoker⁹⁶ have attempted an explanation of such phenomena in terms of strain aging effects and coherency strains, etc., but, as they remark, the explanation cannot be simple. They conclude that for aluminum alloys (i) fracture in single phase and nonprecipitation hardened structures cannot be initiated without measurable prior yielding, even after large degrees of cold work; (ii) fracture below the flow stress is peculiar to the precipitation hardened state, and the severity of embrittlement is greater when precipitates are

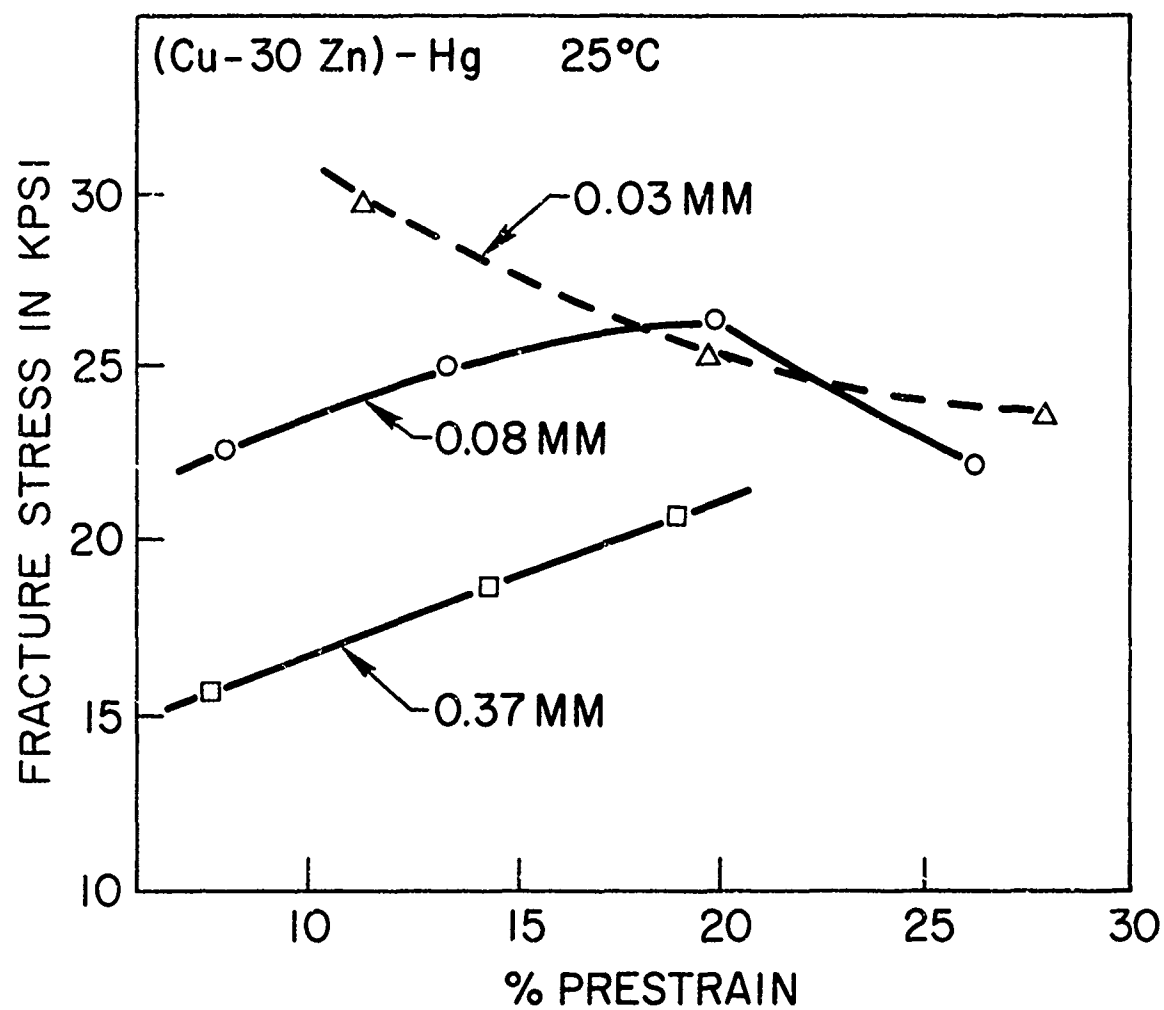


Figure 34. Variation with grain size of effects of prestrain in air on fracture stress of 70-30 brass in liquid mercury at 25°C (after Rosenberg and Cadoff⁴⁸).

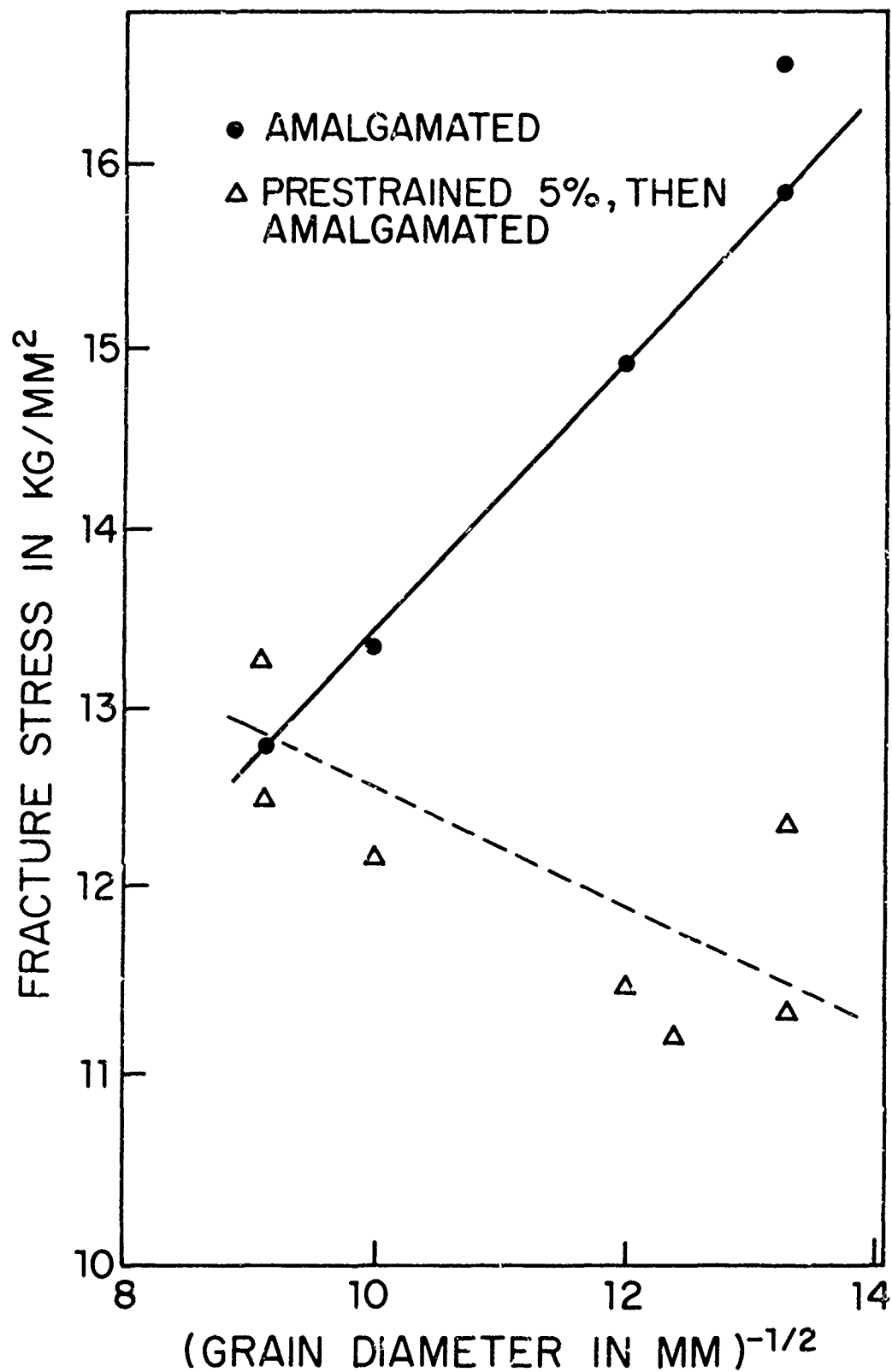


Figure 35. Effects of grain size and prestrain on fracture stress of amalgamated Al 5083 alloy specimens. Note that the data from prestrained specimens do not conform to a Petch relationship (after Rostoker¹⁰⁰).

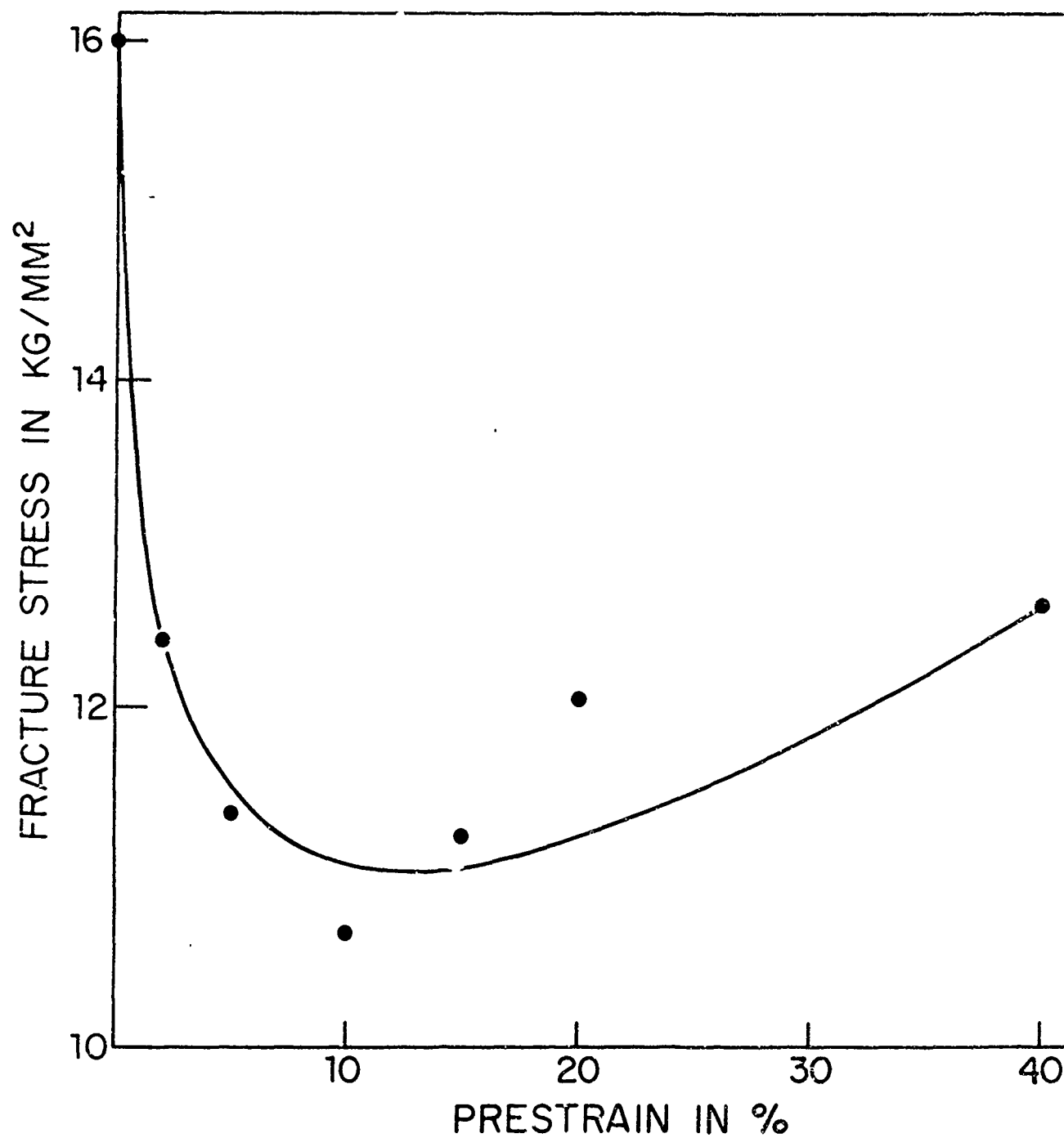


Figure 36. Influence of prestrain on fracture stress of amalgamated polycrystalline Al 2024 alloy specimens in aged condition (100°C for 30 min.) (after Nichols and Rostoker¹⁰⁰).

coherent with the matrix; and (iii) small degrees of cold work superimposed on the aged condition produce the severest embrittlement while large degrees of prior plastic strain cause some reduction in susceptibility.

Recent studies indicate that conclusion (i) also holds for Cu-4% Al alloys in liquid mercury (Pargeter and Ives⁹⁹). However, Work by Westwood⁸² and Kamdar and Westwood⁵⁴ indicates, that conclusion (ii) is not valid for zinc. Polycrystalline pure zinc specimens in liquid mercury can fracture at stresses substantially below those at which any marked deviation from linearity in the stress-strain curve occurs, Figure 21.

Effects of cold work and prestrain on the susceptibility of an alloy to liquid metal embrittlement has been investigated in aluminum^{2,95,102} and copper base alloys.¹⁰³ In aluminum alloys tested in liquid mercury, increased cold work decreases the susceptibility of the alloy to embrittlement. In age hardenable aluminum alloys, cold working first produces an increase in the susceptibility and then a progressive recovery with further cold work. The effects of tensile prestrain on the embrittlement of alpha brass in the presence of liquid mercury showed that susceptibility increases with prestrain. The susceptibility of cold rolled alpha-brass to embrittlement by mercury-sodium amalgam has also been investigated.¹⁰⁴ It was shown that for small amounts of cold work (i.e. up to 25% reduction in area) the alloy is severely embrittled and the failure occurs by intergranular fracture. As the amount of cold work increases, the susceptibility to embrittlement decreases and the mode of failure becomes ductile and transgranular. For large amounts of cold work (90% reduction in area), essentially no embrittlement is observed. The elimination of grain boundaries resulting from cold

work is the dominant factor responsible for the observed change in susceptibility and the fracture mode. It is apparent that the effects of prestrain and cold work on susceptibility to embrittlement are intriguing but they are not well understood.

5.5 Static Fatigue and Strain Rate Effects

When a ductile solid metal is subjected to tensile stress σ_a in an inert environment, the relationship usually observed between time to failure, t_F , and σ_a is

$$t_F = t_0 \exp(U_0 - \alpha \sigma_a / kT)$$

(Zhurkov),¹⁰⁵ where t_0 is a constant of order 10^{-13} sec, U_0 is a term related to the binding energy of the solid and is approximately the heat of sublimation, α is a structure dependent coefficient, and k is Boltzmann's constant. Such a relationship is displayed by the data of Bruyukhanova et al.⁴² for zinc in Figure 37, curves (a) and (c). For amalgamated zinc crystals, however, once a critical tensile stress is exceeded, a very abrupt decrease in lifetime occurs over a small range of stress, curves (b) and (d). For example, amalgamated zinc polycrystals fractured instantaneously at a stress of 1000 g/mm^2 ; under a stress of 960 g/mm^2 they remained unbroken after more than 10^6 sec. The magnitude of this critical stress was not significantly affected by temperature over the range $20^\circ\text{--}100^\circ\text{C}$. Similar results were obtained for cadmium specimens in liquid gallium,⁴³ for silver and cadmium specimens in mercury-indium solutions and for aluminum in mercury gallium solutions.⁴³ The latter observations will be discussed in Section 6. Bruyukhanova et al.⁴² have concluded from their work that in the presence of a pure, embrittling liquid metal, the fracture process is not

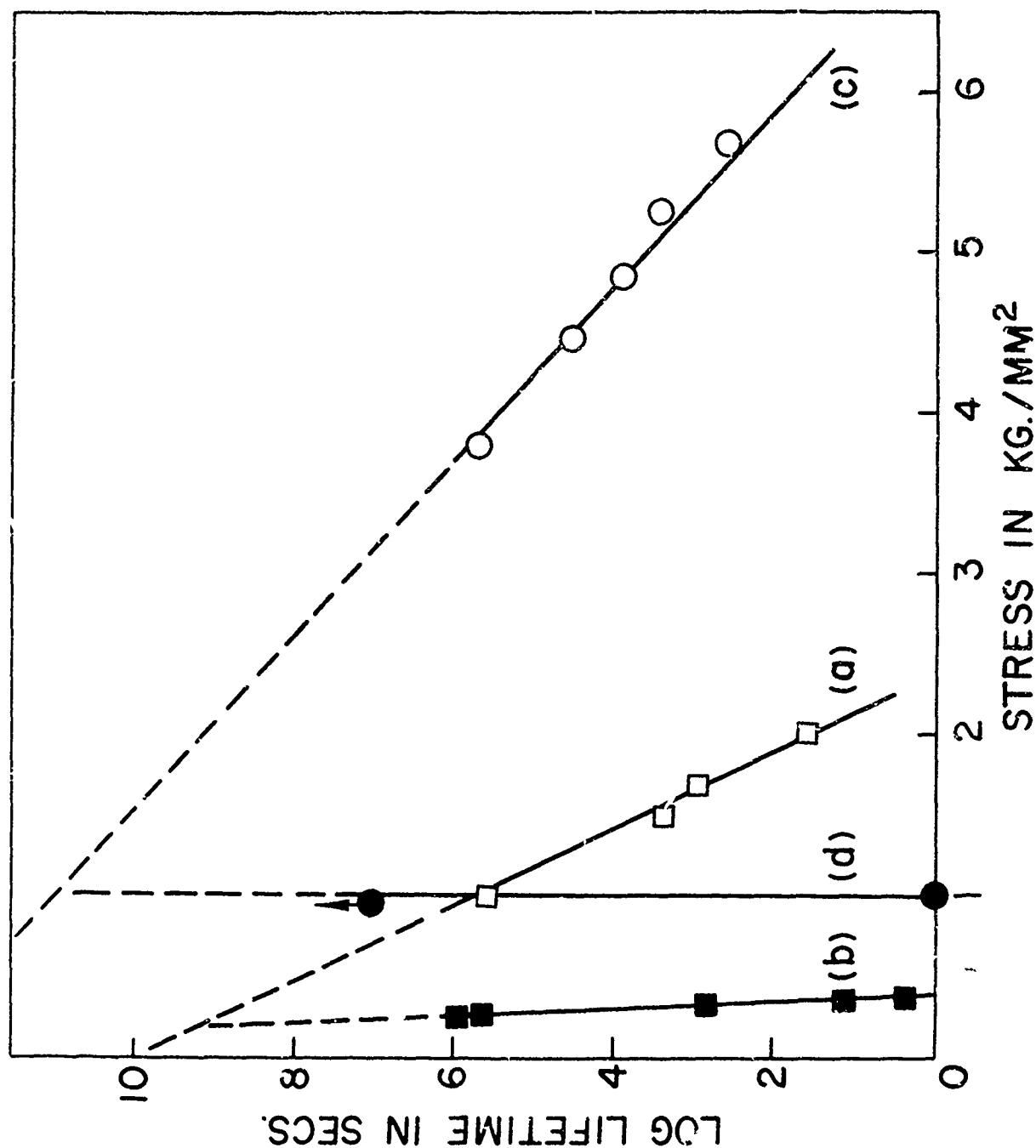


Figure 37. Variation of time to failure with applied stress for zinc at room temperature. Curves (a) and (b) for unamalgamated and amalgamated monocrystals ($\gamma_0 = 50^\circ$, ~ 1 mm dia.), respectively; curves (c) and (d) for unamalgamated and amalgamated polycrystals, respectively (after Bryukhanova et al.⁴²).

thermally activated. The catastrophic nature of the failure process further suggests that fracture under such testing conditions is controlled by the crack initiation process. This view would seem to be in accord with the suggestion of Stroh,⁶⁴ later verified by Smith and Barnby,⁶⁵ that provided the effective fracture surface energy for crack propagation, ϕ_F , is equal to (or less than) the true surface energy at all stages, then in an applied tensile stress field the crack initiation process controls the fracture behavior of the solid.

It is interesting to note that the critical stress for rapid failure in static fatigue tests is approximately equal to the dynamic fracture stress for both zinc in liquid mercury⁴² and cadmium in mercury-indium solutions.^{10,43}

The effects of strain rate on the susceptibility of a solid to liquid metal embrittlement have been described in Section 5.2 while discussing the effects of temperature. In general, increase in strain rate increases embrittlement and the brittle to ductile transition temperature. At low strain rates interesting "plasticizing" effects have been observed when zinc monocrystals were tested in various liquid metal environments. In this connection, Russian workers have reported that the strain at fracture, ϵ_F , of 1mm dia. zinc monocrystals coated with liquid mercury, gallium or tin is markedly dependent on strain rate, $\dot{\epsilon} = 10-15\%$ per min, all three liquid metals reduced ϵ_F from that in air; but at very low strain rates ($10^{-1}-10^{-3}\%$ per min) the ductility of wetted crystals was markedly increased, Figure 38 (lower curve). These results, however, were not confirmed by the more recent investigation of Kamdar and Westwood,⁹ in which carefully prepared and handled 6mm square zinc monocrystals were coated with liquid gallium or

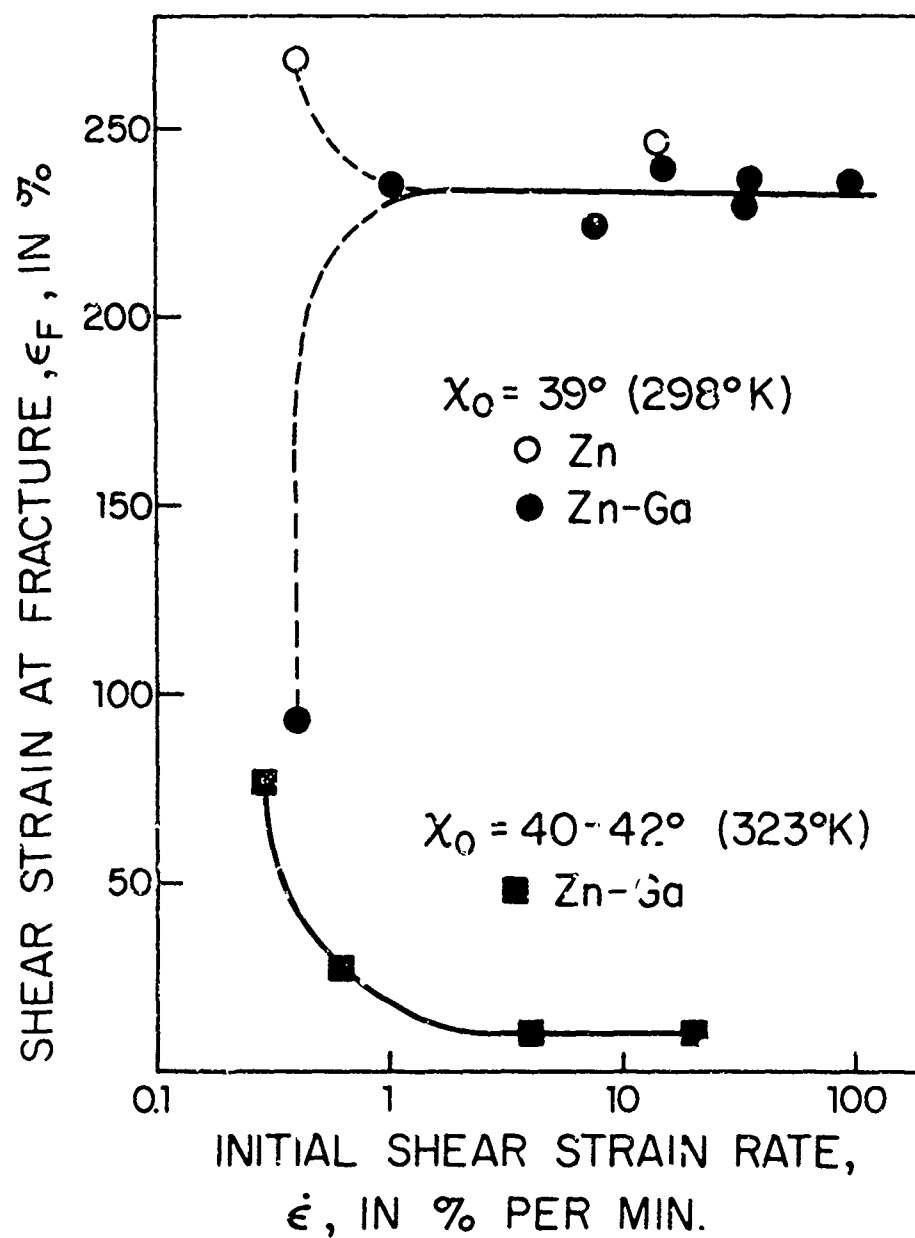


Figure 38. Strain rate dependence of the shear strain at fracture for (i) lower curve, 1mm dia. zinc monocrystals coated with Ga (after Shchukin et al.¹⁰⁷). Note "plasticizing" effect at low strain rates. (ii) upper curves, 6mm square zinc monocrystals partially coated with Ga (black circles) or uncoated (open circles) (Kamdar and Westwood⁹).

liquid mercury in the center of the gauge length only. These workers found that for shear strain rates of 1-100% per min., neither gallium coatings nor mercury coatings produced any significant embrittlement of crystals deforming principally by single slip, Figure 38, upper curves. Moreover, whereas Shchukin et al.¹⁰⁷ reported a "plasticizing" effect for gallium coated specimens tested at $\dot{\epsilon} < 1\%$ per min, the converse effect was found in the more recent work. Specimens tested at $\dot{\epsilon} < 1\%$ per min deformed in a markedly inhomogeneous manner, with well developed kink bands forming in the gauge section. In the presence of liquid mercury or gallium cleavage fractures initiated at such kink bands at relatively low stresses and strains. For uncoated crystals deformed at low strain rates on the other hand, the strains at fracture increased, though fracture stresses were not significantly affected. Since the experiments performed with uncoated crystals at initial shear strain rates of $\sim 0.4\%$ per min required more than 12 hours for completion, it is likely that the increased strains at fracture observed can be explained in terms of simultaneous deformation and recovery in zinc at room temperature.^{70,90}

The discrepancies between the earlier observations and those of Kamdar and Westwood⁹ probably result from problems in handling the mm dia. crystals used by the earlier workers. At "high" strain rates, accidentally introduced damage causes inhomogeneous deformation behavior and kink band formation in such crystals. Cracks then nucleate at these kink bands at relatively low strains. At "low" strain rates, however, sufficient time is available for some of this damage to anneal out, and this results in an apparent plasticization effect. Even so, the "enhanced" value of σ_F

observed for "pre-damaged" specimens at low strain rates ($\sim 75\%$), lower curve of Figure 38 is less than the "reduced" value obtained at similar strain rates for undamaged crystals ($\sim 90\%$), upper curve of Figure 38.

6. EFFECTS OF LIQUID METAL ENVIRONMENTS

It is generally accepted that liquid metal embrittlement is a "specific" phenomenon manifested only by certain solid metal liquid metal couples, Tables 1 and 2. But the fundamental factors which determine whether or not a given liquid metal will embrittle a particular solid metal, and the degree of embrittlement that will be induced, have not been resolved. The mechanism of embrittlement has been based on the hypothesis that embrittlement results from a localized reduction in cohesion (i.e. σ is reduced, Section 4.1) associated with the chemisorption of specific liquid metal atoms at strained bonds, e.g. at a stressed crack tip, or in the vicinity of high concentrations of dislocations⁹ see Section 3. If this hypothesis is correct, then one might expect to observe some correlation between the electronic properties of the liquid and the solid metal atoms, on the one hand and the degree of embrittlement induced in a solid metal on the other. However, no such correlation has been reported so far in the literature. Reductions in chemisorption induced cohesion at a crack tip are difficult to estimate from theoretical considerations. Under these circumstances, it is difficult to predict the occurrence of embrittlement in a given liquid metal-solid metal couple except by the rough and not so reliable empirical rules described in Section 2. Instead of reduction in cohesion, chemisorption of liquid metal atoms at the crack tip may result in a strengthening of the bonds. Dissolving such species in an embrittling environment may result in the inhibition of embrittlement. It has been proposed that the severity of embrittlement of a given solid-liquid metal couple is related to the electronegativities of the participating liquid and the solid metals.^{7,10} It is conceivable that embrittlement is caused by the penetration

Preceding page blank

of the liquid into the grain boundaries of the solid. Such a process should depend upon the time and temperature of test and perhaps also on the level of stress applied to the specimen. Such effects of liquid metal environments may result in penetration dependent delayed failure of the solid metal. Also, embrittlement process should be limited by the transport or diffusion of the liquid phase to the propagating tip and thus should be temperature sensitive. Such effects have been described in Section 5.2. Embrittlement may be controlled, i.e. increased or decreased, by suitable additions to the embrittling liquid phase.^{2,49,48,43} Alternatively, embrittlement may be induced or controlled by dissolving certain solid or liquid metal embrittling species in a non-embrittling liquid phase.^{10,108} In this section, we will describe and discuss various effects which liquid metal and liquid metal solution environments have on the severity of liquid metal embrittlement of the solid.

6.1 Effects of Minor Additions to the Embrittling Liquid Metal

Most work on the effects of the chemical composition of the liquid metal phase on the degree of embrittlement induced in a given solid metal, has customarily utilized an active liquid metal as the embrittling environment, and then attempted to modify its action on the solid metal by additions of solute elements.^{2,48,49,43} Thus, substantial variations in the severity of embrittlement have been induced by changing the chemical composition of the embrittling liquid-metal environment through addition of minor quantities^{*}

* Small additions are dictated by the low solubilities of most elements in the embrittling liquid phase at ambient temperatures.

Table 5

Effects of Minor Solute Additions to Embrittling Liquid on Susceptability of
a Solid to Liquid Metal Embrittlement, (after Stoloff¹¹ and Westwood et al.⁷).

Base Metal	Base Liquid	Temp. °C	Solute in Liquid and Embrittlement		Slight or No effect
			Increase	Decrease	
Copper	Bi	345°		Sb, Pb, Tl, Cd, Zn	
Copper Alloys	Hg	25°	Al	Zn, Cd, In	Au
2024 Al-T3	Hg	25°	Zn, Ga	Sn	Cd
Iron-Aluminum	Hg	25°			In
Iron-Silicon	Hg	25°			In
Cadmium	Hg	25°	In		
Aluminum	Hg	25°	Cd, Zn, Ga, Sn		
Silver	Hg	25°		In	
Zinc	Hg	25°		Ba	
Alpha Brass	Hg	25°		Tl, Zn, Ga	

of other elements in solution, (Table 5). Consider, for example, the fracture behavior of 2024-T3 aluminum alloy specimens in liquid mercury.² Additions of up to 0.84 at. pct. tin to the mercury reduce embrittlement slightly, and additions of some 3 at.pct. zinc or gallium increase embrittlement markedly, i.e. reduce the fracture stress. Other examples of such behavior have been reported for copper alloy-liquid mercury couples, and for the copper-liquid bismuth couple.⁴⁹ In the former systems, additions of zinc, cadmium or indium to the mercury reduce the degree of embrittlement, additions of gold have no observable effect, and additions of aluminum reportedly increase embrittlement. For the pure copper-liquid bismuth couple at 345°C, minor additions to the molten bismuth of either lead, thallium, cadmium or zinc reduce the embrittlement of copper somewhat, but the addition of as little as 0.4 at.pct of antimony produces a considerable effect, raising the fracture stress of copper in bismuth by some 60 pct.⁴⁹ A possibility exists that minor additions of solute improve the wettability of the solid by the embrittling liquid either by breaking or dissolving the thin oxide film which intervenes between the solid and the liquid phase or by reducing the surface tension of the liquid.^{2,12} As yet, satisfactory explanations have not been offered for such effects. Minor additions to the liquid phase have resulted in intriguing effects but have not provided any improved understanding of the chemical nature of the liquid phase on embrittlement. It is possible that large additions of solute to the liquid phase would allow investigation of the embrittlement susceptibility as a function of the composition of the liquid phase. Such studies may lead to improved understanding of the chemical nature of the liquid phase on embrittlement. In this regard the recently developed concept of "inert carriers"¹⁰ is a very useful approach. It will be discussed in the next section.

6.2 The Concept of "Inert Carriers"

In some instances, direct investigation of the embrittlement behavior of a potentially interesting solid metal-liquid metal couple is not feasible. The reason is that the solid metal at temperatures just above the melting temperature of the liquid metal is either too ductile to maintain the stress concentrations necessary to initiate and propagate a "brittle" crack, or it is excessively soluble in the liquid metal, thus allowing crack blunting. It is possible, however, that the embrittlement of a given solid metal by a potentially embrittling "liquid" metal might be achieved at temperatures much below the melting point of this "liquid" metal if one incorporates it, in solution, in an "inert" carrier liquid metal of lower melting point.¹⁰ In this way, the active element can be present "effectively" in the liquid state, though at some temperature far below its melting point. Besides providing a possible means for inducing embrittlement in a potentially interesting system. This approach, also provides a means of investigating the variation in the degree of embrittlement induced in a solid metal as a function of the chemical nature of several active liquid-metal species dissolved separately in a common inert carrier.

To examine the validity of the proposition, experiments were performed with the solid cadmium-liquid (mercury + indium) system.^{10,107} Mercury is known not to embrittle cadmium,⁵⁶ dissolves up to 70 at.pct of indium in homogeneous solid solution at 25°C,^{108,109} and so it served as the inert, low melting point carrier metal. Cadmium and indium do not form inter-metallic compounds and exhibit only limited mutual solubility at 25°C;^{108,109} thus indium is a potentially embrittling species for cadmium (empirical rules, Section 2).

Tensile fracture data for cadmium tested in mercury and mercury-indium solutions are presented in Figure 39. The data demonstrate that mercury or mercury 5 at.pct indium solutions do not embrittle cadmium. Failure in these environments occurred by necking and ductile shear after more than 45 pct. elongation. In mercury 8 at.pct indium solutions, however, intercrystalline failure occurred after only 15-20 pct. elongation, and the degree of embrittlement induced then increased markedly with the indium content of the mercury, Figure 39. In solutions containing more than 40 at.pct. indium, intercrystalline fracture occurred at stresses as low as 55 pct. of the macroscopic flow stress. Such results demonstrate, the validity and usefulness of this approach to embrittlement studies.

In other experiments, chemically polished cadmium specimens were stressed above their flow stress at -10°C . While under stress they were coated with the extremely embrittling mercury -60 at.pct. indium solution. They failed immediately and catastrophically. Further experiments revealed that the degree of embrittlement observed at room temperature was the same whether or not the mercury-indium solutions were presaturated with cadmium. Such observations imply that the operative embrittlement mechanism in this system is not dissolution-dependent.

Several experiments were also performed with cadmium monocrystals. These are normally extremely ductile, failing by shear even at liquid helium temperature.¹¹⁰ Nevertheless, crystals coated with mercury -60 at.pct. indium solution and deformed by bending at room temperature failed in a relatively brittle manner by basal cleavage. Furthermore, monocrystals coated with this solution could be cleaved at room temperature by the impression of a sharp chisel, Figure 7. Monocrystals coated with pure

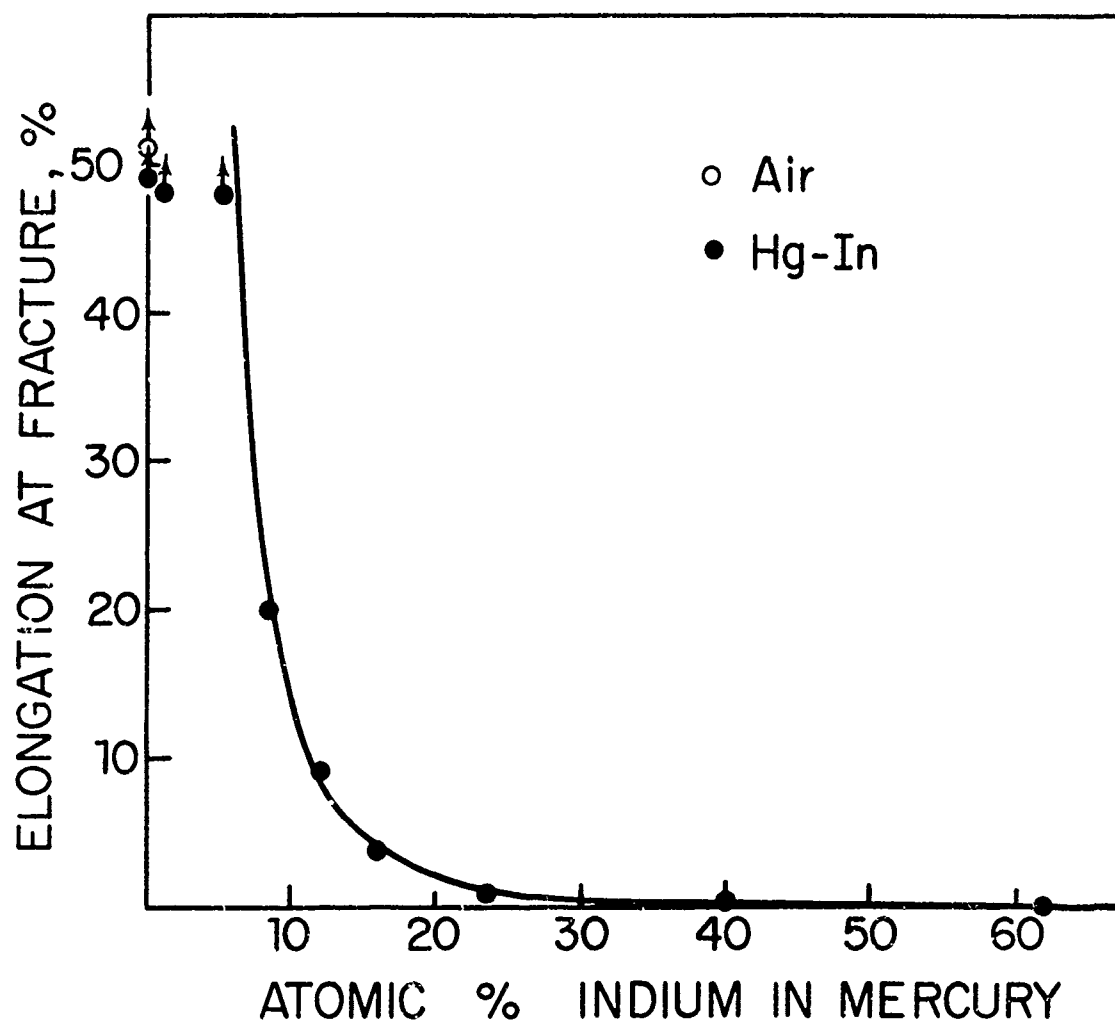


Figure 39. Variation in ductility of polycrystalline cadmium specimens with indium content of mercury-indium surface coatings at 298°K (after Kamdar¹⁰ and Kamdar and Westwood¹⁰⁸).

mercury were extremely ductile and could not be cleaved. These results indicate that the embrittlement of cadmium by indium at temperatures around room temperature is a genuine manifestation of adsorption — induced liquid metal embrittlement and does not involve dissolution or intergranular penetration.

Experiments were also performed to determine the effects of other liquid-metal solutions on the mechanical behavior of polycrystalline cadmium. The results of this work are included in Table 6. It is seen that cadmium is embrittled by neither thallium nor tin, and that indium is a more severe embrittling agent for cadmium than gallium. The significance of these results will be discussed in the next section.

6.3 Severity of Embrittlement and Electronegativity

Perhaps the most significant development from the work with cadmium-mercury-indium solutions is that the data reveals a pattern in embrittlement behavior. There appears to be a correlation between the occurrence and severity of liquid-metal embrittlement in a given system and the electronegativities of the active metals involved. Consider the data on the liquid-metal embrittlement of cadmium, Table 6. The electronegativity* of cadmium is 1.7.¹¹¹ It is most severely embrittled by indium (1.7), less by gallium (1.6), and not at all by thallium (1.8) or mercury (1.9). Thus, for these systems (i) maximum embrittlement occurs when the solid metal and active "liquid" metal are of similar electronegativity, and (ii) the degree of embrittlement induced in the solid metal decreases as the difference in electronegativity between the active metals increases.

*Pauling's¹¹¹ values for electronegativity are used throughout, and are given thus: cadmium (1.7).

TABLE 6

Effects of Several Liquid Metal Environments on the Tensile Fracture Behavior of Polycrystalline Cadmium* (After Kamdar and Westwood¹⁰⁸ and Kamdar¹⁰⁹)

Environment	Electronegativity of Solute Element ¹⁸	Fracture Stress in Kg/mm ²	Elongation at Fracture in pct	Fracture Mode
Ga	1.6	1.01	~ 0.25	Brittle
Hg + 3.0 at.pct. Ga	1.6	> 4.9	> 45	Ductile
Hg + 13 at.pct. In	1.7	3.93	8.0	Semi-Brittle
Hg + 40 at.pct. In	1.7	1.43	~ 0.5	Brittle
Hg + 60 at.pct. In	1.7	0.61	Fractured below flow stress	Brittle
Ca + 13 at.pct. In	1.7	0.57	Fractured below flow stress	Brittle
Hg + 40 at.pct. Tl	1.8	> 4.7	> 45	Ductile
Hg + 42 at.pct. Sn (100°C)	1.8	> 3.0	> 48	Ductile
Hg	1.9	> 4.5	> 45	Ductile

* The electronegativity of cadmium is 1.7.

In examining the possible generality of this correlation, it is convenient to separate the available information on liquid-metal embrittlement phenomena into two categories, (A) embrittlement by pure liquid metals, and (B) embrittlement by liquid metal solutions.

Category (A). Several examples may be cited in support of the correlation described. (i) Aluminum (1.5) alloys are more severely embrittled by gallium (1.6) than mercury (1.9), Table 7.² Aluminum also is embrittled by molten indium (1.7) but not by molten thallium (1.8),² although the high melting temperature of thallium (303°C) may be a factor in the latter system. (ii) Bismuth (1.9) is embrittled by mercury (1.9) but not by gallium (1.6).¹¹² (iii) Copper (1.9) alloys are embrittled by both bismuth⁴⁹ (1.9) and mercury⁴⁸ (1.9) but not by gallium (1.6). (iv) Iron (1.8) alloys containing 8-16 at.pct. aluminum are embrittled by mercury (1.9) but not by gallium (1.6).³⁹ Molten cadmium (1.7) and indium (1.7) also embrittle iron alloys.² (v) Zinc (1.6) is more severely embrittled by gallium (1.6) than by mercury (1.9) at room temperature, Table 8.

Category (B). Systems in this category can be separated into two classes, (I) those in which embrittlement is accomplished by an active element dissolved in an inert carrier liquid metal, and (II) those in which embrittlement by an active liquid metal is affected by minor additions of other elements in solution. Class I includes the embrittlement of cadmium by mercury solutions described in Section 6.2. No other examples of class I type systems are presently known. However, several examples may be cited from class II systems in support of the electronegativity correlation. (i) Aluminum (1.5). Table 7 shows that the embrittlement of aluminum in

TABLE 7

Effects of Mercury and Mercury Solutions on the Tensile
Fracture Load of Polycrystalline 2024-T3 Aluminum^{*}
Alloy Specimens at Room Temperature, Data
from Rostoker et al.²

Environment	Electronegativity of Solute Element ¹¹¹	Fracture Load Kg
Hg + 5.5 at.pct. Ga (Ga present as liquid)	1.6	1008
Hg + 2.8 at.pct. Ga	1.6	1789
Hg + 3.0 at.pct. Zn	1.6	2565
Hg + 3.55 at.pct. Cd	1.7	3000
Hg	1.9	3088

^{*}The electronegativity of aluminum is 1.5.

TABLE 8

Fracture Data for Polycrystalline Zinc^{*}
Specimens Coated with Mercury or Gallium
and Tested in Tension at 30°C (after Kamdar and Westwood^{9,4})

Environment	Electronegativity of Environment Element ¹⁸	Fracture Stress in Kg/mm ²
Gallium	1.6	0.14
Mercury	1.9	0.44

^{*}The electronegativity of zinc is 1.6.

TABLE 9

Effects of Bismuth and Bismuth Solutions on the
Tensile Fracture Stress of Polycrystalline Copper^{*}
at 345°C. Data from Kraai et al.⁴⁹

Environment	Electronegativity of Solute Element ¹¹¹	Fracture Stress Kg/mm ²
Bi	1.9	5.06
Bi + 5 at.pct. Pb	1.8	5.27
Bi + 5 at.pct. Tl	1.8	5.62
Bi + 5 at.pct. Cd	1.7	5.76
Bi + 5 at.pct. Zn	1.6	5.97
<hr/>		
Bi + 0.43 at.pct. Sb	1.9	8.10
Bi + 5 at.pct. Sb	1.9	8.51

^{*}The electronegativity of copper is 1.9.

mercury (1.9) is increased by dissolving in the mercury either gallium (1.6), zinc (1.6) or cadmium (1.7).² At similar solute concentrations, moreover, the order of the effectiveness of these additions is related to their electronegativity. (ii) Cadmium (1.7). The embrittlement of cadmium in gallium (1.6) is increased by additions of indium (1.7) to the gallium, Table 6. (iii) Copper (1.9). The embrittlement of copper alloys in molten bismuth (1.9) is reduced by adding to the bismuth either lead (1.8), cadmium (1.7) or zinc (1.6), and the effectiveness of these additions is again related to their electronegativity, Table 9. It has been reported⁴⁸ that additions of aluminum (1.5) to liquid mercury (1.9) increase the embrittlement of copper alloys in this environment. Such an effect, if valid, would be contrary to what might have been expected on the basis of the electronegativity correlation. This experimental observation appears questionable, however, since the maximum solubility of aluminum in mercury at room temperature is only ~ 0.015 at.pct.¹⁰⁹ It would appear unlikely that the presence of such a small concentration of aluminum in mercury could significantly reduce the fracture strength of ductile copper alloys in this environment.

High Purity Aluminum: In Figure 40 the stress-strain curve shown is an "averaged" curve from a number of high purity aluminum (99.999 + %) specimens, tested under cyclohexane to prevent confusing oxidation effects. The results from tests conducted in liquid mercury or various mercury solutions (also under cyclohexane) are likewise averaged. It can be seen that for equivalent solute element concentrations (~ 3 a/o), the severity of embrittlement is related to the difference in Pauling-electronegativity between aluminum

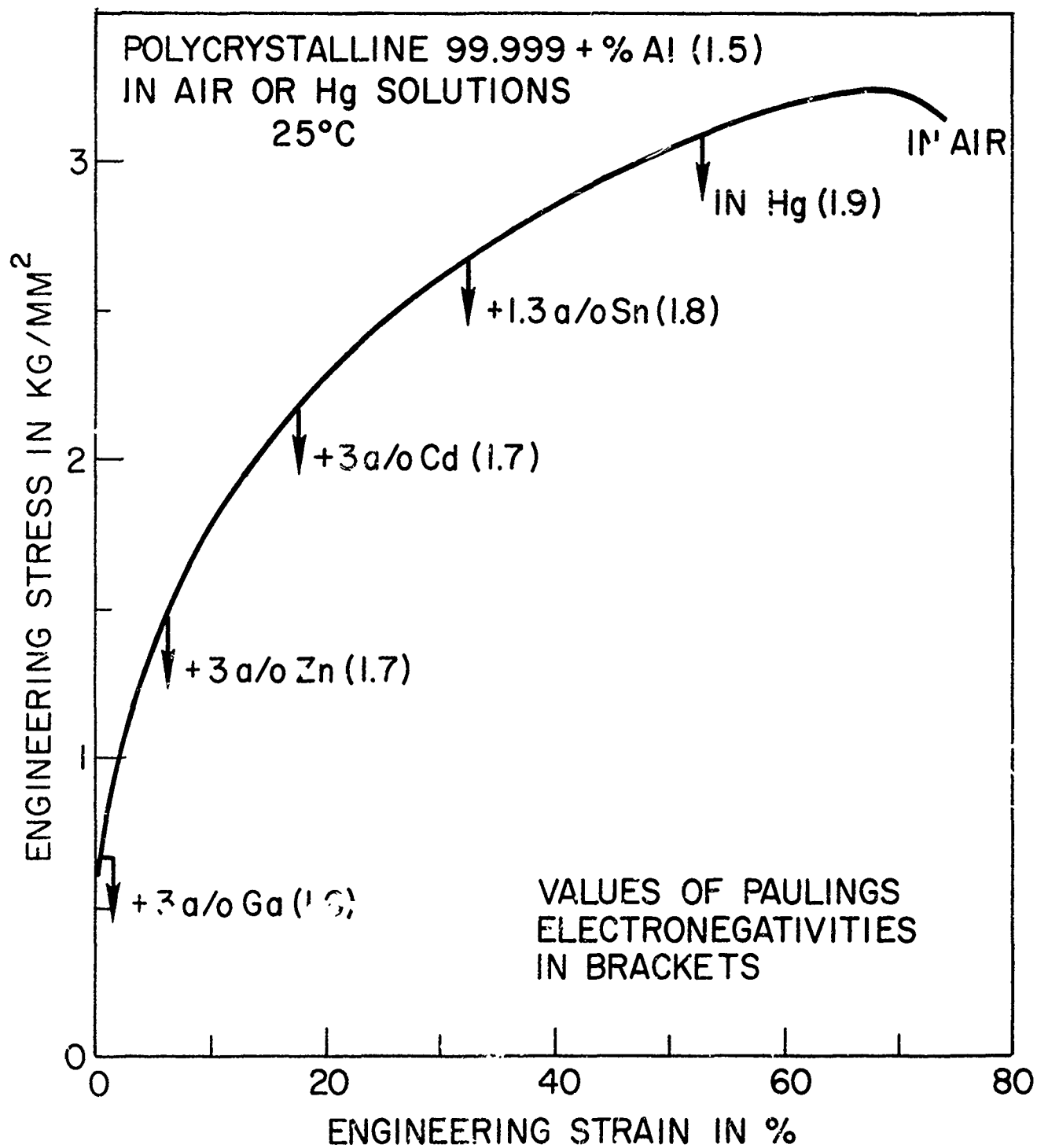


Figure 40. Embrittlement of polycrystalline pure aluminum by various mercury solutions. Note apparent correlation between Pauling electronegativity of solute element and severity of embrittlement (Westwood et al.⁷).

(1.5) and the active species in the liquid mercury namely gallium (1.6), zinc (1.6), cadmium (1.7), thallium (1.8), tin (1.8) or mercury (1.9). In other studies it has been shown that silver (1.9) is severely embrittled by liquid mercury (1.9), but that additions of up to 70 a/o In (1.7) to the mercury gradually restore ductility, Figure 41.⁴³ Note that this is exactly the opposite of that observed for cadmium in these solutions, Figure 41. Exceptions to the electronegativity correlation also can be found. For example, neither copper (1.9) or iron (1.8) is significantly embrittled by lead^{2,49} (1.8). Although their electronegativities are similar, they do not form intermetallic compounds and they do exhibit low mutual solubility. Such behavior may result from the inability of lead to wet these metals. There is recently a report of severe embrittlement of steel by lead.¹⁶ Also, despite a large electronegativity difference, aluminum (1.5) is embrittled by liquid sodium (0.9),² and iron (1.8) is embrittled by liquid lithium (1.0). However, it may be that embrittlement occurs in this and perhaps other apparently anomalous systems by mechanisms involving intergranular penetration or specific dissolution, rather than chemisorption.

The electronegativity difference is a measure of the tendency for two elements to form ionically-bonded compounds. The existence of such a correlation could be regarded simply as a semiquantitative restatement of the empirical rule that embrittlement does not occur in systems which exhibit stable, intermetallic compounds. The absence of or little solubility between the solid and liquid (empirical rule, Section 2) would suggest no chemical affinity. This would predict maximum embrittlement when electronegativities are dissimilar contrary to the observed correlation with

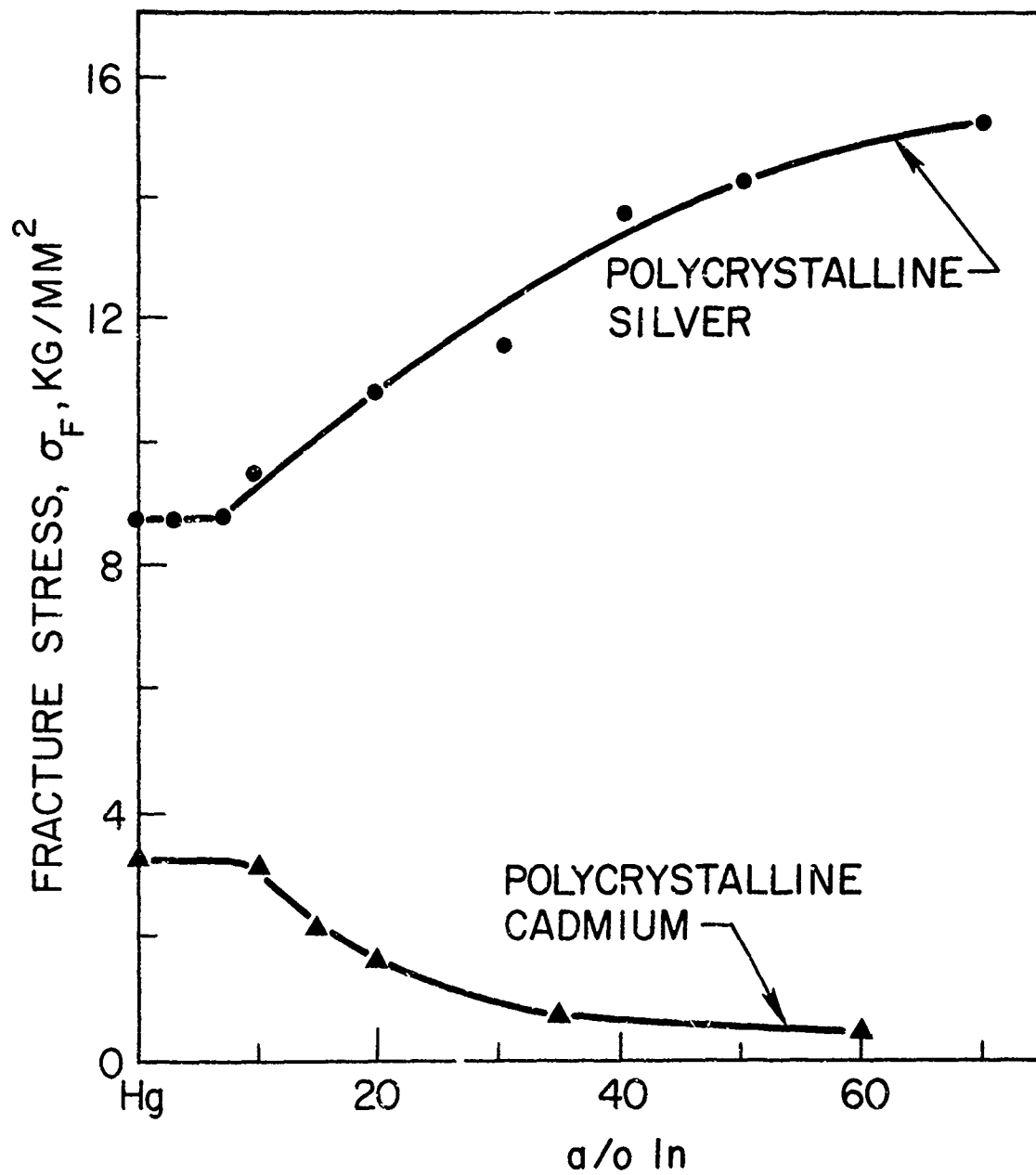


Figure 41. The variation of fracture stress of silver and cadmium with composition of the mercury indium environment (after Preece and Westwood⁴³).

electronegativity. However, the fact that the liquid must be in intimate contact with the solid (See Section 2) and that chemisorption may occur under high local stress, suggest that some chemical affinity must exist under these conditions and thus appear to be in accord with the electronegativity correlation. Questions could also be raised regarding the use of Pauling's values for atomic electronegativity rather than, say, those of Gordy and Thomas.¹¹³ Indeed, there has been much discussion of the whole concept of electronegativity during the past ten years.^{114,115,116} This more recent work has not only involved detailed considerations of the electronic interactions between specific orbitals of the participating atoms, but has also taken into account such factors as the state of hybridization and the self energy of the molecular orbital of the bond formed, etc. Certainly it would be preferable to make any prospective correlation with electronegativity using recently derived values of the electronegativities rather than the less easily interpreted values of Pauling.¹¹¹ It is interesting to note, however, that the values of electronegativities derived by recent workers are, for a wide range of elements in the "atomic" state, related to those of Pauling by a simple numerical formula.⁷

It appears that the chemical prerequisites for the occurrence of liquid-metal embrittlement are that the solid metal and the "active" liquid metal should (i) be of similar electronegativity, (ii) exhibit little tendency to form stable intermetallic compounds, (iii) liquid should wet the solid (Section 2.1), and, possibly, (iv) exhibit limited mutual solubility. The severity of embrittlement then observed is inversely related to the difference in electronegativity between the component metals.

The fundamental significance of the observed correlation with electronegativity* is not yet understood, and while insufficient reliable data are presently available to allow a thorough evaluation of its generality, it does appear to provide some degree of order in what had appeared to be a randomly occurring phenomenon. Under these circumstances, the apparent correlation between severity of embrittlement and electronegativity difference should be regarded as interesting, but not established. It's fundamental significance remains to be discovered.

6.4 Effects of Exposure to the Liquid Metal Environment Prior to Stressing

Penetration of the solid metal by solid state diffusion of liquid metal atoms is not fundamental to the occurrence of adsorption-induced liquid metal embrittlement, Section 3.3. If the specimen is left in contact with the liquid metal environment for a sufficient length of time, however, variations in subsequent mechanical behavior can result from intergranular or sub-boundary penetration processes. The occurrence of such variations and the magnitude of the effects observed are dependent upon such factors as the particular solid metal-liquid metal couple, time, temperature, grain size, state of stress and amount of liquid metal available. No general rules for predicting the occurrence of such effects appear to have been developed as yet. Observations on a few systems will serve to demonstrate the types of phenomena that may result.

(i) Aluminum-mercury-3% zinc and Brass-mercury systems. Ichinose³ has studied the effects of prior exposure of polycrystalline brass and pure

*The qualitative definition of electronegativity as the power of an atom in a molecule to attract electrons to itself is generally accepted. However, there is considerable disagreement as to the quantitative definition of the term.¹¹⁷

aluminum to mercury-3% zinc solution at room temperature, Figure 42. It is seen that the fracture stress of aluminum and brass is independent of the time of exposure. His analysis of the behavior of these systems, based on measurements of the magnitude of decreases in strength with pre-exposure at temperatures between 150° and 250°C and known diffusion constants at 20°C, suggests that times of exposure of the order 875 and 4500 days, respectively, would be required to produce a 5% reduction in the fracture stress of the brass or aluminum specimens.

(ii) Zinc-liquid mercury or liquid gallium: Flegontova et al.¹¹⁸ have shown that a variety of effects can be produced at room temperature in systems depending on the ratio, C_0 , of the mass of liquid metal available to the mass of the zinc sample. Specimens of zinc of about 98.7% purity and 50 μ grain diameter were used, and the variations in fracture stress obtained with time of pre-exposure and C_0 are shown in Figure 43. Though it may not be readily apparent from this figure, the fracture strength of 9.6 Kg/mm² recorded immediately on wetting the zinc with mercury decreased to about 8.4 Kg/mm² after 20-35 min. [For zinc in contact with liquid gallium the fracture stress decreased from 4.8 Kg/mm² to about 1 Kg/mm² in this initial period.] For small values of C_0 , say ≤ 0.002 , all of the mercury diffused into the zinc in about 80 hours producing an alloyed surface layer and consequent strengthening; note that curves a, b, and c cross over the line to indicate the strength of zinc in air. For much greater values of C_0 , e.g., $C_0 \sim 0.01$, despite surface alloying effects, there was always an adequate supply of liquid Hg to embrittle the crystal. Accordingly, the fracture strength was not particularly sensitive to time of prior exposure (curve f).

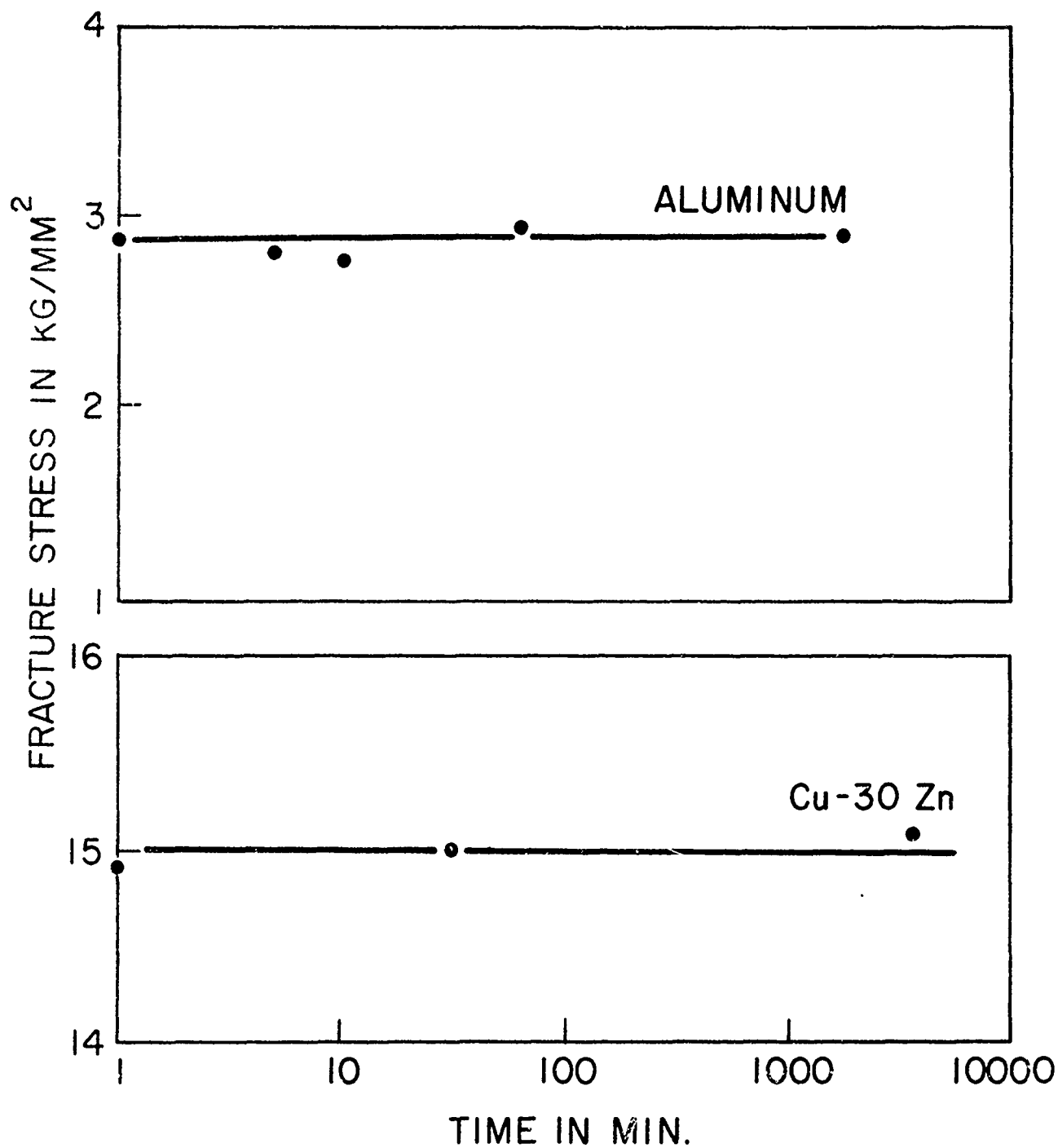


Figure 42. Fracture stress of polycrystalline aluminum or 70-30 brass as a function of time of exposure to liquid mercury prior to testing in this environment (after Ichinose³).

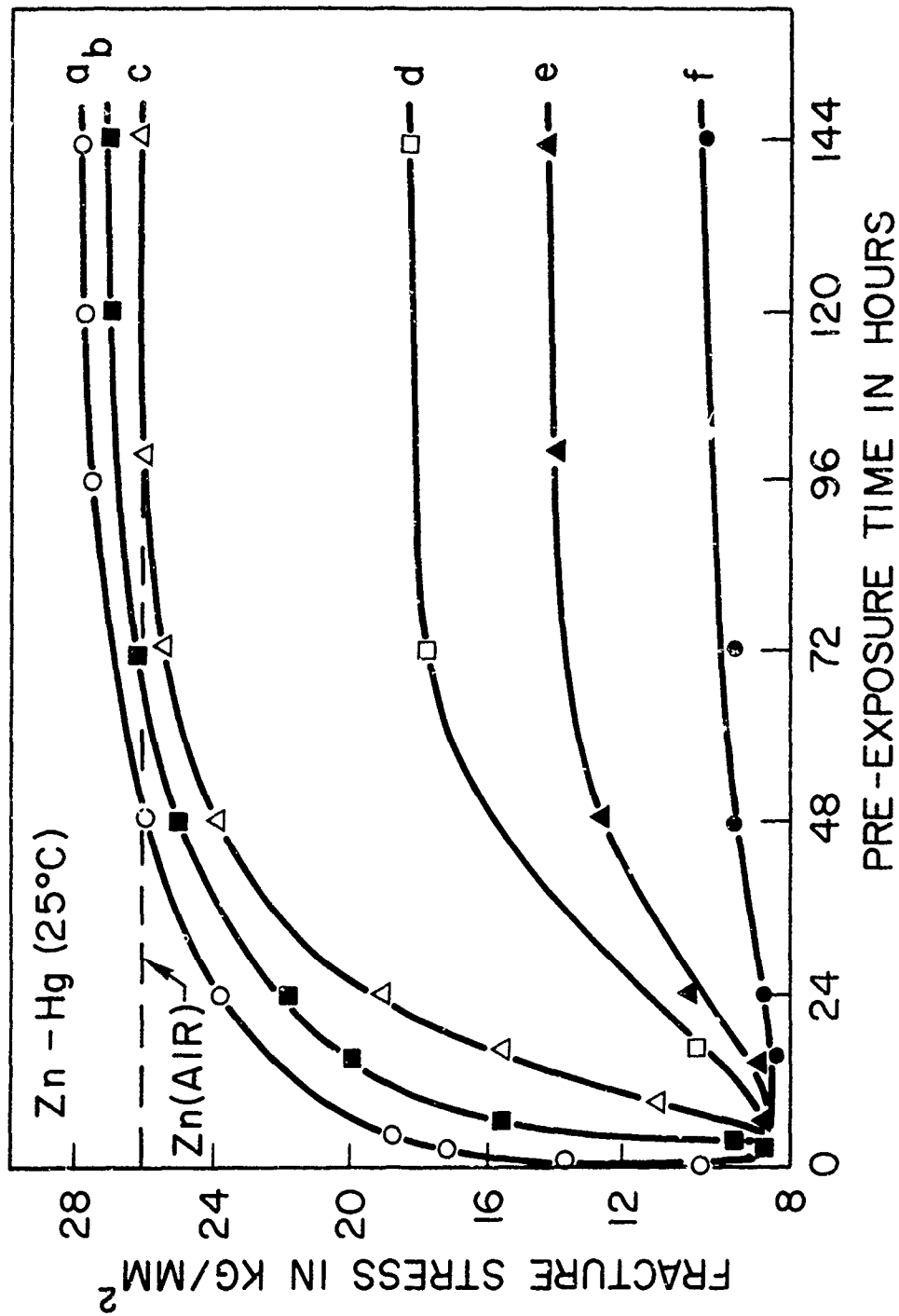


Figure 43. Fracture strength of polycrystalline zinc as function of (i) time of exposure to mercury environment prior to testing in this environment (ii) ratio, C_0 , of mass of Hg on the surface to mass of the specimen. Values of C_0 are: a - 3×10^{-3} ; b - 7×10^{-4} ; c - 2×10^{-3} ; d - 3×10^{-3} ; e - 7×10^{-3} ; f - 1×10^{-2} (after Flegontova et al.¹¹⁸).

According to Flegontova et al.¹¹⁸ the extra reduction in strength occurring after short exposure times is associated with intergranular (or sub-boundary) penetration. These workers suggest that this process results in an "adsorption drop" in strength of the boundary. It can be seen from Figure 43, on the other hand that for small values of C_0 as time of pre-exposure increases and the mercury atoms diffuse into the zinc, the strength actually increases to values greater than that for pure zinc. Westwood et al.⁷ have suggested that, once in the solid, the mercury atoms segregated at the grain boundary would produce boundary hardening, and that this would result from solid solution strengthening and source locking rather than from adsorption-induced reduction in strength. This suggests a more likely explanation for the initial drop in strength namely that diffusion of mercury into grain boundaries or sub-boundaries at the surface will harden (not weaken) these boundaries, thus facilitating crack initiation at the surface. In view of the recent observations of embrittlement of steel containing 0.3 w/o lead at the melting temperature of lead²³ (Section 2.2), however, it can be suggested that since mercury is in a liquid state within zinc, a crack will nucleate in the bulk of the solid upon stressing. Such a crack may not propagate to failure, perhaps because the supply of the liquid mercury at the sites of crack nucleation and subsequently at the tip of the propagating crack is insufficient and also because crack blunting may have occurred. Thus, fracture in zinc would be propagation rather than nucleation controlled, as discussed in Section 5.1. Such cracks will link up and will lead to ultimate failure at a much higher stress in accord with the observations of Levine and Cadoff.^{83,97} Metallographic examinations of specimens loaded to a stress just below the fracture stress could resolve this possibility.

6.5 Effects of Liquid Metal Environment on Static Fatigue

An important aspect of liquid metal embrittlement is the possibility that grain boundary penetration of the solid metal by the liquid metal occurs in the presence of applied stress. This penetration then gives rise to embrittlement or delayed failure. There has been no successful attempt to induce delayed failure in notch-sensitive metals like zinc,⁴² cadmium and iron-aluminum alloys in appropriate liquid metal environments.¹¹ For these metals, the typical behavior is that described for the zinc-mercury couple in Section 5.4. For zinc-mercury couple it was shown that fracture nucleates instantaneously at some threshold or critical stress, Figure 37. Thus, fracture is essentially nucleation controlled. The critical stress for failure is generally of the same magnitude as the dynamic fracture stress of solid metal in the same liquid metal environment. Also, crack propagation occurs almost instantly when liquid mercury is introduced in a partially cracked zinc monocrystal (crack initiated and stopped on the basal plane) maintained under a constant load.⁴ Crack nucleation and propagation in notch sensitive zinc therefore occur instantaneously.

Delayed failure has been reported for notch-insensitive aluminum-copper^{11,9} and copper-beryllium^{98,20} alloys in liquid mercury environments, Figure 44. Nichols and Rostoker¹¹⁹ reported that delayed failure occurs in copper-beryllium alloy only when the alloy is cold worked or age hardened. Age hardening causes maximum propensity for embrittlement whereas the solution treated and overaged alloys do not show delayed failure. There is no evidence of microcreep; cracking apparently occurs only during the last

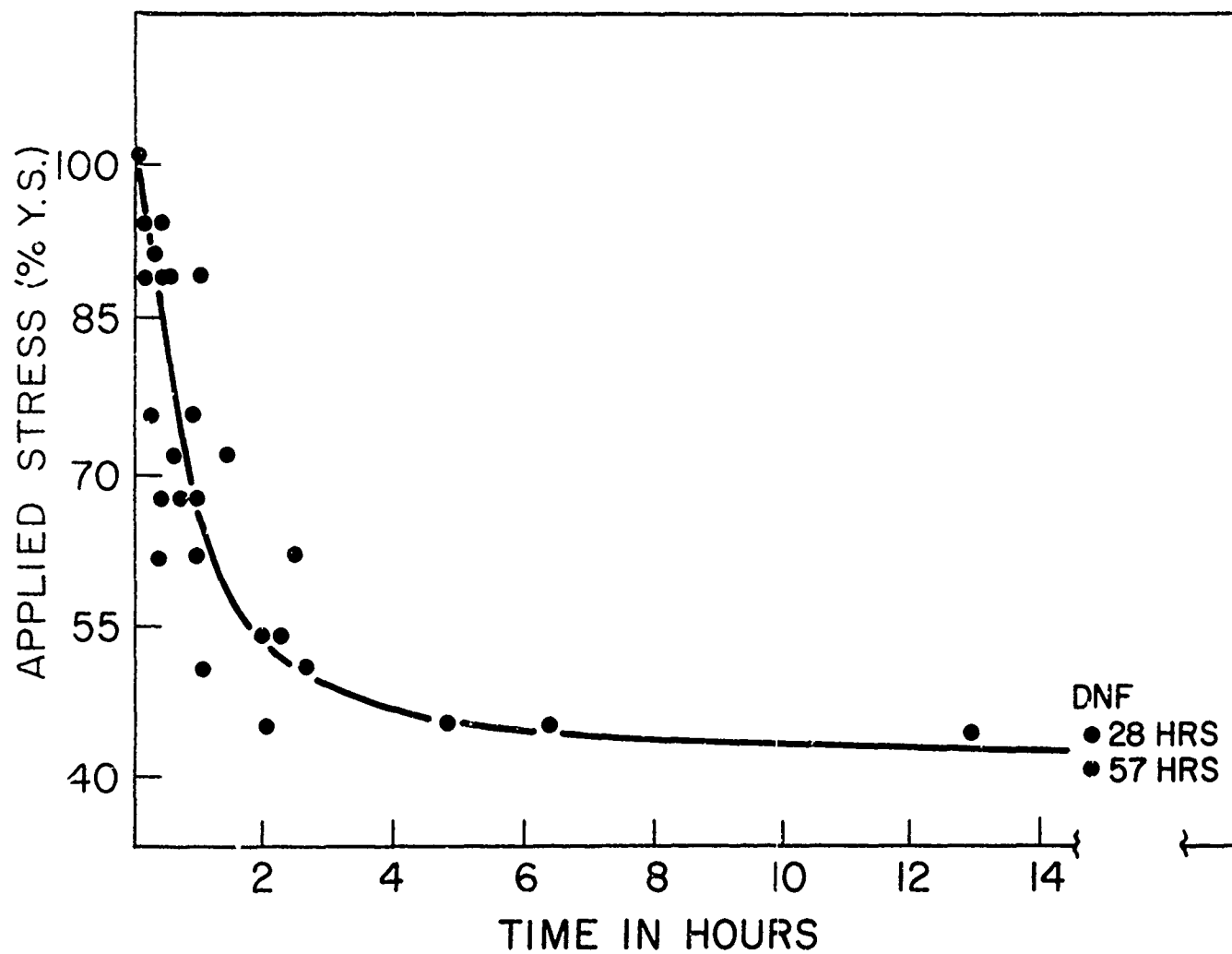


Figure 44. Delayed failure of copper -2% beryllium alloy at room temperature wetted with mercury -2% sodium amalgam. The alloy was initially aged for one hour at 700° F (yield stress ~150000 psi) (after Rinnevetore et al.¹²⁰).

minutes under stress. Nevertheless, there is evidence that a combination of stress and temperature accelerates failure. It was also suggested that grain boundary penetration is perhaps related to delayed failure, although such penetration is considered too small to be detected metallographically. On the other hand Kinnovatore et al.⁹⁸ have shown that unstressed copper-beryllium alloy exposed to liquid mercury-sodium amalgam for extended periods of time exhibited grain boundary penetration and subsequent loss of strength as a result of such penetration. In other more extensive studies these workers¹²⁰ noted that grain boundary penetration occurs in delayed failure and that a critical depth of penetration is related inversely to the applied stress. Penetration itself, however, is not sufficient to cause embrittlement. Although a critical depth of penetration is necessary, Griffith type analysis for crack propagation is not directly applicable to the phenomenon of delayed failure. Thus, the role of liquid metal penetration on the embrittlement of a solid metal is yet not well understood. It is suggested that delayed failure in these metals should be investigated in specimens containing sharp notches or cracks. It may then be possible to evaluate the effects of local high stress concentrations rather than over-all applied stress as used in the smooth specimens on grain boundary penetration of liquid. Conceivably, under such conditions rapid penetration of liquid into the grain boundary of the solid occurs and that fracture nucleates when the depth of penetration reaches some critical value corresponding to a Griffith flaw size.

6.6 Effects of Variation in the Composition of the Environment

The effects of minor additions to the embrittling liquid have been shown to cause significant variations in the susceptibility of a solid to

embrittlement, Section 6.1. It might be suspected that the influence of minor alloying additions is a consequence of the "wetting" problem (See Section 6.1) or is caused by the preferential adsorption of the solute species at the solid metal surface or at the crack tip of the solid. If this were so, however, then once sufficient solute atoms are available to form a few monolayers near a crack tip or over the surface of the solid, little or no variation in fracture strength with solute concentrations would be expected. In practice, a continuous variation in fracture stress over a wide range of liquid alloy composition has been observed in a number of systems.⁴³ For example, while pure liquid mercury reduces the fracture stress of polycrystalline silver by some 50%, increasing additions of more than 7% indium to mercury gradually restores the fracture stress of silver to its value in air, Figure 41. This means that embrittlement is inhibited. On the other hand, mercury does not embrittle cadmium but additions of more than 7% indium to mercury induce embrittlement,^{10,158} Figure 39; in mercury-40% indium solution the fracture stress is reduced to the flaw stress, Figure 41. These results indicate that a wide range of control over embrittlement can be achieved by alloying the liquid environment with an appropriate concentration of a suitable solute. Indium in mercury solutions containing less than 7% indium is apparently inactive with regard to its influence on the embrittlement behavior of cadmium and silver. This can be rationalized in terms of the solute-solvent interactions in the liquid which are thought to be responsible for similar anomalies in certain physical properties of mercury-indium solutions such as thermopower.⁴³ A tentative explanation for such behavior has been offered

by Mott¹²¹ in terms of the existence of a minimum in the density of states curve for mercury near the Fermi energy level. Solute additions conceivable influence the position of the energy level with respect to this minimum and also eventually blunt and cause the disappearance of the minimum. Thus mercury-indium solutions appear to exhibit strong solvent-solute interactions which serve in some way to reduce the surface activity of the solute species; perhaps by providing a solvation sheath of mercury atoms around indium atoms. The significance of the observations reported in Figure 41 is that solvent-solute interactions can play an important role in determining the embrittlement behavior of solid metals in liquid metal solutions. The important questions regarding the mechanism of the inhibition or enhancement of embrittlement observed at concentrations higher than 7% indium in mercury still remain unresolved. It is possible that at large concentrations, availability of the active species at the crack tip or at the sites of crack nucleation are limited by their concentration; these factors would then determine the susceptibility to embrittlement.

6.7 Effects of Liquid Metals Solutions on Static Fatigue Behavior

The static fatigue behavior of notch sensitive metals in pure liquid metal environments have been described. It was shown that in zinc-mercury and cadmium-gallium couples, fracture initiated in a catastrophic manner. This indicated that the fracture process was nucleation controlled. Also, it was suggested that once a crack is initiated in a notch sensitive metal subsequent propagation may occur in the absence of the liquid metal at the crack tip by mechanical means. The role of pure liquid metal in embrittlement may then be limited to the initiation stage of the fracture process.

It is conceivable, however, that failure in liquid metal solutions containing only low concentrations of some active species would be controlled by the rate of arrival of these species at the propagating crack tip, and therefore would be propagation controlled. Preece and Westwood⁴³ have investigated the effects of liquid metal solutions on the static fatigue behavior of polycrystalline aluminum in mercury-gallium solutions and cadmium and silver exposed to mercury-indium solutions. Their results indicate that fracture in liquid metal solutions is initiation rather than propagation controlled. The typical static fatigue behavior of these embrittlement couples is exemplified by the fracture behavior of cadmium in various mercury-indium solutions, Figure 45. Note that failure occurred in a catastrophic manner at some critical stress, σ and that this stress varied with the indium content of the solution, Figure 45. The static fatigue behavior of silver in mercury-indium was also found to be identical to that of cadmium; with the exception that susceptibility to embrittlement decreased with increasing indium content, i.e. inhibition of embrittlement occurred. These results are in agreement with the tensile fracture data reported for silver in indium-mercury solutions, Figure 41. The reasons for this behavior have been discussed earlier in Sections 6.3 and 6.6. Thus fracture behavior under static loading conditions is identical to that observed under continuous loading. These investigations demonstrate that additions of metallic solutes to liquid metal environments can be used to control, (sometimes over a wide range) the stress to induce catastrophic failure in polycrystalline metals under static loading conditions. Additions can be used to enhance or inhibit embrittlement. The influence of solute

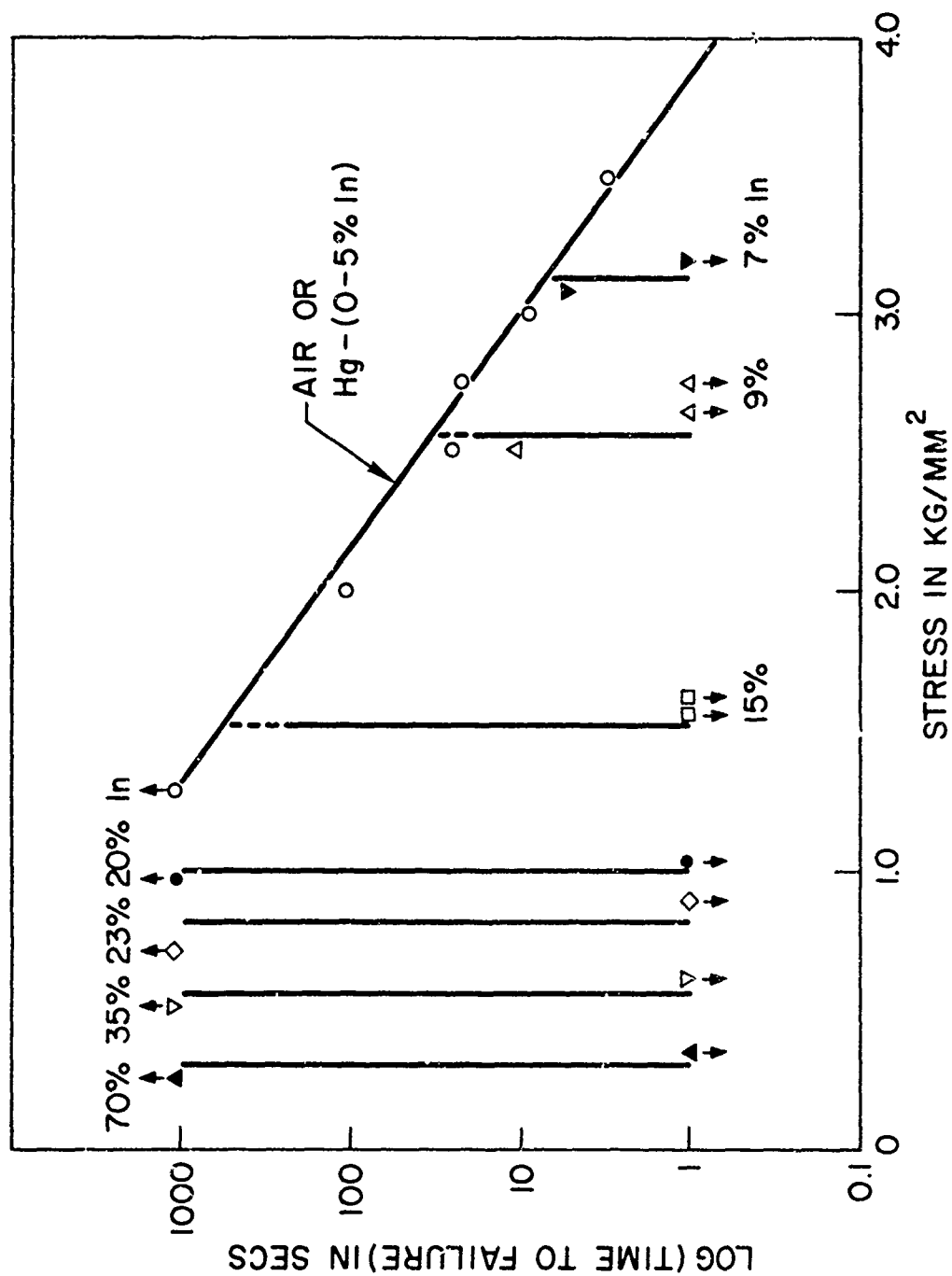


Figure 45. Effects of applied stress and (Hg-In) environments on the time to failure of statically loaded polycrystalline cadmium at room temperature (grain diam. $\approx 1.0\text{mm}$). Note that for indium concentrations of more than ~ 7 a/o, severity of embrittlement increases with indium concentration (after Preece and Westwood²³).

addition on the applied stress is, related to the concentration of the active species. This indicates that in most cases neither solvent nor solute elements are preferentially adsorbed at the metal surfaces. If preferential adsorption were involved, then addition to the environment of less than 1% solute would provide more than a sufficient number of monolayers of solute on the metal surface to cause fracture to initiate and propagate, Section 3.2. The applied stress, therefore, would not be expected to vary significantly with composition of the liquid-metal environment. The variation of the applied stress with composition indicates, that a dynamic equilibrium exists between metallic surfaces and liquid metal solution environments.

From Figure 45, it is seen that embrittlement occurs either in a catastrophic manner or not at all. This indicates that the failure is controlled by the crack initiation process, and that the rate of arrival of the most active species at the crack tip is sufficient to maintain crack propagation in a brittle manner, even in intrinsically notch insensitive solids such as pure aluminum and silver. As discussed earlier in Section 4.7, such fracture behavior may be anticipated, if the effective fracture surface energy to cause both crack nucleation and propagation in a liquid metal environment is equal to or less than the true surface free energy, γ , for intercrystalline failure.^{74,75}

It is possible that fracture in liquid metal solutions would occur by propagation controlled processes if the concentration of the active species were sufficiently low, say, one hundredth of one percent. For example, embrittlement of steel in hydrogen environment occurs by slow

crack growth when only several parts per million of hydrogen atoms are present.

6.8 Effects of Liquid Metal Solutions on Brittle-Ductile Transitions

The effects of pure liquid metals in causing brittle to ductile transitions in solid metals were described in Section 5.2. It was shown that the transition temperature, T_c , varies with grain size and strain rate. The variation in T_c with these factors was based on three assumptions, (i) that the temperature dependence of yields stress, σ_y , is the controlling factor, i.e. τ , the metallurgical parameter is affected; (ii) that T_c is that temperature at which $\sigma_y \approx \sigma_F$, the fracture stress; and (iii) σ , the environment sensitive parameter is not affected by temperature. Preece and Westwood¹²² have shown that brittle-ductile transitions occur in face centered cubic metals in liquid metal solutions and that the transition temperature varies with the composition of the environment. Aluminum, brass and silver undergo transitions in mercury base solutions (containing 0-4 a/o gallium and 0 to 70 a/o indium) and the transition temperature, T_c , varied with composition of the environment, Figures 46 and 47. Figure 46 shows that high purity aluminum is not significantly embrittled by pure mercury at room temperature. Lowering the test temperature by 40°C produces marked increase in the severity of embrittlement, however, and a sharp brittle to ductile transition occurs at $\sim 10^\circ\text{C}$. Specimens tested in pure gallium, on the other hand, do not exhibit such transitions, Figure 46. The absence of ductile-brittle transition in gallium is to be expected, because pure gallium embrittles aluminum by intergranular penetration even in the absence of stress;¹²³ any diffusion dependent embrittlement process would

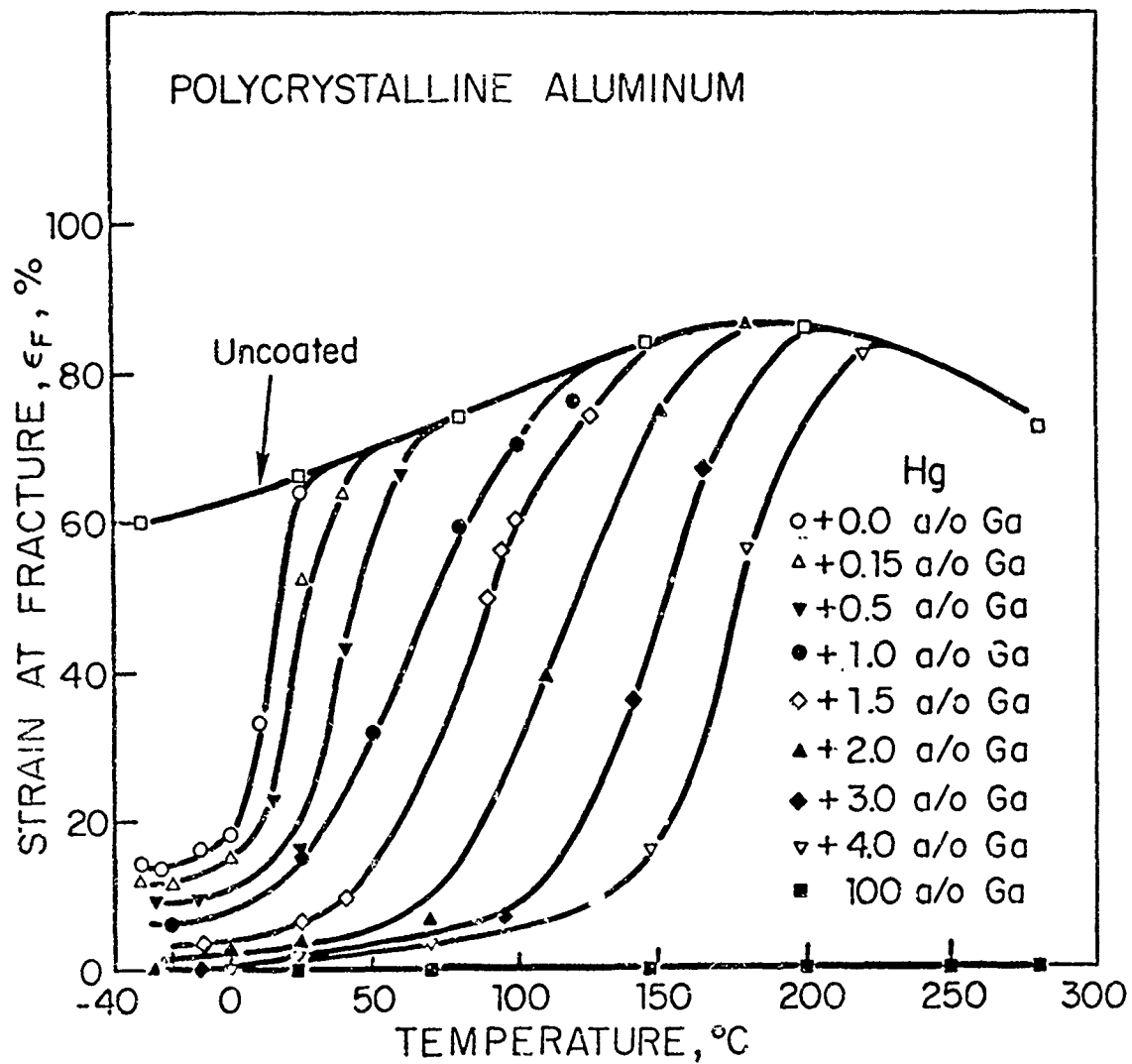


Figure 46. Influence of mercury, gallium or mercury-gallium environments on the strain at fracture of aluminum (grain diam ≈ 1 mm) as a function of temperature (after Preece and Westwood¹²²).

therefore be expected to increase rather than decrease severity of embrittlement with temperature. Fracture data for mercury-4 at/o gallium solutions suggest that gallium dissolved in mercury embrittles aluminum primarily by an adsorption process rather than by grain boundary penetration. This is because brittle to ductile transitions are observed and these occur at temperatures higher than those for pure mercury, Figure 46. The variation in the transition temperature, T_c , with concentration of gallium in mercury is shown in Figure 47. Brass and silver are both embrittled by pure mercury. The transition temperature in these metals increases with a decrease in the indium content of the mercury solutions. In silver, the transition temperature was shown to be essentially independent of grain size. The effects of grain size, however, were not investigated in other systems.

The temperature sensitive embrittlement behavior of face centered cubic metals in liquid metal solutions described above has been interpreted by Preece and Westwood¹²² as follows: They found that σ_y , the yield stress of these metals varies but little in the temperature range in which transitions occur and that a significant amount of plastic deformation occurs before embrittlement, suggesting that $\sigma_y \approx \sigma_F$ at any temperature of relevance. Assumptions (i) and (ii) apply to transitions occurring in pure liquid metal environments. An analysis based on these assumptions developed by Ichinose⁸⁰ and Robertson,¹⁶ Section 5.2, for brittle-ductile transition in pure liquid metals should not be applied to transitions occurring in liquid metal solutions. Preece and Westwood suggest that σ , the environment sensitive parameter mentioned in assumption (iii), must be affected by the composition of the environment. They propose that the effective value of the bond strength in the presence of chemisorbed

POLYCRYSTALLINE ALUMINUM

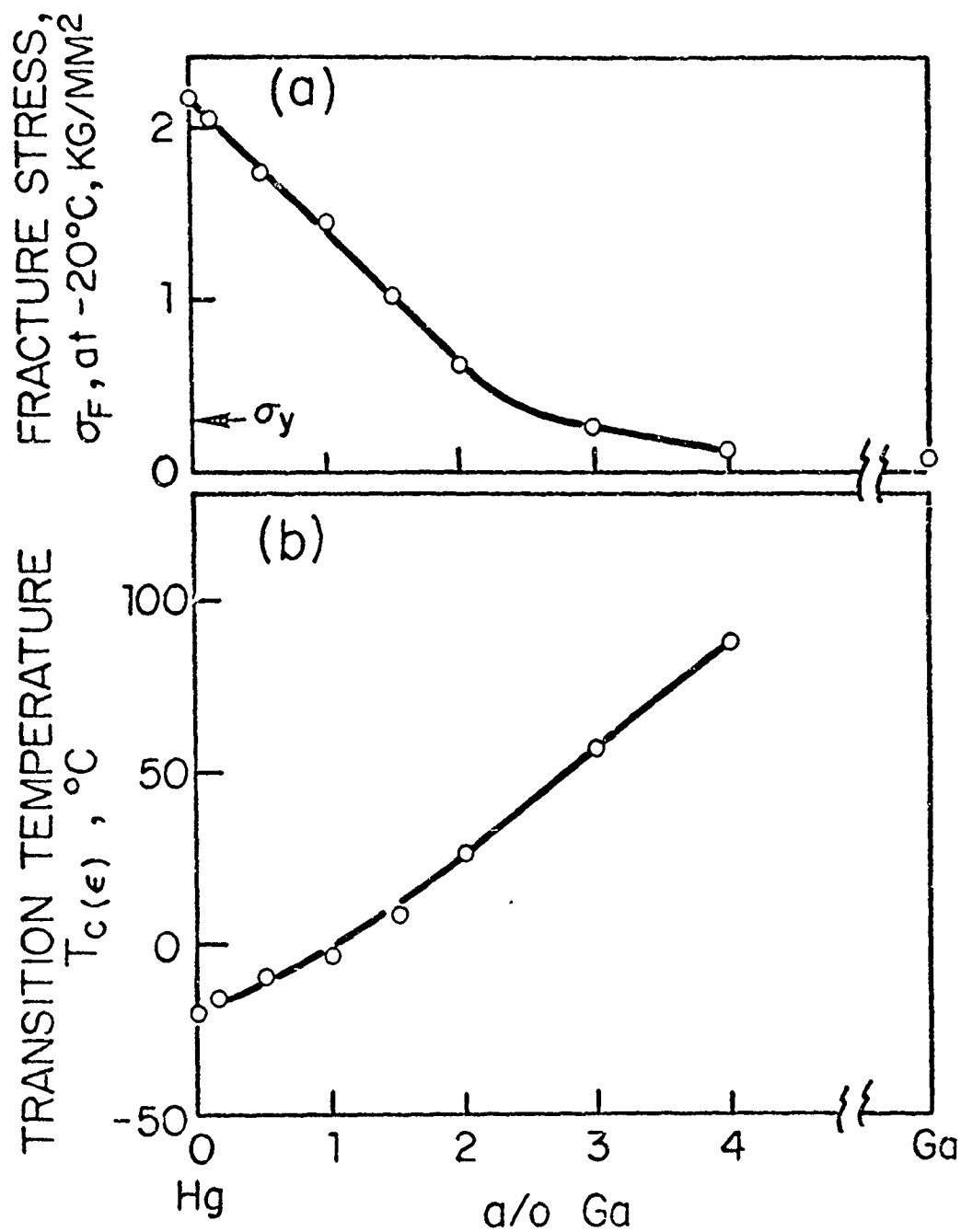


Figure 47. Effects of gallium concentration of (Hg-Ga) environments on (a) fracture stress at -20°C and (b) transition temperatures, T_C for aluminum. Values of T_C were derived from the data of Fig. 46 (after Preece and Westwood¹²²).

embrittling species, σ_e , should be temperature sensitive. The reason is that adsorption is a dynamic and thermally activated process. Using this idea they developed a relation, $\sigma_e = \sigma(1-\beta\theta)$, when β is a constant for a particular system, σ is the cohesive bond strength at the crack tip, and θ is a fraction of the surface sites covered with adsorbed liquid metal atoms that causes embrittlement. For liquid alloy environments, in which one of the species is considerably more embrittling than the other, θ for these species will increase with concentration. At any given temperature, a large value of θ will result in a lower value of σ_e . Because σ does not change with temperature, the ratio σ_e/τ will decrease and consequently susceptibility to embrittlement will increase, as discussed in Section 4.1. Thus, the transition temperature of the metal will increase with the concentration of the more active species, as shown in Figures 46 and 47. The magnitude of the constant β determines the maximum degree of embrittlement that can occur in a particular system.

Although, above analysis of Preece and Westwood¹²² has been shown to be applicable to face centered cubic metals, the results for aluminum are not in agreement with those of Ichinose⁸⁰ for brittle-ductile transition in pure aluminum in pure liquid mercury, Figure 23. Figure 23 shows that T_c for one mm grain size aluminum is estimated to be $\sim 180^\circ\text{C}$ compared to $\sim 10^\circ\text{C}$ for the same grain size material, Figure 46. The reasons for this variation in T_c tested under identical conditions are not known. Of particular significance, however, is the result that T_c in aluminum does vary with grain size and strain rate.

Ichinose⁸⁰ also reports that the yield stress of aluminum varies with temperature in the range 50 to 180°C and that the fracture stress of

aluminum in air is about the same as that in mercury at the transition temperature, Figure 23. In the same range of temperatures, Preece and Westwood observed transitions to occur in aluminum in liquid metal solutions. Preece and Westwood however, assumed that for face centered cubic metals, σ_y and σ_F did not vary with temperature. Using these assumptions, they developed the analysis for the ductile-brittle transitions in liquid metal solutions. These points therefore require clarification.

The brittle-ductile transitions in pure embrittling metals are related to variations in the property of the solid via factors such as grain size and strain rate.^{80,16} These factors, considered unimportant for the transitions occurring in liquid metal solutions, are related to variations in reduction in the effective bond strength with composition of the active species in the environment.¹²² It is conceivable that ductile-brittle transition would be related to the properties of both the solid and the liquid solutions. It may be that the data shown in Figures 23, 46 and 47 are caused by a particular set of experimental conditions. A detailed analysis of such transitions should consider the factors that affect both the solid as well as the liquid. Such an analysis may be developed by substituting the relation for σ_e for γ in the Cottrell-Petch equations and its modification by Robertson.⁸⁰

7. SUMMARY

A brief summary of the review on liquid metal embrittlement presented in the foregoing sections is given below:

(i) On the basis of some empirical observations, it may be anticipated that a solid and a liquid metal will constitute an embrittlement couple, providing that they have little or no mutual solubility and do not form stable intermetallic compounds.^{2,5}

(ii) It is considered that embrittlement results from liquid metal adsorption induced reduction in cohesion at the sites of crack nucleation or at the tip of a crack.^{4,6} Embrittlement is not limited by the adsorption process, apparently adsorption occurs spontaneously. The liquid metal phase or atoms, however, must be present at the crack tip for continued propagation of a crack, specially if the metal is notch-sensitive. The transport of liquid phase to crack tip may occur by diffusion of liquid metal atom over liquid and such processes apparently are relatively temperature insensitive.

In notch insensitive metals, once a crack is initiated in a liquid metal environment, and has grown to some critical size, subsequent propagation may occur in the absence of liquid at the tip by mechanical means.

In general, time and temperature dependant diffusion controlled penetration of liquid or corrosion type processes are not considered responsible for the occurrence of embrittlement in a solid. However, the former is a likely possibility when delayed failure occurs in liquid metal environments.¹²⁰

(iii) It appears well established that liquid metal embrittlement is a special case of brittle fracture and prerequisites for its occurrence are the same as those for brittle fracture^{7,9} (see Section 4, for extensive investigations with zinc-mercury couples)

(iv) In general, factors that normally induce brittle behavior in a solid also cause increase in the severity of embrittlement. Such factors are large grain size, high strain rates, low temperature, metallurgical structures that lead to high stress concentrations in a solid rather than relief of stress concentration via plastic flow, e.g. slip character, presence of stress raisers or a sharp notch in a solid, alloying additions, etc.

(v) Embrittlement is a specific phenomenon and the severity of its occurrence appears to be related to the electronegativities of the participating solid and liquid metal. Maximum embrittlement occurs when electronegativity of these metals are identical.^{10,7}

(vi) The concept of "inert career" liquid metal (Section 6.2) can be used to induce and control the severity of embrittlement.¹⁰⁸ Small as well as large variations in the composition of the liquid can cause significant variations in the severity of embrittlement and in some instances may even cause inhibition of embrittlement.^{43,122} The role of liquid metal and its solutions in controlling the severity of embrittlement and the associated mechanism(s) are not well understood.

(vii) A consideration of the effects of adsorption of the liquid metal atoms at a crack tip on the shear and cohesive strength in the vicinity of or at the crack tip provide reasonable explanation for the occurrence and severity of embrittlement.⁷ Also, these considerations provide a rational explanation for the effects of variables on the severity of embrittlement that affect both the solid and the liquid. Theoretical investigations based on the above considerations have not been made so far and thus it is not possible to predict embrittlement characteristics, i.e. the occurrence or the severity of embrittlement, in a particular solid metal liquid metal couple.

8. SUGGESTIONS FOR FUTURE WORK

The foregoing review and the summary presented in Section 7 indicate that significant progress has been made in the past ten years in achieving an improved understanding of the phenomenon of liquid metal embrittlement. This is primarily due to the fact that investigations of liquid metal embrittlement utilized critical experiments and studied the effects of one variable at a time. Also, these experiments used simple model embrittlement couples and direct experimental techniques to provide readily interpretable results. It is not always possible, however, to design appropriate critical experiments because (i) liquid metal embrittlement is a specific phenomena and occurs but in a limited number of couples, (ii) in most instances, the solubility of active embrittling or nonembrittling species in a carrier liquid phase is limited to small amounts, and (iii) the temperature range in which embrittlement studies can be performed is limited before diffusion or penetration dependent processes become significant. In spite of these limitations, it is clear that the above approach should be used in future work in each of the three interrelated areas of liquid metal embrittlement, namely, solid-liquid interaction, chemical nature of the liquid and its solutions, and metallurgical factors that influence the fracture characteristics of the solid. Some suggestions regarding future work in these areas are given below:

(i) Solid-Liquid Metal Interactions and Embrittlement

Assuming that the phenomenon of embrittlement discussed in this paper does involve chemisorption, then theoretical and experimental studies are

required of the manner in which the electrons in surface bonds are redistributed during chemisorption such that significant reductions in cohesive strength result.

Reliable measurements of the fracture surface energies of solid metals of known band structure, exposed both to active and inactive liquid metal environments, would be of particular use in conjunction with the above theoretical and experimental studies of the chemisorption process. In addition to fracture studies, investigations are needed which will make physical measurements of reduction in chemisorption induced cohesion using nondestructive, novel physical experimental techniques.

The search for some parameter of the solid metal-liquid metal system which will correlate with severity of embrittlement should be continued. However, this possibility has yet to be investigated by researchers equipped with both an interest in embrittlement, and a sufficient knowledge of the fundamentals of surface physics and the band structure approach to chemisorption.

(ii) Metallurgical Factors and Embrittlement

Considerably improved understanding of metallurgical factors on severity of embrittlement has occurred. Nevertheless, studies on simple embrittlement couples are still required. These should be quantitative whenever possible, preferably involving direct determination of changes in the fracture surface energy. Studies of cleavage crack propagation in suitable monocrystals, crack initiation in asymmetric bicrystals, and the propagation of intercrystalline cracks in suitably oriented bicrystals as a function of temperature, composition of both solid and liquid components, amount of prestrain, rate of loading, etc. would be most useful.

(iii) Liquid Metals, Liquid Metal Solutions and Embrittlement

This is by far the most important area of investigation, however, very little work of any significance has been performed so far. For example, the high rates of crack propagation in ductile metals in the presence of liquid metal environment are considered limited by the transport of the liquid metal atoms to the propagating tip. However, the precise mechanism of transport of liquid metal atoms to the crack tip is not yet known. The severity of embrittlement can be controlled by varying the composition of the liquid phase (Section 6). This must be related to solute-solvent interactions, diffusion of active species, and adsorption of these at a crack tip. Also penetration of liquid into the solid and associated delayed failure in smooth specimens (Section 6) suggest possible embrittlement by time and temperature dependent diffusion controlled processes. In this regard, penetration of liquid at sites of high stress concentrations and its effect, if any, on embrittlement should be investigated in specimen containing sharp notches or cracks.

In general, little is known concerning the chemical nature of the liquid and its solutions on the occurrence and severity of embrittlement. It is necessary therefore to become familiar with the nature of liquid metal and its solution, i.e. with the structure and type of atomic interaction in the liquid as well as diffusion characteristics and adsorption kinetics.

Such work in each of the above three areas of liquid metal embrittlement should aid considerably our understanding of this phenomenon.

REFERENCES

1. Likhtman, V.I., and Shchukin, E.D., 1958, Soviet Physics - Uspekhi, 1, 91.
2. Rostoker, W., McCaughey, J.M., and Markus, M., 1960, "Embrittlement by Liquid Metals," New York, Reinhold.
3. Ichinose, M., 1966, Trans. Jap. Inst. Met., 7, 57.
4. Westwood, A.R.C., and Kamdar, M.H., 1963, Phil. Mag., 8, 787.
5. Likhtman, V.I., Shchukin, E.D., and Rebinder, P.A., 1962, Physico-Chemical Mechanics of Metals," Acad. Sci. of U.S.S.R., Moscow.
6. Likhtman, V.I., Rebinder, P.A., and Karpenko, G.V., 1958, "Effects of Surface Active Medium on Deformation of Metals," H.M.S.O., London.
7. Westwood, A.R.C., Preece, C.M., and Kamdar, M.H., "Fracture" 1971, Vol. 3, 589, ed. H. Leibowitz, Academic Press, New York.
8. Stoloff, N.S., and Johnston, T.L., 1963, Acta. Met., 11, 251.
9. Kamdar, M.H., and Westwood, A.R.C., "Environment Sensitive Mechanical Behavior," 1966, 581, Ed. Westwood, A.R.C. and Stoloff, N.S., Gordon and Breach, New York.
10. Kamdar, M.H., Phys. Stat. Solidi., 1971, 4, 225.
11. Stoloff, N.S., Liquid Metal Embrittlement, "Surface and Interfaces," II 14, Sagamore Army mat. Res. Conf., 1968, 159, Ed. J. Burke, J., Reed, N. Weiss, W.
12. Klein Wassink, R.J., J. Inst. Met., 1967, 95, 38.
13. Kamdar, M.H., Unpublished work, RIAS, 1964.
14. Fager, D.W., and Spurr, W.F., Corrosion, 1969, 24, 209.
15. Fager, D.W., and Spurr, W.F., Corrosion-NACE, 1971, 27, 72.
16. Robertson, W.M., Met. Trans., 1970, 1, 2607.
17. Nichols, H., and Rostoker, W., Acta. Met., 1961, 9, 504.
18. Felbeck, D.K., and Orowan, E., Weld. Jour. Res. Suppl., 1955, 34, 570.
19. Low, J.R., "Fracture," 1959, 58, Wiley & Sons, New York.
20. Gilman, J.J., "Plasticity," 1960, 43, Pergamon, New York.
21. Bennett, A.J., and Felicov, L.M., Phys. Rev., 1966, 151, 512.

Preceding page blank

22. Grimley, T.B. Proc. Phys. Soc., 1967, 90, 751.
23. Mostovoy, S. and Breyer, N.N., Trans. ASM. Quart. 1968, 61, 219.
24. Schmidt, L.D. and Comer, R., J. Chem. Phys., 1966, 45, 1605.
25. Geuss, J.W., Surface Sci., 1964, 2, 48.
26. Inglis, C.E., Trans. Inst. Naval. Architects, 1913, 55, 219.
27. Griffith, A.A., Phil. Trans., 1920-21, A221, 163.
28. Orowan, E., Rep. Prog. Phys., 1949, 12, 186.
29. Gilman, J.J., J. Appl. Phys., 1960, 31, 2208.
30. Westwood, A.R.C., and Hitch, T.T., J. Appl. Phys., 1963, 34, 3085.
31. Govila, R.K., and Kamdar, M.H., Met. Trans., 1970, 2, 1011.
32. Gilman, J.J., "Fracture," Ed. Averbach, B.L., Felback, D.K., Hahn, G.T., and Thomas, D.C., 1959, John Wiley and Sons, New York.
33. Maitland, A.H., and Chadwick, G.A., Phil. Mag., 1969, 19, 1305.
34. Maitland, A.H., and Chadwick, G.A., Phil. Mag., 1969, 12, 645.
35. Hull, D., Beardmore, P., and Valentine, A.P., Phil. Mag., 1965, 12, 1021.
36. Bell, R.L., and Cahn, R.W., J. Inst. Metals., 1957-58, 86, 433.
37. Perrone, N., and Leibowitz, H., 1965, Second Int. Conf. on Fracture, Sendai, Japan.
38. Kamdar, M.H., Report to ARO(D) 1 through 13, on Contract # DA-33-124-ARO-D-63, 1963-1969.
39. Stolloff, N.S., Davies, R.G., and J. Asten, T.L., "Environment Sensitive Mechanical Behavior," 1966, 613, Ed. Westwood, A.R.C., and Stolloff, N.S., Gordon and Breach, New York.
40. Robertson, W.M., Trans. AIME, 1966, 236, 1478.
41. Rozhanskii, V.N., Pertsov, N.V., Shchukin, E.D., and Rebinder, P.A., Soviet Phys. Doklady, 1957, 2, 460.
42. Bryukhanova, L.S., Andreeva, I.A., and Likhtman, V.I., Soviet. Phys. Solid-State, 1962, 3, 2025.
43. Preece, C.M., and Westwood, A.R.C., 1969, Proceedings of the Second Int. Conf. on Fractures, Brighton. Ed. P.L. Pratt.

44. Kelly, A., Tyson, W.R., and Cottrell, A.H., *Phil. Mag.*, 1967, 15, 567.
45. Brattain, W.H., "The Surface Chemistry of Metals and Semiconductors," 1959, 9. Wiley and Sons, New York.
46. Stern, E.A., *Phys. Rev.*, 1967, 162, 565.
47. Westwood, A.R.C., Preece, C.M., and Kamdar, M.H., *ASM. Trans. Quart.* 1967, 60, 723.
48. Rosenberg, R., and Cadoff, J., "Fracture of Solids," 1963, 607, Interscience, New York.
49. Kraai, D.A., Floreen, S., Stickles, C.A., Ragone, D.V., and Huccke, E.E., AFOSR, 1960, Rept. No. TR-60-116.
50. Summ, B.D., Ivanova, L.V., Goryunov, U.V., *Physico-chemical mechanics of Materials (in Russian)*, 1965, 1, 648.
51. Summ, B.D., Ivanova, L.V., Goryunov, U.V., and Dekartov, A.P., *Phys. of Metals and Metallography*, 1966, 21, 26.
52. Shchukin, E.D., and Yuschenco, V.S., *Physico-chemical Mechanics of Materials (in Russian)*, 1966, 2, 133.
53. Hayden, H.W., and Floreen, S., *Phil. Mag.*, 1969, 20, 135.
54. Kamdar, M.H., and Westwood, A.R.C., *Acta. Met.*, 1968, 16, 1335.
55. Morgan, W.A., Ph.D. Thesis, 1944, Cambridge University.
56. Shchukin, E.D., Pertsov, N.V., and Goryunov, U.V., *Soviet-Phys. Crystallography*, 1960, 4, 840.
57. Garber, R.I., and Gindin, I.A., *Soviet-Phys-Uspekhi*, 1960, 3, 41.
58. Morton, P.H., Treon, R., and Baldwin, W.M., *J. Mech. Phys. Sol.*, 1954, 2, 177.
59. Gilman, J.J., *Trans. AIME*, 1958, 212, 783.
60. Eshelby, J.D., Frank, F.C., and Nabarro, F.R.N., *Phil. Mag.*, 1951, 42, 351.
61. Stroh, A.H., *Phil. Mag.*, 1958, 3, 597.
62. Bullough, R., *Phil. Mag.*, 1964, 9, 917.
63. Bullough, R., 1956, Quoted in Deruyterre, A and Greenough, G.B., *J. Inst. Met.*, 1956, 34, 337.

64. Rozhanskii, V., Soviet-Physics-Doklady, 1959, 3, 1193.
65. Smith, E., and Barnby, J.T., Metal. Sci. Jour., 1967, 1, 56.
66. Heald, P., Scripta. Met., 1969, 3, 393.
67. Huntington, H.B., Solid State Physics, 1958, 7, 213.
68. Ku, R.C., and Johnston, T.L., Phil. Mag., 1964, 9, 231.
69. Kamdar, M.H., Met. Trans., 1971, 2, 2937.
70. Deruyettere, A., and Greenough, A.B., J. Inst. Met., 1956, 34, 337.
71. Shchukin, E.D., and Likhtman, V.I., Soviet-Physics-Doklady, 1959, 4, 111.
72. Kamdar, M.H., Met. Trans., 1971, 2, 485.
73. Kamdar, M.H., and Westwood, A.R.C., "Physical Basis for Yield and Fracture," 1966, Physical Society, London.
74. Stroh, A.H., Adv. in Phys., 1957, 6, 418.
75. Smith, E., Acta. Met., 1966, 14, 985.
76. Cottrell, A.H., Trans. AIME., 1958, 212, 192.
77. Petch, N.J., J. Iron. Steel. Inst., 1953, 173, 25.
78. Petch, N.J., Progress in Metal Physics, 1954, 5, 1.
79. Armstrong, R.W., Phil. Mag., 1964, 9, 1063.
80. Ichinose, H., Trans. Jap. Inst. Met., 1968, 9, 35.
81. Ichinose, H., and Oouchi, C., Trans. Jap. Inst. Met., 1968, 9, 41.
82. Westwood, A.R.C., Phil. Mag., 1964, 9, 199.
83. Levine, E., and Cadoff, I.B., Trans. AIME., 1964, 230, 1116.
84. Nichols, H., and Rostoker, W., Acta. Met., 1960, 8, 848.
85. Rhines, F.N., Alexander, J.A., and Barklay, W.F., Trans. ASM, 1962, 55, 22.
86. Smithells, C.J., "Metals Ref. Book," II, p. 558, 1955, Interscience, New York.
87. Johnston, T.L., Davies, R.G., and Stoloff, N.S., Phil. Mag., 1965, 12, 305.

88. Kamdar, M.H., and Westwood, A.R.C., Trans. Jap. Inst. Met. Suppl., 1968, 9.
89. Worthington, P.J., and Smith, E., Acta. Met., 1964, 12, 1277.
90. Gilman, J.J., and Reed, T.A., Trans. Met. Soc. AIME., 1953, 197, 49.
91. Madar, S., "Electron Microscopy and Strength of Crystals," 1963, p. 219, Interscience, New York.
92. Howie, A., and Swann, P.R., Phil. Mag., 1961, 6, 1215.
93. Foley, J.H., Cahn, R.W., and Raynor, G.V., Acta. Meta., 1963, 11, 355.
94. Smallman, R.E., and Westmacott, K.H., Phil. Mag., 1957, 2, 669.
95. Neighbours, J.R., and Smith, C.S., Acta. Met., 1954, 2, 591.
96. Nichols, H. and Rostoker, W., Trans. AIME, 1962, 224, 1258.
97. Levine, E., and Cadoff, I.B., Trans. AIME, 1964, 230, 1113.
98. Rinnevatore, J.V., Corrie, J.D., and Markus, H., Trans. ASM, 1964, 57, 474.
99. Pargeter, F.W.J., and Ives, M.B., Canadian Jour. Phys., 1967, 45, 1235.
100. Rostoker, W. 1963. Rept. No. ARF-B183-12 on Contract No DA-11-GFC-022-3108, Nov. Armour. Res. Found. Chicago.
101. Nichols, H., and Rostoker, W., Trans. ASM., 1963, 56, 494.
102. Nichols, H., and Rostoker, W., Trans. AIME., 1964, 251.
103. Rinnevatore, J.V., McCaughey, J., and Markus, H., Acta. Met., 1964, 12, 383.
104. Rinnevatore, J.V., Corrie, J.D., and Meakin, J.D., Trans. ASM., 1968, 61, 321.
105. Zhurkhov, S.N., 1966, "Proc. First. Inst. Conf. on Fracture," Vol 2, p. 1167., Jap. Soc. for Strength and Fracture of Materials.
106. Labzin, V.A., and Likhtman, V.I., Soviet-Physics-Doklady, 1959, 4, 1282.
107. Shchukin, E.D., Kochanova, L.A., and Pertsov, N.V., Societ-Physics-Crystallography, 1963, 8, 49.
108. Kamdar, M.H. and Westwood, A.R.C., Phil. Mag., 1967, 15, 567.
109. Hansen, M., "Constitution of Binary Alloys," 2nd Edition, McGraw-Hill, 1958.

110. Schmid, E., and Boas, W., "Plasticity of Crystals," p. 147, 1950, Hughes and Co., London.
111. Pauling, L., "The Nature of the Chemical Bond," 1960, p. 91. Cornell Univ. Press, Ithaca, N.Y.
112. Westwood, A.R.C., and Goldheim, D.L., unpublished work, RIAS, 1966.
113. Gordy, W. and Thomas, W.J.O., J. Chem. Phys., 1956, 24, 439.
114. Hinze, J., and Jaffe, J.H., J. Am. Chem. Soc., 1962, 84, 540.
115. Peters, D., J. Chem. Soc., A., 1966, 656.
116. Huheey, J.E., J. Phys. Chem., 1965, 69, 3264.
117. Cotton, F.A., and Wilkinson, A., "Advanced Inorganic Chemistry," 1962, p. 89, Interscience, New York.
118. Flegontova, N.I., Summ, B.D., and Goryunov, U.V., Physics of Metals and Metallography, 1964, 18, 85.
119. Nichols, H., and Rostoker, W., Trans. ASM., 1965, 58, 155.
120. Rinnovetore, J.V., Corrie, J.D., and Markus, H., Trans. ASM., 1966, 59, 665.
121. Mott, N.F., Phil. Mag., 1966, 13, 989.
122. Preece, C.M., and Westwood, A.R.C., Trans. ASM, 1969, 62, 419.
123. Gogging, W.R., and Moberly, J.W., Trans. ASM., 1966, 59, 315.